



Search for light neutral particles decaying promptly into collimated pairs of electrons or muons in pp collisions at $\sqrt{s} = 13$ TeV with the ATLAS detector

ATLAS Collaboration*

CERN, 1211 Geneva 23, Switzerland

Received: 16 July 2024 / Accepted: 10 February 2025
© CERN for the benefit of the ATLAS Collaboration 2025

Abstract A search for a dark photon, a new light neutral particle, which decays promptly into collimated pairs of electrons or muons is presented. The search targets dark photons resulting from the exotic decay of the Standard Model Higgs boson, assuming its production via the dominant gluon-gluon fusion mode. The analysis is based on 140 fb^{-1} of data collected with the ATLAS detector at the Large Hadron Collider from proton-proton collisions at a center-of-mass energy of 13 TeV. Events with collimated pairs of electrons or muons are analysed and background contributions are estimated using data-driven techniques. No significant excess in the data above the Standard Model background is observed. Upper limits are set at 95% confidence level on the branching ratio of the Higgs boson decay into dark photons between 0.001% and 5%, depending on the assumed dark photon mass and signal model.

1 Introduction

Hidden sectors near the weak scale that are motivated by naturalness, thermal dark matter, and electroweak baryogenesis are particularly compelling proposals for new phenomena beyond the Standard Model (SM) [1–4]. Several minimal extensions of the SM introduce new symmetries and hidden sectors of particles that can be investigated at the Large Hadron Collider (LHC), assuming their interaction with SM particles through specific portals. Unstable dark states may be produced at colliders and decay into SM particles with sizeable branching ratios, depending on the dark sector's structure.

This paper focuses on a blueprint extension of the SM that considers an additional broken $U'(1)$ gauge symmetry mediated by a massive vector boson, referred to as 'dark photon' (γ_d). The only interaction between the dark photon and SM particles is via kinetic mixing [5] with the SM photon

and the Z boson, with a coupling denoted by ϵ . Additionally, if a dark Higgs mechanism drives the spontaneous breaking of the new $U'(1)$ gauge symmetry, the dark Higgs boson will generally have a coupling to the SM Higgs boson (H), leading to mixing between the two physical scalar states. The production of dark photons at the LHC can be enhanced by exotic decay modes of the Higgs boson, while its observation may be possible thanks to the kinetic mixing of the γ_d with the SM photon.

The most stringent 95% CL upper limit on the branching ratio for the SM Higgs boson decay into undetected final states is 12% [6, 7], leaving ample room for the Higgs boson decay mode investigated in this paper. In the absence of lighter hidden-sector states, a dark photon with a mass (m_{γ_d}) up to a few GeV kinetically mixes with the SM photon and decays into leptons or light quarks. Under this assumption, the dark photon decay branching ratios coincide with those of virtual SM photons, which are directly measured in e^+e^- experiments [8]. The kinetic mixing parameter ϵ is related to the γ_d mean proper lifetime. This paper targets values $\epsilon \gtrsim 10^{-5}$ – 10^{-3} , which correspond to prompt γ_d decays [4].

The dark photon mass range targeted by this search goes from $\mathcal{O}(10 \text{ MeV})$ to $\mathcal{O}(10 \text{ GeV})$. Therefore, the small mass of the γ_d relative to the Higgs boson mass implies that the dark photon decay products are highly collimated and can be identified as bundles of electrons or muons, referred to as *Lepton-Jets* (LJ) in the following. At masses greater than $\mathcal{O}(10 \text{ GeV})$, the decay products of the dark photon become less collimated and can no longer be identified as LJs.

This paper presents a search for $\gamma_d \rightarrow e^+e^-$ and $\gamma_d \rightarrow \mu^+\mu^-$ reconstructed as LJs. The search is performed on proton–proton (pp) collision data at $\sqrt{s} = 13$ TeV, collected with the ATLAS detector at the LHC between 2015 and 2018 and corresponding to an integrated luminosity of 140 fb^{-1} . While sufficiently massive γ_d can decay into quark–antiquark ($q\bar{q}$) or τ -lepton pairs, these channels are not considered in this study, given the presence of neutrinos from τ

* e-mail: atlas.publications@cern.ch

decays and the overwhelming multi-jet background. SM processes that can lead to a LJ signature include the production of light vector mesons and off-shell photons. Due to the high cross-section of these background processes, the analysis is restricted to events where two LJs are reconstructed.

Two minimal signal models where dark photons can be pair-produced are the Hidden Abelian Higgs Model (HAHM) [4] and the Falkowski–Ruderman–Volansky–Zupan (FRVZ) model [9,10]. The former allows the Higgs boson decay into a pair of γ_d , mainly via the diagram shown in Fig. 1a, while the latter includes additional dark-sector fermions coupled to the γ_d . The two dark-sector fermions (f_d) are produced by the Higgs boson decay, and they subsequently decay into a γ_d and a hidden lightest stable particle (HLSP), as shown by the diagram in Fig. 1b. More complex scenarios where multiple pairs of γ_d are produced are not considered in this paper, but the definition of the LJ and the selection implemented in the analysis are designed to allow the interpretation of models with richer phenomenology.

Related searches targeting multiple production of γ_d via the identification of LJs were conducted by the ATLAS Collaboration on the Run 1 pp collisions data at $\sqrt{s} = 8$ TeV [11–13]. Two recent results by ATLAS [14,15] have investigated the production of long-lived dark photons using $\sqrt{s} = 13$ TeV data, with masses in the $\mathcal{O}(10\text{ MeV})$ – $\mathcal{O}(10\text{ GeV})$ range, probing the HAHM and FRVZ models and relying on the identification of LJs from displaced γ_d decays (referred to as ‘Dark-Photon-Jets’ in the papers). Other ATLAS searches targeted the scenario of dark photons with masses above $\mathcal{O}(1\text{ GeV})$ produced by Higgs boson decays, identifying resolved prompt [16] or displaced [17] decays of the γ_d . Similar searches were performed by the CMS Collaboration for prompt [18–21] and long-lived [22,23] dark photon production. Other searches conducted by the LHCb [24,25], CMS [26] and FASER [27] Collaborations do not require the H -mediated production of dark photons, but assume kinetic mixing for both dark photon production and decay. These results target dark photon decays into muons and hence probe the mass regime $m_{\gamma_d} > 2m_\mu$. Several constraints on sub-GeV dark photons are set, without assuming the production from Higgs boson decays, by beam-dump and fixed-target experiments [28–38], by measurements of the anomalous magnetic moment of electrons and muons [39–41] and by astrophysical observations [42,43]. Experiments at e^+e^- colliders [44–56] also constrain the production of dark photons with masses smaller than $\mathcal{O}(10\text{ GeV})$.

This paper significantly improves the previous Run 1 result [13] thanks to a novel event selection, optimised considering multiple γ_d mass scenarios, to a new background estimate based on a bump-hunt strategy, and to the larger integrated luminosity and increased Higgs boson production cross section at $\sqrt{s} = 13$ TeV. The HAHM model, not considered by the previous search, is also constrained for the first

time using prompt LJs, probing a complementary m_{γ_d} range with respect to that probed by Ref. [16].

2 ATLAS detector

The ATLAS detector [57] at the LHC covers nearly the entire solid angle around the collision point.¹ It consists of an inner tracking detector surrounded by a thin superconducting solenoid, electromagnetic and hadronic calorimeters, and a muon spectrometer incorporating three large superconducting air-core toroidal magnets with eight coils each.

The inner-detector system (ID) is immersed in a 2 T axial magnetic field and provides charged-particle tracking in the range $|\eta| < 2.5$. The high-granularity silicon pixel detector covers the vertex region and typically provides four measurements per track, the first hit generally being in the insertable B-layer (IBL) installed before Run 2 [58,59]. It is followed by the SemiConductor Tracker (SCT), which usually provides eight measurements per track. These silicon detectors are complemented by the transition radiation tracker (TRT), which enables radially extended track reconstruction up to $|\eta| = 2.0$. The TRT also provides electron identification information based on the fraction of hits (typically 30 in total) above a higher energy-deposit threshold corresponding to transition radiation.

The calorimeter system covers the pseudorapidity range $|\eta| < 4.9$. Within the region $|\eta| < 3.2$, electromagnetic calorimetry is provided by barrel and endcap high-granularity lead/liquid-argon (LAr) calorimeters, with an additional thin LAr presampler covering $|\eta| < 1.8$ to correct for energy loss in material upstream of the calorimeters. Hadronic calorimetry is provided by the steel/scintillator-tile calorimeter, segmented into three barrel structures within $|\eta| < 1.7$, and two copper/LAr hadronic endcap calorimeters. The solid angle coverage is completed with forward copper/LAr and tungsten/LAr calorimeter modules optimised for electromagnetic (EM) and hadronic energy measurements respectively.

The muon spectrometer (MS) comprises separate trigger and high-precision tracking chambers measuring the deflection of muons in a magnetic field generated by the superconducting air-core toroidal magnets. The field integral of the toroids ranges between 2.0 and 6.0 T m across most of

¹ ATLAS uses a right-handed coordinate system with its origin at the nominal interaction point (IP) in the centre of the detector and the z -axis along the beam pipe. The x -axis points from the IP to the centre of the LHC ring, and the y -axis points upwards. Polar coordinates (r, ϕ) are used in the transverse plane, ϕ being the azimuthal angle around the z -axis. The pseudorapidity is defined in terms of the polar angle θ as $\eta = -\ln \tan(\theta/2)$ and is equal to the rapidity $y = \frac{1}{2} \ln \left(\frac{E+p_z c}{E-p_z c} \right)$ in the relativistic limit. Angular distance is measured in units of $\Delta R \equiv \sqrt{(\Delta y)^2 + (\Delta \phi)^2}$.

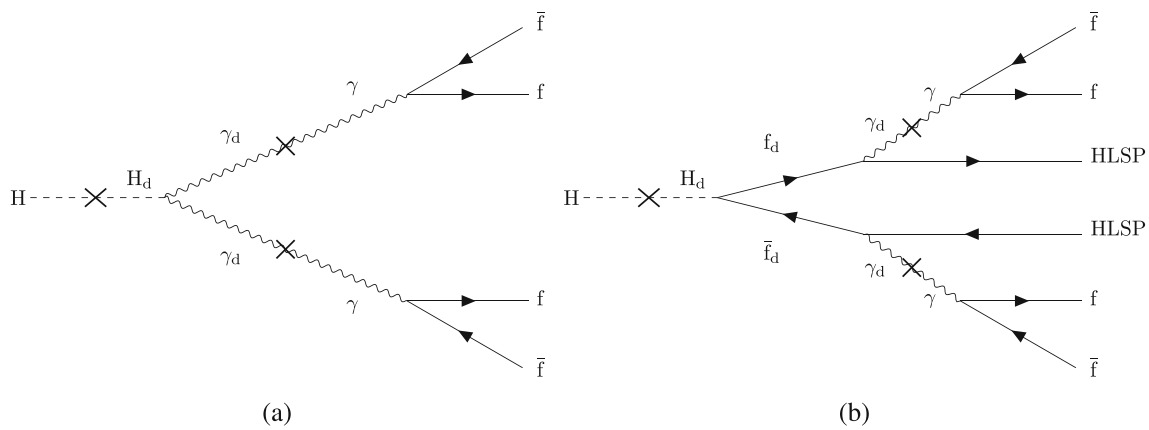


Fig. 1 Representative diagrams for the Higgs boson decay in the (a) HAHM and (b) FRVZ models. In the HAHM model, dark photons (γ_d) are produced from the decay of the Higgs boson, while in the FRVZ

model, the Higgs boson decays in a pair of hidden fermions (f_d), both decaying into a dark photon and a stable hidden fermion (HLSP)

the detector. Three layers of precision chambers, each consisting of layers of monitored drift tubes, cover the region $|\eta| < 2.7$, complemented by cathode-strip chambers in the forward region, where the background is highest. The muon trigger system covers the range $|\eta| < 2.4$ with resistive-plate chambers in the barrel, and thin-gap chambers in the endcap regions.

The luminosity is measured mainly by the LUCID-2 [60] detector that records Cherenkov light produced in the quartz windows of photomultipliers located close to the beampipe.

Events are selected by the first-level trigger system implemented in custom hardware, followed by selections made by algorithms implemented in software in the high-level trigger [61]. The first-level trigger accepts events from the 40 MHz bunch crossings at a rate below 100 kHz, which the high-level trigger further reduces in order to record complete events to disk at about 1 kHz.

A software suite [62] is used in data simulation, in the reconstruction and analysis of real and simulated data, in detector operations, and in the trigger and data acquisition systems of the experiment.

3 Data and simulated event samples

Data are collected by the ATLAS detector during Run 2 of the LHC (2015–2018) at $\sqrt{s} = 13$ TeV and correspond to an integrated luminosity of 140 fb^{-1} . The highest peak instantaneous luminosity reached $2.1 \times 10^{34} \text{ cm}^{-2} \text{ s}^{-1}$, with an average number of inelastic interactions per bunch crossing ranging from 13.4 to 37.8, depending on the data-taking year. These are collected using a set of triggers that require the presence of electrons [63] or muons [64] with thresholds in the transverse energy for electrons and the transverse

momentum (p_T) for muons that are in the range of 6–26 GeV, depending on the lepton flavour, the number of leptons and the data-taking period [65]. Stringent data quality requirements [66] are applied, ensuring the optimal operation of all sub-detectors and stable-collision mode of the LHC beams.

Simulated Monte Carlo (MC) event samples are used to optimise the analysis selections and characterise the signal and backgrounds. The signal samples consist of events where dark photons are produced, according to the HAHM and FRVZ models, via the decay of the SM Higgs boson with mass set to 125 GeV and considering only the dominant gluon–gluon fusion production mechanism. Several samples with different γ_d masses were generated, varying from 17 MeV to 20 GeV. For the HAHM model, dark photon masses were set to 17, 100, 400, 2000, 10,000 and 20,000 MeV, while for the FRVZ model the generated samples include dark photon masses of 17, 30, 60, 100, 240, 400, 900, 2000, 6000, 10,000 MeV. The decays of the Higgs boson into dark photons through dark fermions or directly into two dark photons were simulated at the matrix-element level during the generation. The branching ratios of the dark photon decay into leptons were enhanced during event generation and the events are weighted in order to match the expected decay branching ratios of a virtual SM photon. In the FRVZ model, the mass of f_d was chosen to be small relative to the Higgs boson mass, and far from the kinematic threshold at $m_{f_d} = m_{\text{HLSP}} + m_{\gamma_d}$. The values of the dark fermions masses have a negligible impact on the analysis results. In the HAHM, the Higgs boson can decay directly into a pair of dark photons leading to more boosted final states. Simulated signal events were generated with MADGRAPH5_AMC@NLO 2.2.3 [67] interfaced to PYTHIA 8.186 [68] for the parton showering and hadronisation. The matrix-element calculation was performed at tree level and

the parton distribution function (PDF) set used for the generation was NNPDF2.3LO [69]. Signal samples were normalised to a total cross-section of 48.61 pb [70, 71], using dedicated cross-sections calculations at NNLO in QCD and including electroweak corrections at NLO.

Simulated SM background samples were generated in order to optimise the event selection and include Z boson production in association with jets (Z +jets) and top-quark pair production ($t\bar{t}$). The production of Z +jets was simulated with the SHERPA 2.2.1 [72] generator using NLO matrix elements for up to two partons, and leading-order (LO) matrix elements for up to four partons calculated with the COMIX [73] and OPENLOOPS [74–76] libraries. They were matched with the SHERPA parton shower [77] using the MEPS@NLO prescription [78–81] using the set of tuned parameters developed by the SHERPA authors. The NNPDF3.0NNLO set of PDFs [82] was used and the samples were normalised to a NNLO prediction [83]. The production of $t\bar{t}$ events was modelled using the POWHEG BOX v2 [84–87] generator at NLO with the NNPDF3.0NLO PDF set [82] and the h_{damp} parameter set to 1.5 times the mass of the top quark [88]. The events were interfaced to PYTHIA 8.230 [89] to model the parton shower, hadronisation, and underlying event, with parameters set according to the A14 tune [90] and using the NNPDF2.3LO PDF set. The decays of bottom and charm hadrons were performed by EVTGEN 1.6.0 [91].

All MC simulated events were processed through a full simulation of the ATLAS detector geometry and detector response [92] using the GEANT4 [93] toolkit. This simulation accounts for multiple pp interactions per bunch crossing (pile-up), as well as the detector response to interactions in bunch crossings before and after the one producing the hard interaction. The multiple pp interactions were included using simulated events generated with PYTHIA 8.186 [68] using the NNPDF2.3LO PDF set and the A3 minimum-bias tune [94]. Simulated events are weighted to reproduce the distribution of the average number of interactions per bunch crossing observed in data.

4 Event reconstruction

The presence of at least one collision vertex, reconstructed from at least two ID tracks with $p_{\text{T}} > 500$ MeV, is required for each event [95]. When multiple vertices satisfy this requirement, the one with the largest $\sum p_{\text{T}}^2$ is selected as the primary vertex of the event.

Electrons are identified by associating a cluster of energy deposits in the electromagnetic calorimeter to at least one track in the ID. Their p_{T} must be greater than 4.5 GeV and they must be found within $|\eta| < 2.47$, with the exclusion of the transition region between the barrel and endcap electromagnetic calorimeter, defined by $1.37 < |\eta| < 1.52$. Elec-

trons must also satisfy the *Medium* identification working point defined in Ref. [96]. In addition, for tracks associated to electrons the significance on the transverse impact parameter is required to be $|d_0| / \sigma_{d_0} < 5$ and the longitudinal impact parameter must be $|\Delta z_0 \sin \theta| < 0.5$ mm, where both impact parameters are computed with respect to the primary vertex. Track-based and calorimeter-based isolation are required according to the *Loose* criterion defined in Ref. [96]. Electromagnetic showers from light γ_{d} decaying in two electrons are often merged into a single cluster, which is then reconstructed as a single electron with two associated tracks. The impact of the isolation requirement, when two close-by electrons are identified as a single EM shower, is found to be negligible for electrons identified from simulated γ_{d} decays into electrons.

Muon tracks in the ID and the MS are used in a *Combined* muon fit [97]. For each muon, a minimum p_{T} of 3 GeV is required as well as $|\eta| < 2.5$ and the *Loose* identification working point [97] must be satisfied. Muon ID tracks are required to satisfy $|d_0| / \sigma_{d_0} < 3$ and $|\Delta z_0 \sin \theta| < 0.5$ mm. Muon isolation requirements are based on the presence of track-based or calorimeter-based energy contributions around a muon. Muons used for the definition of the regions where the background modelling is performed are required to satisfy the *PFlowLoose* isolation requirement with variable cone radius [97]. Such requirements are found to be inefficient when applied on muons originating from boosted $\gamma_{\text{d}} \rightarrow \mu\mu$ decays, due to the contribution of one muon to the isolation cone of the other. A custom isolation variable, defined without considering the contribution due to nearby muons found in a 0.4 cone, is applied to muons used in the LJ reconstruction, leading to an increase of up to 80% in the selection efficiency with respect to standard requirements.

Hadronic jets are reconstructed from clusters of energy deposits in the calorimeter [98] using the anti- k_t algorithm [99, 100], with a radius parameter $R = 0.4$. The energy calibration procedure described in Ref. [101] is also applied and the jets are required to have $p_{\text{T}} > 20$ GeV, $|\eta| < 2.5$ and they must satisfy the *Loose* selection defined in [102]. To suppress jets from pile-up interactions, jets with $p_{\text{T}} < 60$ GeV, $|\eta| < 2.5$ are required to satisfy a selection on a multivariate jet vertex tagger [103] based on tracking information.

In order to avoid double-counting of objects, electrons sharing an ID track with muons are removed. Reconstructed jets are discarded if they are found within a $\Delta R = 0.2$ cone around a lepton (and only if they have less than three ID tracks in case of muons). Remaining jets are retained against leptons if they satisfy $\Delta R < \min(0.4, 0.04 + 10 \text{ GeV} / p_{\text{T}}^{\ell})$, where p_{T}^{ℓ} is the p_{T} of the lepton.

LJs are identified from collimated muons or electrons originating from the decay of light γ_{d} . Two exclusive types of LJs are identified: *muon LJs* (μ LJs) or *electron LJs*

(e LJs). Cambridge–Aachen clustering [104] is adopted, starting from the first lepton in the collection ordered by p_T and adding the same-flavour ones found within a $\Delta R = 0.4$ cone around the initial one. For each lepton added to the LJ, the momentum axis is recomputed as the vector sum of the four-momentum of each constituent. The procedure is repeated until no other particle can be added and until no other LJ can be reconstructed. If a different-flavour lepton is found within the cone of a given LJ, such LJ is discarded, in order to ensure orthogonality between the two types. The LJ definition is inclusive in the number of leptons to allow the interpretation of the analysis in the context of more complex models, as mentioned in Sect. 1. LJs are expected to be reconstructed with all the electrons or muons originating from the decay of a neutral particle, hence the sum of the charges of the LJ components (muons in case of μ LJs and the associated ID tracks in case of e LJs) is required to be zero.

Muon LJs contain at least two muons and target the signature where one or more γ_d decay into muons. Electron LJs are required to contain at least one electron and at least two ID tracks associated to electrons, to accommodate for the scenarios in which the electrons from the γ_d decay are identified as two resolved objects, as well as the one in which the EM showers from the two electrons are merged and identified as a single electron with two associated tracks. In addition, only e LJs with $|\eta| < 1.37$, for which the leading track has a $p_T > 5$ GeV, are retained for the selection.

The mass of a LJ is defined as the invariant mass of its components: for μ LJs this corresponds to the invariant mass of the muon constituents while, for e LJs, the definition depends on the number of electron objects that are clustered. For an e LJ reconstructed from two or more electrons, its mass is taken as the invariant mass of the system of electrons. On the other hand, for an e LJ containing two ID tracks associated to one electron, the invariant mass is computed by using the associated ID tracks. This definition was found to be optimal in order to correctly reconstruct the mass of the γ_d in simulated signal events. Since this search targets the pair-production of two particles decaying into electron/muon pairs, it is also expected that the masses of the two LJs that are reconstructed are similar, hence the absolute value of the ratio between the difference and the sum of the masses of the LJs (hereafter referred to as ‘mass imbalance’), is used when defining the analysis regions.

Two additional variables are defined exclusively for e LJs. The imbalance in p_T (p_T^{imb}) is defined as the absolute value of the ratio between the difference and the sum of the p_T of the ID tracks associated to an e LJ. If more than two tracks are associated to an e LJ, the p_T^{imb} is computed by considering the two leading tracks in p_T with opposite charge. The p_T^{imb} is expected to be smaller for e LJ originating from resonance decays, with respect to e LJs formed from prompt electrons matched to additional ID tracks. On the other hand, the shape

of a merged EM shower originating from two close-by electrons is expected to be wider in ϕ for an e LJ originating from a γ_d decay, compared to that of a prompt electron matched to an additional track. Hence, the ratio between the energy of the EM shower, in the cells around the most energetic energy cluster measured in a $(\eta \times \phi) = 3 \times 3$ region and the one measured 3×7 region (hereafter referred to as R_ϕ) is used when defining the signal region (SR).

The presence of at least two LJs is required in each event and the event selection is performed on the leading LJ in p_T and the LJ with largest $\Delta\phi$ from the leading LJ (denoted farthest LJ). The event selection continues with two analysis channels, which are defined depending on the type of the leading and farthest LJs. The *muon channel* includes events where at least one μ LJ is found and is described in Sect. 5, while the *electron channel* includes events where both LJs are of the electron type and is described in Sect. 6. Events with a single reconstructed LJ are not considered as the constraints they provide are not competitive due to the large background yields.

5 Event selection and background estimation in the muon channel

Events with at least one reconstructed μ LJ are required to satisfy single-lepton or multi-lepton (dilepton and trilepton) triggers, including triggers based on mixed lepton flavour. Offline leptons used in the LJ reconstruction are required to be found within a $\Delta R = 0.2$ cone around the trigger seed and, in the case of multi-lepton triggers, the leptons matching the online objects must belong to two different LJs. Moreover, a selection on the p_T , identification and isolation of the leptons matching the trigger is applied, tighter than the requirements applied online, to be on the trigger efficiency plateau [63, 64]. In order to avoid overlaps between events selected with the di-muon and the tri-muon triggers, the latter ones are utilised only for events outside the fiducial region of the di-muon triggers.

Two orthogonal regions are defined, based on the LJ multiplicity: events with at least two reconstructed μ LJs and no e LJs, the μ LJ– μ LJ region, and events where a μ LJ and an e LJ are reconstructed, the μ LJ– e LJ region. While no further requirement is applied in the μ LJ– μ LJ region, the μ LJ– e LJ region requires $p_T^{\text{imb}} < 0.8$ for e LJ and that the two LJs are back-to-back, with a minimum separation in the azimuthal angle of at least two radians, in order to improve the purity of the selection. The requirements are summarised in Table 1.

The final result of the search in the μ LJs regions is obtained by fitting the invariant mass of the μ LJ. In the μ LJ– μ LJ region, there are two entries per event, corresponding to the invariant masses of both μ LJs. In the μ LJ– e LJ region, only the μ LJ invariant mass is utilised, as the overlapping

Table 1 Definition of the muon signal regions. In signal regions requiring events with at least two LJs, only the leading LJ and the farthest LJ are considered for the event classification

Requirement/region	$\mu\text{LJ}-\mu\text{LJ}$	$\mu\text{LJ}-e\text{LJ}$
Number of μLJs	≥ 2	≥ 1
Number of $e\text{LJs}$	0	≥ 1
Muon triggers	Yes	Yes
Electron-muon triggers	–	Yes
Electron triggers	–	Yes
$e\text{LJ } p_{\text{T}}^{\text{imb}}$	–	< 0.8
$\Delta\phi(\mu\text{LJ}, e\text{LJ})$	–	> 2

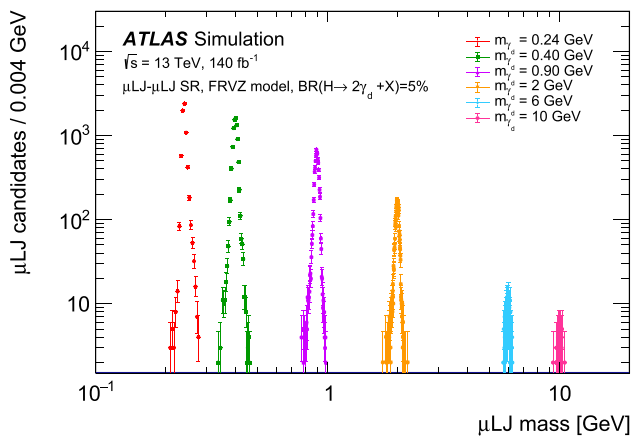


Fig. 2 Simulated distributions of the number of μLJ candidates for a selection of γ_d mass values. The shape and normalisation of the distributions are extracted from the parameterisation obtained for $\mu\text{LJ}-\mu\text{LJ}$ SR, using the FRVZ model and assuming a branching ratio of the Higgs boson decay to dark photons of 5%

electron showers in the calorimeter prevented a well-defined $e\text{LJ}$ mass reconstruction. The SM background affecting these search regions is characterised by a non-resonant component due to the production of muon pairs from virtual photons decays, plus a resonant component due to the pair-production of low-mass resonances, such as the J/ψ meson, decaying into muons. For the signal, the μLJ mass distribution is modelled using a parametric function, with parameters interpolated to include signal masses for which MC simulation is not available. A double-sided Crystal Ball function [105] is found to be an excellent choice for modelling the shape of the signal invariant mass distribution.

Examples of simulated distributions of the number of μLJ candidates within the mass range used for this region are shown in Fig. 2. The μLJ invariant mass resolution ranges from 10 to 300 MeV in the investigated mass range.

The background distribution corresponds to a smooth falling spectrum and vector meson resonances. This enables the background estimate to be performed using a data-driven method, in which the continuum shape is parameterised by an

analytical function derived from two control regions (CRs). The CRs are obtained by selecting events with one reconstructed μLJ , no reconstructed $e\text{LJs}$, and two additional pairs of muons or electrons separated by $\Delta R \geq 1.8$, which are not used for the reconstruction of LJs. The μLJ distribution is then used to characterise the modelling of the μLJ distribution in the SR. The CR built from one μLJ and two muons is used to characterise the modelling of the $\mu\text{LJ}-\mu\text{LJ}$ search region, while for the $\mu\text{LJ}-e\text{LJ}$ region the CR built from one μLJ and two additional electrons is used. These additional leptons must fulfil the same requirements as the μLJ or $e\text{LJ}$ constituents, ensuring that the CR closely resembles the SR. In order to minimise any signal contamination in the CRs, a requirement on the mass imbalance of the μLJ and the di-muon system, or the μLJ and di-electron system is applied, requiring it to be greater than 0.2, or 0.6, respectively.

The parametric form of the μLJ distribution for the background has two components: a double exponential function to describe the bulk non-resonant distributions, and Gaussian probability functions to capture the $\phi(1020)$, J/ψ , and $\psi(2S)$ resonances. It is parameterised as follows:

$$\begin{aligned}
 B(m_{\mu\text{LJ}}) = & N_{\text{exp1}} e^{-m_{\mu\text{LJ}}/\tau_2} + N_{\text{exp2}} e^{-m_{\mu\text{LJ}}/\tau_1} \\
 & + N_{J/\psi} e^{-\left(\frac{m_{\mu\text{LJ}} - \mu_{J/\psi}}{\sigma_{J/\psi}}\right)^2} + N_{\psi(2S)} e^{-\left(\frac{m_{\mu\text{LJ}} - \mu_{\psi(2S)}}{\sigma_{\psi(2S)}}\right)^2} \\
 & + N_{\phi} e^{-\left(\frac{m_{\mu\text{LJ}} - \mu_{\phi}}{\sigma_{\phi}}\right)^2}, \quad (1)
 \end{aligned}$$

where N_i , with $i = \text{exp1}, \text{exp2}, \phi, J/\psi, \psi(2S)$, are the normalisation factors associated to the i -th SM background process relative to the total amount of events; τ_1 and τ_2 are the parameters of the two exponential distributions. The parameters μ_{res} with $\text{res} = \phi, J/\psi, \psi(2S)$ are fixed and set to 1.02, 3.097 and 3.69 GeV, respectively [8]. The parameters σ_{res} , with $\text{res} = \phi, J/\psi, \psi(2S)$ are fixed to the fitted values in the CR. This functional form is chosen for its ability to accurately model the background shape in several control regions.

The bias from the functional form choice is evaluated by fitting signal and background contributions to data templates in signal-free regions. This *spurious signal* estimate helps gauge biases inherent in the method [106]. Various templates are created using data or simulation in the control region, and used as probability distribution functions to generate expected distributions in the SR. The extracted values of the signal yields for each γ_d mass assumption define an envelope approximating the method's bias, which is included as a systematic uncertainty in the final fit.

Post-fit μLJ mass distributions in the $\mu\text{LJ}-\mu\text{LJ}$ and $\mu\text{LJ}-e\text{LJ}$ signal regions are shown in Fig. 3. In this figure, a representative γ_d signal with a mass of 1 GeV is shown, assuming a branching ratio of $H \rightarrow 2\gamma_d$ of 0.5%.

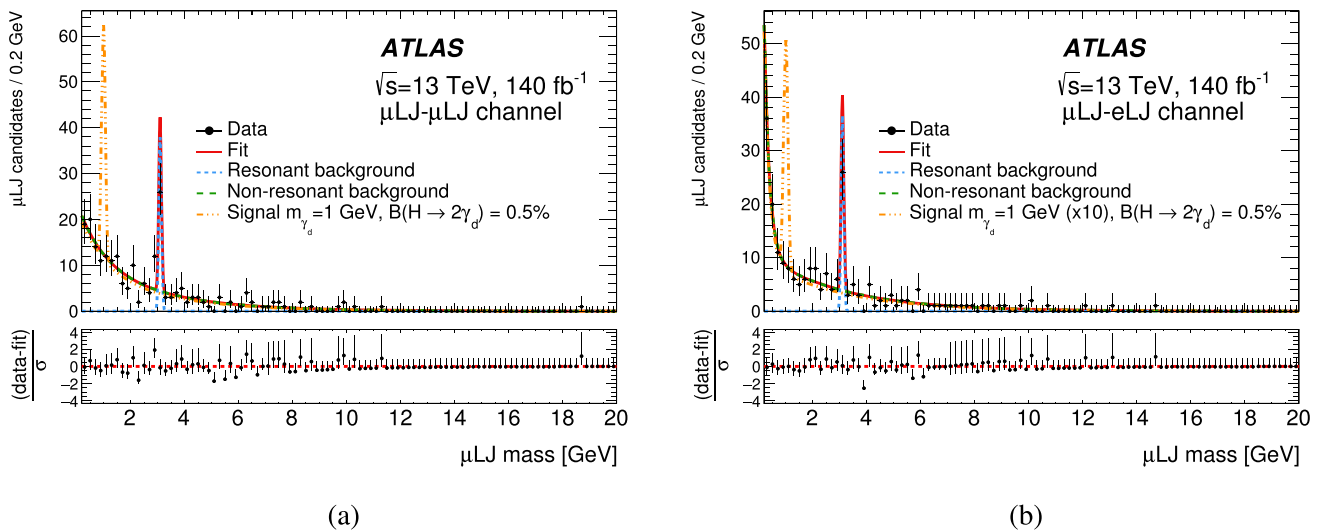


Fig. 3 The background-only fit (solid red line) with its background (dashed blue and green lines) and signal (dot-dashed orange line) components of the μ LJ mass distributions for the (a) μ LJ- μ LJ and (b) e LJ- μ LJ regions. For the μ LJ- μ LJ region, both the μ LJs are included.

6 Event selection and background estimation in the electron channel

Events with two e LJs are selected by the logical or of single and di-electron triggers. As mentioned in Sect. 5, the electrons used for the e LJ reconstruction are required to be within a $\Delta R = 0.2$ cone around the trigger seed. Additional requirements on their p_T , identification and isolation are also applied, with tighter requirements than those applied online. In events selected by di-electron trigger, the two online electrons are required to match the two different e LJs.

This analysis channel is optimised for the scenarios where the mass of the dark photon is smaller than the mass of a muon pair. To improve the sensitivity in this mass range, all the e LJ candidates are required to be formed by two electrons with merged EM clusters. In addition, the LJs are required to be back-to-back, with a minimum separation in the azimuthal angle of at least 2.5 radians. Events are retained only if the mass imbalance of the two e LJs is below 0.8.

The main background is composed by the random overlap of prompt electrons, produced in Z boson decays or $t\bar{t}$ events, with additional ID tracks. In order to reduce the contribution of $t\bar{t}$ processes, selected events are rejected if at least one hadronic jet with $p_T > 40$ GeV is present. Moreover, to remove events where one Z boson decays into two electrons, the invariant mass of the system of the two e LJs ($m(eLJ, eLJ)$) must be outside of the interval between 80 and 100 GeV. The SR is finally defined by requiring p_T^{imb} to be smaller than 0.8 for the leading e LJ, while R_ϕ has to be

smaller than 0.96 for the farthest e LJ. The distributions of these two variables are shown in Fig. 4.

After these selections, the residual background is estimated directly from data using the so-called *ABCD* method. The overlapping electron showers in the calorimeter for the low-mass range considered in this region prevent a well-defined e LJ mass reconstruction and the use of the bump-hunting method, as in the muon channel. In the plane defined by the p_T^{imb} and R_ϕ variables, the four regions A, B, C and D, are identified: region A corresponds to the SR, while regions B, C, D correspond to three CRs defined by reversing the selection on R_ϕ , p_T^{imb} , and both the variables, respectively.

The requirements on the p_T^{imb} and R_ϕ adopted in the definition of the SR are determined as the one that maximise the signal-to-background sensitivity, while minimising the signal contamination in regions B, C and D. These variables are considered uncorrelated when p_T^{imb} is considered for the leading e LJ and R_ϕ for the sub-leading e LJ, with R_ϕ being a calorimeter-based variable and p_T^{imb} being track-based.

The number of background events in the SR (N_A) can be estimated by $N_A = (N_B \times N_C)/N_D$, where N_i with $i = B, C, D$ is the number of observed data events in the three CRs. This relation is extended using a likelihood-based method analogous to the one used in Ref. [15], which fits the number of background and signal events simultaneously, taking into account any potential signal contamination in the CRs.

This method for the background estimate is validated in regions where the signal contribution is expected to be small. A first set of validation regions (VRs) is defined by combin-

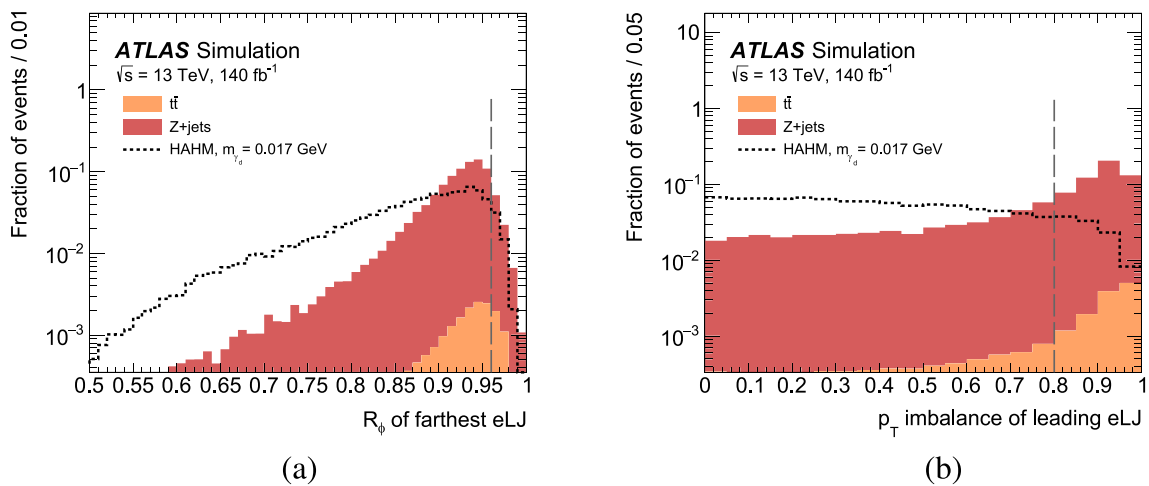


Fig. 4 Distribution of the (a) $eLJ R_\phi$ and (b) $eLJ p_T$ imbalance, obtained for signal events generated with the HAHM model with a γ_d mass set to 17 MeV and for simulated background events. Events are selected from the electron channel, with only the trigger require-

ment applied. Signal and background distributions are normalised to unit area. The dashed grey line corresponds to the selection applied in the definition of the SR

ing CRs C and D, and CRs B and D, while another region (VR_Z) is defined by reversing the selection on the invariant mass of the two eLJ s in the event, hence targeting pairs of LJ s originating in $Z \rightarrow e^+e^-$ events. The Pearson linear correlation coefficient between the two variables defining the ABCD plane in all control and validation regions was observed to be below 2%. The signal leakage in these regions was found to be less than 10% of the total signal in the ABCD plane for all signal scenarios considered in the analysis.

The definitions of the SR A, CRs B, C and D, as well as the VR_Z are summarised in Table 2.

For each VR, alternative A, B, C, D regions are defined by dividing the plane in increasing steps of p_T^{imb} and R_ϕ , in order to assert the reliability of the method in each of these regions. In all the tested regions, the observed number of events is found to be in agreement with the expected value within one standard deviation.

Figure 5 shows the distribution of events in the ABCD planes, for observed data and events simulated with the HAHM model assuming a mass of the γ_d of 17 MeV and a decay branching ratio of the Higgs boson to dark sector particles of 0.5%. The number of observed data events in the eLJ ABCD plane is reported in Table 3, where the yields in SR A are extracted by a background-only fit performed on data in all ABCD regions.

7 Systematic uncertainties

The overall uncertainty in the SRs yields is dominated by the background statistical uncertainty. For the electron channel, the uncertainty in the observed yields in the ABCD con-

trol regions are propagated to the SR expectation obtained from the ABCD method, amounting to 5%. Other potential sources of experimental uncertainties are considered for the background estimates and the simulated signal yields.

The following experimental uncertainties are taken into account in the signal distributions for the μLJ , eLJ , and μLJ – eLJ channels, as well as in the background estimations. All systematic uncertainties are incorporated into the fits using nuisance parameters, which are constrained by Gaussian terms in the likelihood function.

The background parameterisation in the muon channels is data-driven and extracted from the fit in the control region, thus only systematic uncertainties related to the background modelling and the fit are considered. The bias from the choice of the background model is evaluated with the spurious signal method, as discussed in Sect. 5. At most three spurious signal events are extracted across the full spectrum and this number is taken as an uncertainty on the signal yields independent of the assumed dark photon mass.

To account for potential biases in the signal model description, an injection test is performed to determine if the correct number of events can be extracted using a signal-plus-background fit. Pseudo-data generated from the background model with a known number of injected signal events is used and a fit is performed. The obtained value for signal yields is then compared with the injected value. The largest difference per mass point between the injected and fitted signal for each of the configurations is assigned as a systematic uncertainty, which ranges from 1% and up to 5% increasing with the mass of the dark photon.

The uncertainty in the integrated luminosity of the combined data samples from 2015 to 2018 is 0.83%, calculated

Table 2 Definition of the analysis regions of the electron channel

Requirement/region	SR	CR B	CR C	CR D	VR _Z
Applied to both leading and farthest eLJ					
Number of EM clusters in eLJ			1		
eLJ mass imbalance			< 0.8		
Selection on event-level variables					
$\Delta\phi(eLJ, eLJ)$			> 2.5		
Number of jets ($p_T > 40$ GeV)			0		
$m(eLJ, eLJ) \notin [80, 100]$ GeV	Yes	Yes	Yes	Yes	Veto
Leading eLJ p_T^{imb}	< 0.8	< 0.8	> 0.8	> 0.8	–
Farthest eLJ R_ϕ	< 0.96	> 0.96	< 0.96	> 0.96	–

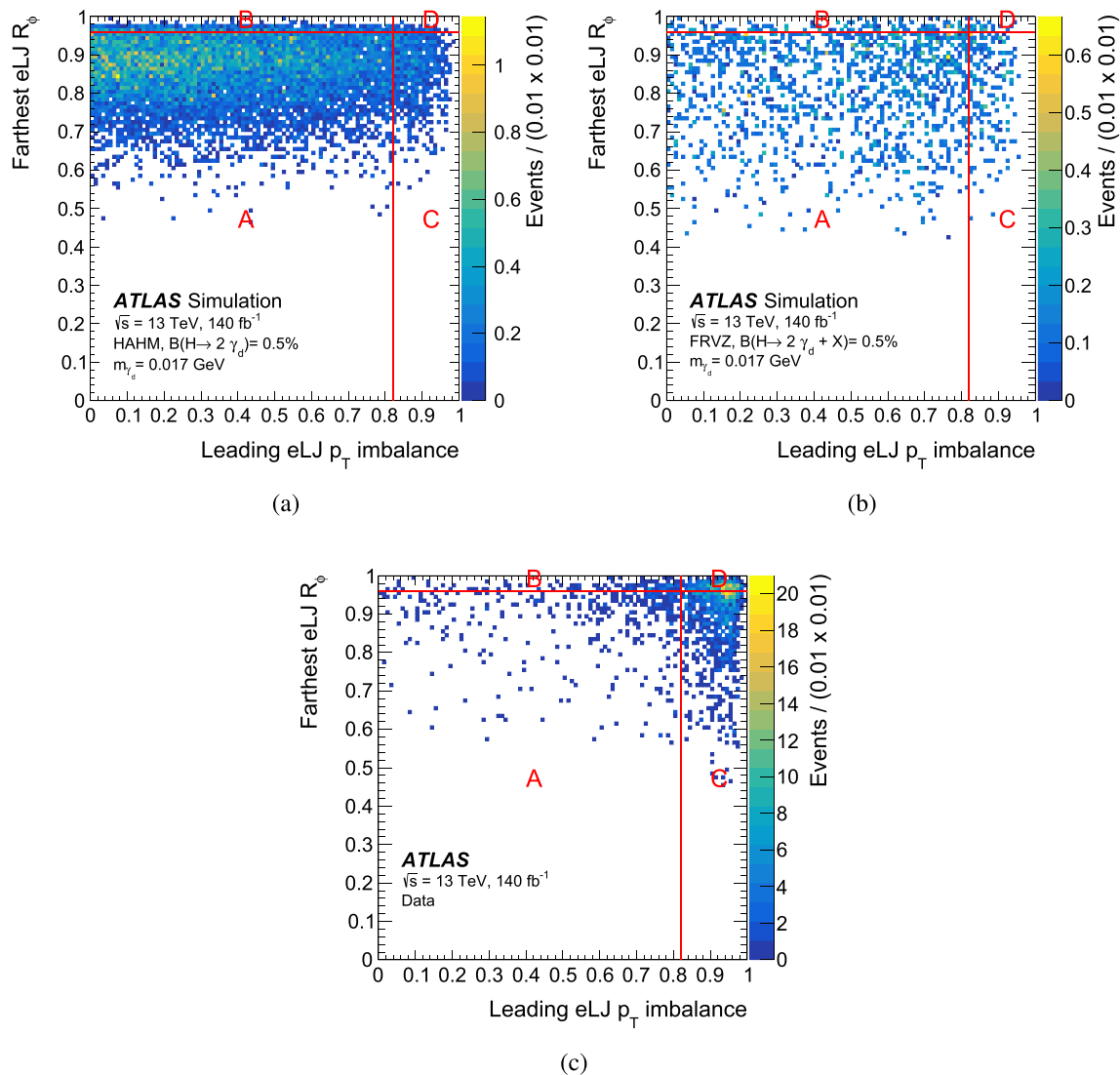


Fig. 5 Distribution of (a, b) expected signal and (c) observed data events in the ABCD regions defined by the leading eLJ p_T^{imb} and farthest eLJ R_ϕ variables in the electron channel. Signal events are simulated

according to the (a) HAHM and (b) FRVZ models, for a γ_d mass of 17 MeV and assuming a branching ratio of the Higgs boson decay to dark photons of 0.5%

Table 3 Observed data events in the four ABCD regions and the expected yields in the SR A were extracted with a background-only fit of the electron channel, assuming no signal. The a priori scenario

does not consider data yields in SR A, whereas the a posteriori scenario includes data in all ABCD regions in the fit. The expected number of events is reported together with its statistical uncertainty

Region	CR B	CR C	CR D	SR expected a priori	SR expected a posteriori	SR observed
$eLJ-eLJ$	125	862	356	303 ± 33	334 ± 17	351

using the methodology described in Ref. [107]. The uncertainty is determined using the LUCID-2 detector [60] for primary luminosity measurements, supplemented by measurements using the inner detector and calorimeters.

The pile-up modelling uncertainty that accounts for the difference between the simulated and measured inelastic pp cross-section [108] is evaluated with a data-to-MC reweighting method of the distribution of the average number of interactions per bunch crossing. This uncertainty is propagated through the event selection, and results in a less than 4% effect on the event yield of all the signal samples.

The experimental uncertainties are related to the lepton reconstruction, identification and isolation, and are evaluated using $Z \rightarrow \ell\ell$, $J/\Psi \rightarrow \ell\ell$ events in data and MC [96,97]. The dominant uncertainties arise from muon isolation and electron identification found to be less than 1% and 2% for μLJ and eLJ channels respectively. The impact of electron isolation, lepton momentum resolution and energy scale, and muon identification are found to be sub-dominant. No additional systematic uncertainty is considered due to the additional correction added on top of the standard isolation variables. The experimental uncertainties related to the jet energy resolution and jet energy scale, evaluated from the standard calibration scheme [101], amount to up to 3% of the expected signal yields. This uncertainty is relevant only for the $eLJ-eLJ$ channel where jets are used in the selection.

Uncertainty in the efficiency of trigger influence the expected yields and are estimated to be less than 2.2% across all signal samples. The estimates are based on studies of the detector performance using Run 2 data and changes to the MC simulation [63,64].

A summary of the experimental systematic uncertainties considered for the signal samples in this search is presented in Fig. 6. The average uncertainties represent the bulk of the signal samples, with minor variations, typically of a few percent, observed as a function of the γ_d mass.

8 Results and interpretations

The statistical analysis of the muon channel uses an unbinned maximum-likelihood fit of the μLJ mass distribution. The search is conducted in the γ_d mass range between twice the muon mass and 20 GeV for the HAHM model, while this range is limited up to 10 GeV for the FRVZ model. The fit

is performed with a step size of 10 MeV, smaller than the invariant mass resolution of the reconstructed LJ. Instead, the electron channel uses a binned maximum-likelihood fit to the signal region (A) and the three control regions (B, C and D), describing the ABCD constraint and taking into account any possible signal contamination in the control regions. For the electron channel, limits are computed for the γ_d masses available from signal simulated samples (ranging from 0.017 GeV to 0.4 GeV), as no parameterisation of the signal model is performed.

No significant excesses are observed, thus expected and observed 95% confidence level (CL) exclusion limits on the cross-section times branching ratio of the process $H \rightarrow 2\gamma_d + X$ are computed as a function of the dark photon mass using the CL_s [109] modified frequentist approach. The exclusion limits are computed using the asymptotic approximation [110]. The validity of the asymptotic approximation is evaluated by comparing it with a full calculation using pseudo-experiments. The CL_s values from both methods agree within 2%, with the largest discrepancy being 10% in the high mass region. The 95% CL upper limits for the HAHM and FRVZ models are depicted in Fig. 7 for the muon and electron search channels. The muon channel sets limit for γ_d masses larger than twice the muon mass, while the electron channel covers the complementary region, down to the mass of the lightest signal sample available (0.017 GeV). The electron channel is not combined with the muon channel for γ_d masses above twice the muon mass, given the dominant sensitivity of the muon channel in this range. The upper limit is not extracted in regions where background resonances are present.

The search excludes a range of $H \rightarrow 2\gamma_d + X$ branching ratios from 0.001% to 5%, depending on the assumed dark photon mass, improving the previous search by ATLAS during Run 1 [13] by a factor of 50 when considering a dark photon with a mass of 400 MeV. This improvement is mainly due to the renewed background estimate based on the invariant mass shape fit. The muon channels are valid only for dark photon masses greater than twice the muon mass and complement the electron channel, which is covered only by ATLAS. In the FRVZ scenarios, limits are derived down to 17 MeV for the first time, significantly extending previous CMS and ATLAS searches for prompt LJs. In the HAHM scenarios, where the Higgs boson decays directly into a pair of dark photons, the sensitivity improves compared to the FRVZ

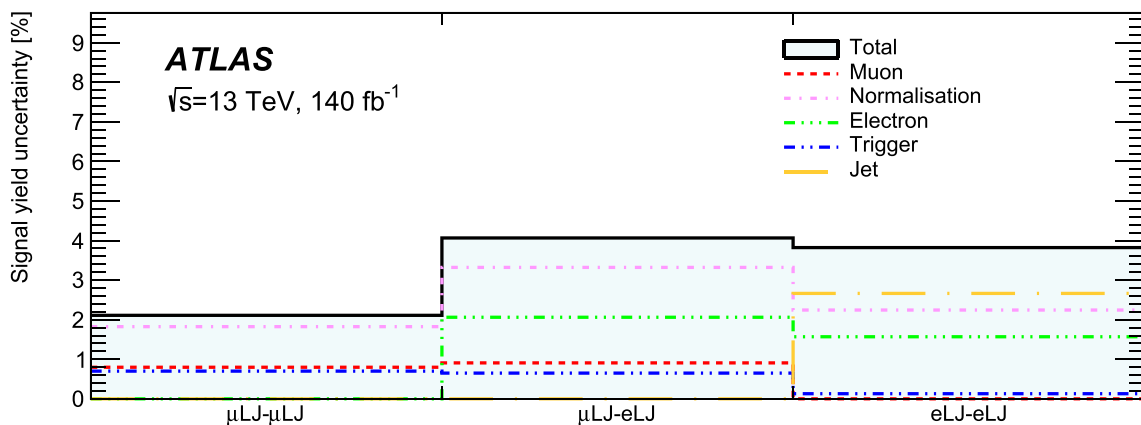
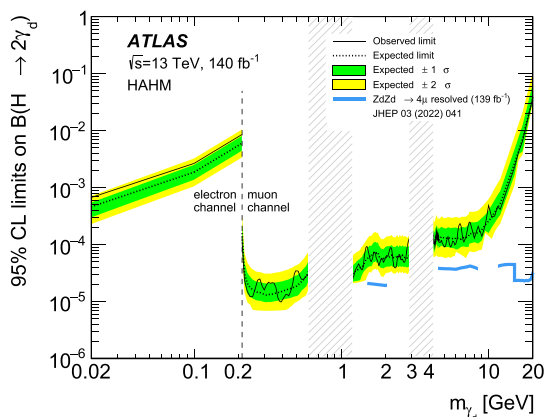
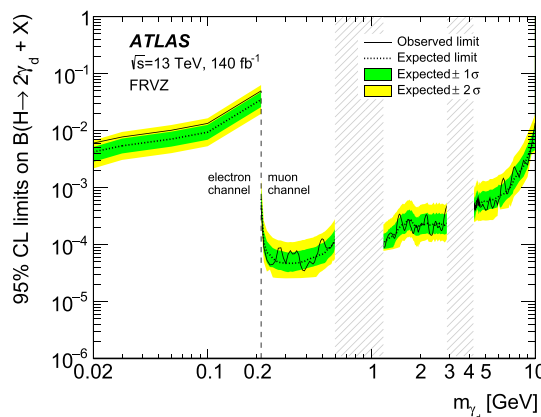


Fig. 6 Contributions from the different sources of uncertainty to the signal yields in the search channels over all simulated signal samples. The reported uncertainties are averaged over all signal MC. The ‘Muon’ and ‘Electron’ sources contain all lepton-related systematic uncertainties and are dominated by the uncertainty in the muon isolation and

electron identification. The ‘Triggers’ source contains all trigger systematic uncertainties. The ‘Jet’ source, relevant only for the electron channel, contains the jet energy scale and resolution uncertainties. The ‘Normalisation’ source contains all systematic uncertainties affecting the overall normalisation of the yields



(a)



(b)

Fig. 7 95% CL exclusion limits on the branching ratio of the Higgs boson to dark photons as a function of the γ_d mass for the (a) HAHM and (b) FRVZ models. The solid (dashed) black curve shows the observed (expected) exclusion limit and the green and yellow bands represent

$\pm 1\sigma$ and $\pm 2\sigma$ uncertainty intervals around the expected limit. The grey hatched regions indicate where the upper limit is not extracted. The figure also shows the exclusion limit from the ATLAS search for resolved prompt γ_d decays [16] (blue line)

model due to the harder dark photon energy spectrum. In the high-mass range, when the muons from the dark-photon decay have large angular separation, making lepton-jet reconstruction inefficient, the analysis steeply loses sensitivity. The result is complementary to the ATLAS search for four resolved prompt muons [16], which sets stronger limits at larger masses and remains competitive around $m_{\gamma_d} = 2$ GeV. These are the first results for this model in ATLAS with the prompt LJ signature.

Figure 8 presents the 90% CL upper limits as a function of the kinetic mixing parameter ϵ , which determines the lifetime of the dark photon, and γ_d mass in both the HAHM vector-portal and FRVZ models, showing exclusion contours

on the Higgs branching ratio to dark photons for branching fractions ranging from 0.01 to 10%. The limits are interpolated between different masses by branching fraction variations [111] as a function of the γ_d mass, corrected by a linear interpolation of the signal efficiency between adjacent available MC signal samples. Simple reweighting techniques [14] were applied to determine the analysis efficiency as a function of the lifetime for each mass point, using additional generated samples with varied lifetimes. Exclusion regions from the complementary ATLAS search for displaced dark-photon [14] are also shown (orange line).

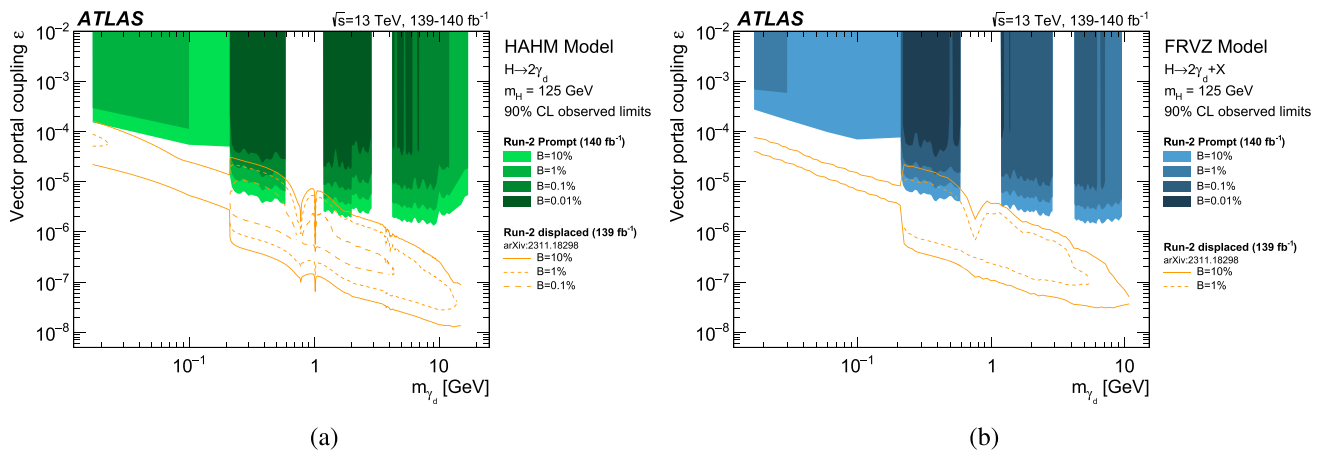


Fig. 8 90% CL exclusion limit contours on the branching ratio of the Higgs boson to dark photons as functions of the γ_d mass and kinetic mixing parameter ϵ for the (a) HAHM model and (b) FRVZ model. These exclusions assume Higgs boson branching fractions to dark pho-

tons within a 0.01% and 10% range. Excluded regions from the complementary ATLAS displaced dark-photon search [14] are displayed (orange lines) for comparison

9 Conclusion

This paper details the first Run 2 search for light neutral particles decaying into collimated pairs of muons or electrons with the ATLAS detector at the LHC. By analysing data corresponding to an integrated luminosity of 140 fb^{-1} of pp collisions at a centre-of-mass energy of 13 TeV, the study investigates dark photons from Higgs boson decays, with a mass between 17 MeV and 20 GeV, extending the range of the previous search. The data is consistent with background predictions and 95% confidence level upper limits are set on the branching ratio of the Higgs boson to dark photons, ranging from 0.004 and 5% for the FRVZ model and from 0.001 to 1% for the HAHM model, depending on the dark photon mass. Compared with the previous search conducted by ATLAS during Run 1, for the FRVZ model with a dark photon with a mass of 0.4 GeV, the upper limit on the branching ratio of the Higgs boson to dark photons is improved by approximately a factor of 50. When accounting for the contributions from the increased integrated luminosity and cross-section at a higher centre-of-mass energy, this results in an improvement by a factor of about 13. The sensitivity of the muon channel has improved due to resonance search approach adopted, compared to simple use of the total event counts in the Run 1 analysis. This is the first search for prompt Lepton-Jets in the electron channel using Run 2 data of the LHC and sets the most stringent limits to date. The limits are extended down to 17 MeV in dark photon mass, significantly improving previous CMS and ATLAS results for prompt Lepton-Jets.

Acknowledgements We thank CERN for the very successful operation of the LHC and its injectors, as well as the support staff at CERN and at our institutions worldwide without whom ATLAS could not be operated efficiently. The crucial computing support from all WLCG part-

ners is acknowledged gratefully, in particular from CERN, the ATLAS Tier-1 facilities at TRIUMF/SFU (Canada), NDGF (Denmark, Norway, Sweden), CC-IN2P3 (France), KIT/GridKA (Germany), INFN-CNAF (Italy), NL-T1 (Netherlands), PIC (Spain), RAL (UK) and BNL (USA), the Tier-2 facilities worldwide and large non-WLCG resource providers. Major contributors of computing resources are listed in Ref. [112]. We gratefully acknowledge the support of ANPCyT, Argentina; YerPhI, Armenia; ARC, Australia; BMWF and FWF, Austria; ANAS, Azerbaijan; CNPq and FAPESP, Brazil; NSERC, NRC and CFI, Canada; CERN; ANID, Chile; CAS, MOST and NSFC, China; Minciencias, Colombia; MEYS CR, Czech Republic; DNR and DNSRC, Denmark; IN2P3-CNRS and CEA-DRF/IRFU, France; SRNSFG, Georgia; BMBF, HGF and MPG, Germany; GSRI, Greece; RGC and Hong Kong SAR, China; ISF and Benozzi Center, Israel; INFN, Italy; MEXT and JSPS, Japan; CNRST, Morocco; NWO, Netherlands; RCN, Norway; MNiSW, Poland; FCT, Portugal; MNE/IFA, Romania; MSTDI, Serbia; MSSR, Slovakia; ARIS and MVZI, Slovenia; DSI/NRF, South Africa; MICIU/AEI, Spain; SRC and Wallenberg Foundation, Sweden; SERI, SNSF and Cantons of Bern and Geneva, Switzerland; NSTC, Taipei; TENMAK, Türkiye; STFC/UKRI, United Kingdom; DOE and NSF, United States of America. Individual groups and members have received support from BCKDF, CANARIE, CRC and DRAC, Canada; CERN-CZ, FORTE and PRIMUS, Czech Republic; COST, ERC, ERDF, Horizon 2020, ICSC-NextGenerationEU and Marie Skłodowska-Curie Actions, European Union; Investissements d’Avenir Labex, Investissements d’Avenir IDEX and ANR, France; DFG and AvH Foundation, Germany; Herakleitos, Thales and Aristeia programmes co-financed by EU-ESF and the Greek NSRF, Greece; BSF-NSF and MINERVA, Israel; NCN and NAWA, Poland; La Caixa Banking Foundation, CERCA Programme Generalitat de Catalunya and PROMETEO and GenT Programmes Generalitat Valenciana, Spain; Göran Gustafssons Stiftelse, Sweden; The Royal Society and Leverhulme Trust, United Kingdom. In addition, individual members wish to acknowledge support from Armenia: Yerevan Physics Institute (FAPERJ); CERN: European Organization for Nuclear Research (CERN PJAS); Chile: Agencia Nacional de Investigación y Desarrollo (FONDECYT 1230812, FONDECYT 1230987, FONDECYT 1240864); China: Chinese Ministry of Science and Technology (MOST-2023YFA1605700, MOST-2023YFA1609300), National Natural Science Foundation of China (NSFC - 12175119, NSFC 12275265, NSFC-12075060); Czech Republic: Czech Science Foun-

dation (GACR - 24-11373S), Ministry of Education Youth and Sports (FORTE CZ.02.01.01/00/22_008/0004632), PRIMUS Research Programme (PRIMUS/21/SCI/017); EU: H2020 European Research Council (ERC - 101002463); European Union: European Research Council (ERC - 948254, ERC 101089007), Horizon 2020 Framework Programme (MUCCA - CHIST-ERA-19-XAI-00), European Union, Future Artificial Intelligence Research (FAIR-NextGenerationEU PE00000013), Italian Center for High Performance Computing, Big Data and Quantum Computing (ICSC, NextGenerationEU); France: Agence Nationale de la Recherche (ANR-20-CE31-0013, ANR-21-CE31-0013, ANR-21-CE31-0022, ANR-22-EDIR-0002), Investissements d'Avenir Labex (ANR-11-LABX-0012); Germany: Baden-Württemberg Stiftung (BW Stiftung-Postdoc Eliteprogramme), Deutsche Forschungsgemeinschaft (DFG - 469666862, DFG - CR 312/5-2); Italy: Istituto Nazionale di Fisica Nucleare (ICSC, NextGenerationEU), Ministero dell'Università e della Ricerca (PRIN - 20223N7F8K - PNRR M4.C2.1.1); Japan: Japan Society for the Promotion of Science (JSPS KAKENHI JP22H01227, JSPS KAKENHI JP22H04944, JSPS KAKENHI JP22KK0227, JSPS KAKENHI JP23KK0245); Netherlands: Netherlands Organisation for Scientific Research (NWO Veni 2020 - VI.Veni.202.179); Norway: Research Council of Norway (RCN-314472); Poland: Ministry of Science and Higher Education (IDUB AGH, POB8, D4 no 9722), Polish National Agency for Academic Exchange (PPN/PPO/2020/1/00002/U/00001), Polish National Science Centre (NCN 2021/42/E/ST2/00350, NCN OPUS nr 2022/47/B/ST2/03059, NCN UMO-2019/34/E/ST2/00393, NCN & H2020 MSCA 945339, UMO-2020/37/B/ST2/01043, UMO-2021/40/C/ST2/00187, UMO-2022/47/O/ST2/00148, UMO-2023/49/B/ST2/04085, UMO-2023/51/B/ST2/00920); Slovenia: Slovenian Research Agency (ARIS grant J1-3010); Spain: Generalitat Valenciana (Artemisa, FEDER, IDIFEDER/2018/048), Ministry of Science and Innovation (MCIN & NextGenEU PCI2022-135018-2, MICIN & FEDER PID2021-125273NB, RYC2019-028510-I, RYC2020-030254-I, RYC2021-031273-I, RYC2022-038164-I), PROMETEO and GenT Programmes Generalitat Valenciana (CIDEGENT/2019/027); Sweden: Carl Trygger Foundation (Carl Trygger Foundation CTS 22:2312), Swedish Research Council (Swedish Research Council 2023-04654, VR 2018-00482, VR 2022-03845, VR 2022-04683, VR 2023-03403, VR grant 2021-03651), Knut and Alice Wallenberg Foundation (KAW 2018.0157, KAW 2018.0458, KAW 2019.0447, KAW 2022.0358); Switzerland: Swiss National Science Foundation (SNSF - PCEFP2_194658); United Kingdom: Leverhulme Trust (Leverhulme Trust RPG-2020-004), Royal Society (NIF-R1-231091); United States of America: U.S. Department of Energy (ECA DE-AC02-76SF00515), Neubauer Family Foundation.

Data Availability Statement This manuscript has no associated data. [Author's comment: Data sharing not applicable to this article as no datasets were generated or analysed during the current study.]

Code Availability Statement This manuscript has no associated code/software. [Author's comment: ATLAS collaboration software is open source, and all code necessary to recreate an analysis is publicly available. The Athena (<http://gitlab.cern.ch/atlas/athena>) software repository provides all code needed for calibration and uncertainty application, with configuration files that are also publicly available via Docker containers and cvmfs. The specific code and configurations written in support of this analysis are not public; however, these are internally preserved.]

Open Access This article is licensed under a Creative Commons Attribution 4.0 International License, which permits use, sharing, adaptation, distribution and reproduction in any medium or format, as long as you give appropriate credit to the original author(s) and the source, provide a link to the Creative Commons licence, and indicate if changes were made. The images or other third party material in this article are included in the article's Creative Commons licence, unless indi-

cated otherwise in a credit line to the material. If material is not included in the article's Creative Commons licence and your intended use is not permitted by statutory regulation or exceeds the permitted use, you will need to obtain permission directly from the copyright holder. To view a copy of this licence, visit <http://creativecommons.org/licenses/by/4.0/>.
Funded by SCOAP³.

References

1. N. Arkani-Hamed, N. Weiner, LHC signals for a super unified theory of dark matter. *JHEP* **12**, 104 (2008). <https://doi.org/10.1088/1126-6708/2008/12/104>. [arXiv:0810.0714](https://arxiv.org/abs/0810.0714) [hep-ph]
2. M. Baumgart, C. Cheung, J.T. Ruderman, L.-T. Wang, I. Yavin, Non-abelian dark sectors and their collider signatures. *JHEP* **04**, 014 (2009). <https://doi.org/10.1088/1126-6708/2009/04/014>. [arXiv:0901.0283](https://arxiv.org/abs/0901.0283) [hep-ph]
3. A. Falkowski, R. Vega-Morales, Exotic Higgs decays in the golden channel. *JHEP* **12**, 037 (2014). [https://doi.org/10.1007/JHEP12\(2014\)037](https://doi.org/10.1007/JHEP12(2014)037). [arXiv:1405.1095](https://arxiv.org/abs/1405.1095) [hep-ph]
4. D. Curtin, R. Essig, S. Gori, J. Shelton, Illuminating dark photons with high-energy colliders. *JHEP* **02**, 157 (2015). [https://doi.org/10.1007/JHEP02\(2015\)157](https://doi.org/10.1007/JHEP02(2015)157). [arXiv:1412.0018](https://arxiv.org/abs/1412.0018) [hep-ph]
5. S.A. Abel, M.D. Goodsell, J. Jaeckel, V.V. Khoze, A. Ringwald, Kinetic mixing of the photon with hidden U(1)s in string phenomenology. *JHEP* **07**, 124 (2008). <https://doi.org/10.1088/1126-6708/2008/07/124>. [arXiv:0803.1449](https://arxiv.org/abs/0803.1449) [hep-ph]
6. ATLAS Collaboration, A detailed map of Higgs boson interactions by the ATLAS experiment ten years after the discovery, *Nature* **607**, 52 (2022), <https://doi.org/10.1038/s41586-022-04893-w> [arXiv:2207.00092](https://arxiv.org/abs/2207.00092) [hep-ex], Erratum: *Nature* **612**, E24 (2022) <https://doi.org/10.1038/s41586-022-05581-5>
7. CMS Collaboration, A portrait of the Higgs boson by the CMS experiment ten years after the discovery, *Nature* **607**, 60 (2022). <https://doi.org/10.1038/s41586-022-04892-x> [arXiv:2207.00043](https://arxiv.org/abs/2207.00043) [hep-ex], Erratum: *Nature* **623**, E4 (2023). <https://doi.org/10.1038/s41586-023-06164-8>
8. Particle Data Group, P. Zyla et al., Review of particle physics. *Prog. Theor. Exp. Phys.* **2020**, 083C01 (2020). <https://doi.org/10.1093/ptep/ptaa104>
9. A. Falkowski, J.T. Ruderman, T. Volansky, J. Zupan, Hidden Higgs decaying to lepton jets. *JHEP* **05**, 077 (2010). [https://doi.org/10.1007/JHEP05\(2010\)077](https://doi.org/10.1007/JHEP05(2010)077). [arXiv:1002.2952](https://arxiv.org/abs/1002.2952) [hep-ph]
10. A. Falkowski, J.T. Ruderman, T. Volansky, J. Zupan, Discovering Higgs boson decays to lepton jets at hadron colliders. *Phys. Rev. Lett.* **105**, 241801 (2010). <https://doi.org/10.1103/PhysRevLett.105.241801>. [arXiv:1007.3496](https://arxiv.org/abs/1007.3496) [hep-ph]
11. ATLAS Collaboration, Search for WH production with a light Higgs boson decaying to prompt electron-jets in proton-proton collisions at $\sqrt{s} = 7$ TeV with the ATLAS detector. *New J. Phys.* **15**, 043009 (2013). <https://doi.org/10.1088/1367-2630/15/4/043009>. [arXiv:1302.4403](https://arxiv.org/abs/1302.4403) [hep-ex]
12. ATLAS Collaboration, A search for prompt lepton-jets in pp collisions at $\sqrt{s} = 7$ TeV with the ATLAS detector. *Phys. Lett. B* **719**, 299 (2013). <https://doi.org/10.1016/j.physletb.2013.01.034>. [arXiv:1212.5409](https://arxiv.org/abs/1212.5409) [hep-ex]
13. ATLAS Collaboration, A search for prompt lepton-jets in pp collisions at $\sqrt{s} = 8$ TeV with the ATLAS detector. *JHEP* **02**, 062 (2016). [https://doi.org/10.1007/JHEP02\(2016\)062](https://doi.org/10.1007/JHEP02(2016)062). [arXiv:1511.05542](https://arxiv.org/abs/1511.05542) [hep-ex]
14. ATLAS Collaboration, Search for light long-lived neutral particles that decay to collimated pairs of leptons or light hadrons in pp collisions at $\sqrt{s} = 13$ TeV with the ATLAS detector.

- JHEP **06**, 153 (2023). [https://doi.org/10.1007/JHEP06\(2023\)153](https://doi.org/10.1007/JHEP06(2023)153). [arXiv:2206.12181](https://arxiv.org/abs/2206.12181) [hep-ex]
15. ATLAS Collaboration, Search for light long-lived neutral particles from Higgs boson decays via vector-boson-fusion production from pp collisions at $\sqrt{s} = 13$ TeV with the ATLAS detector. *Eur. Phys. J. C* **84**, 719 (2023). <https://doi.org/10.1140/epjc/s10052-024-12902-7>. [arXiv:2311.18298](https://arxiv.org/abs/2311.18298) [hep-ex]
 16. ATLAS Collaboration, Search for Higgs bosons decaying into new spin-0 or spin-1 particles in four-lepton final states with the ATLAS detector with 139 fb^{-1} of pp collision data at $\sqrt{s} = 13$ TeV. *JHEP* **03**, 041 (2022). [https://doi.org/10.1007/JHEP03\(2022\)041](https://doi.org/10.1007/JHEP03(2022)041). [arXiv:2110.13673](https://arxiv.org/abs/2110.13673) [hep-ex]
 17. ATLAS Collaboration, Search for long-lived particles in final states with displaced dimuon vertices in pp collisions at $\sqrt{s} = 13$ TeV with the ATLAS detector. *Phys. Rev. D* **99**, 012001 (2019). <https://doi.org/10.1103/PhysRevD.99.012001>. [arXiv:1808.03057](https://arxiv.org/abs/1808.03057) [hep-ex]
 18. C.M.S. Collaboration, Search for light resonances decaying into pairs of muons as a signal of new physics. *JHEP* **07**, 098 (2011). [https://doi.org/10.1007/JHEP07\(2011\)098](https://doi.org/10.1007/JHEP07(2011)098). [arXiv:1106.2375](https://arxiv.org/abs/1106.2375) [hep-ex]
 19. C.M.S. Collaboration, Search for a non-standard-model Higgs boson decaying to a pair of new light bosons in four-muon final states. *Phys. Lett. B* **726**, 564 (2013). <https://doi.org/10.1016/j.physletb.2013.09.009>. [arXiv:1210.7619](https://arxiv.org/abs/1210.7619) [hep-ex]
 20. C.M.S. Collaboration, A search for pair production of new light bosons decaying into muons. *Phys. Lett. B* **752**, 146 (2016). <https://doi.org/10.1016/j.physletb.2015.10.067>. [arXiv:1506.00424](https://arxiv.org/abs/1506.00424) [hep-ex]
 21. C.M.S. Collaboration, Search for low-mass dilepton resonances in Higgs boson decays to four-lepton final states in proton-proton collisions at $\sqrt{s} = 13$ TeV. *Eur. Phys. J. C* **82**, 290 (2022). <https://doi.org/10.1140/epjc/s10052-022-10127-0>. [arXiv:2111.01299](https://arxiv.org/abs/2111.01299) [hep-ex]
 22. C.M.S. Collaboration, Search for long-lived particles decaying into muon pairs in proton-proton collisions at $\sqrt{s} = 13$ TeV collected with a dedicated high-rate data stream. *JHEP* **04**, 062 (2022). [https://doi.org/10.1007/JHEP04\(2022\)062](https://doi.org/10.1007/JHEP04(2022)062). [arXiv:2112.13769](https://arxiv.org/abs/2112.13769) [hep-ex]
 23. CMS Collaboration, Search for long-lived particles decaying to final states with a pair of muons in proton-proton collisions at $\sqrt{s} = 13.6$ TeV. *JHEP* **05**, 047 (2024). [https://doi.org/10.1007/JHEP05\(2024\)047](https://doi.org/10.1007/JHEP05(2024)047). [arXiv:2402.14491](https://arxiv.org/abs/2402.14491) [hep-ex]
 24. LHCb Collaboration, Search for hidden-sector bosons in $B^0 \rightarrow K^{*0} \mu^+ \mu^-$ decays. *Phys. Rev. Lett.* **115**, 161802 (2015). <https://doi.org/10.1103/PhysRevLett.115.161802>. [arXiv:1508.04094](https://arxiv.org/abs/1508.04094) [hep-ex]
 25. LHCb Collaboration, Search for $A' \rightarrow \mu^+ \mu^-$ Decays. *Phys. Rev. Lett.* **124**, 041801 (2020). <https://doi.org/10.1103/PhysRevLett.124.041801>. [arXiv:1910.06926](https://arxiv.org/abs/1910.06926) [hep-ex]
 26. C.M.S. Collaboration, Search for direct production of GeV-scale resonances decaying to a pair of muons in proton-proton collisions at $\sqrt{s} = 13$ TeV. *JHEP* **12**, 070 (2023). [https://doi.org/10.1007/JHEP12\(2023\)070](https://doi.org/10.1007/JHEP12(2023)070). [arXiv:2309.16003](https://arxiv.org/abs/2309.16003) [hep-ex]
 27. FASER Collaboration, Search for dark photons with the FASER detector at the LHC. *Phys. Lett. B* **848**, 138378 (2024). <https://doi.org/10.1016/j.physletb.2023.138378>
 28. A. Bross et al., Search for short-lived particles produced in an electron beam dump. *Phys. Rev. Lett.* **67**, 2942 (1991). <https://doi.org/10.1103/PhysRevLett.67.2942>
 29. M. Reece, L.-T. Wang, Searching for the light dark gauge boson in GeV-scale experiments. *JHEP* **07**, 051 (2009). <https://doi.org/10.1088/1126-6708/2009/07/051>. [arXiv:0904.1743](https://arxiv.org/abs/0904.1743) [hep-ph]
 30. J.D. Bjorken, R. Essig, P. Schuster, N. Toro, New fixed-target experiments to search for dark gauge forces. *Phys. Rev. D* **80**, 075018 (2009). <https://doi.org/10.1103/PhysRevD.80.075018>. [arXiv:0906.0580](https://arxiv.org/abs/0906.0580) [hep-ph]
 31. R. Essig, R. Harnik, J. Kaplan, N. Toro, Discovering new light states at neutrino experiments. *Phys. Rev. D* **82**, 113008 (2010). <https://doi.org/10.1103/PhysRevD.82.113008>. [arXiv:1008.0636](https://arxiv.org/abs/1008.0636) [hep-ph]
 32. J. Blümlein, J. Brunner, New exclusion limits for dark gauge forces from beam-dump data. *Phys. Lett. B* **701**, 155 (2011). <https://doi.org/10.1016/j.physletb.2011.05.046>. [arXiv:1104.2747](https://arxiv.org/abs/1104.2747) [hep-ex]
 33. A1 Collaboration, Search for light gauge bosons of the dark sector at the mainz microtron. *Phys. Rev. Lett.* **106**, 251802 (2011). <https://doi.org/10.1103/PhysRevLett.106.251802>. [arXiv:1101.4091](https://arxiv.org/abs/1101.4091) [nucl-ex]
 34. S. Abrahamyan et al., Search for a new gauge boson in electron-nucleus fixed-target scattering by the APEX experiment. *Phys. Rev. Lett.* **107**, 191804 (2011). <https://doi.org/10.1103/PhysRevLett.107.191804>. [arXiv:1108.2750](https://arxiv.org/abs/1108.2750) [hep-ex]
 35. S.N. Gninenko, Constraints on sub-GeV hidden sector gauge bosons from a search for heavy neutrino decays. *Phys. Lett. B* **713**, 244 (2012). <https://doi.org/10.1016/j.physletb.2012.06.002>. [arXiv:1204.3583](https://arxiv.org/abs/1204.3583) [hep-ph]
 36. WASA-at-COSY Collaboration, Search for a dark photon in the $\pi^0 \rightarrow e^+ e^- \gamma$ decay. *Phys. Lett. B* **726**, 187 (2013). <https://doi.org/10.1016/j.physletb.2013.08.055>. [arXiv:1304.0671](https://arxiv.org/abs/1304.0671) [hep-ex]
 37. J. Blümlein, J. Brunner, New exclusion limits on dark gauge forces from proton Bremsstrahlung in beam-dump data. *Phys. Lett. B* **731**, 320 (2014). <https://doi.org/10.1016/j.physletb.2014.02.029>. [arXiv:1311.3870](https://arxiv.org/abs/1311.3870) [hep-ph]
 38. HADES Collaboration, Searching a dark photon with HADES. *Phys. Lett. B* **731**, 265 (2014). <https://doi.org/10.1016/j.physletb.2014.02.035>. [arXiv:1311.0216](https://arxiv.org/abs/1311.0216) [hep-ex]
 39. M. Pospelov, Secluded U(1) below the weak scale. *Phys. Rev. D* **80**, 095002 (2009). <https://doi.org/10.1103/PhysRevD.80.095002>. [arXiv:0811.1030](https://arxiv.org/abs/0811.1030) [hep-ph]
 40. H. Davoudiasl, H.-S. Lee, W.J. Marciano, Dark side of Higgs diphoton decays and muon $g - 2$. *Phys. Rev. D* **86**, 095009 (2012). <https://doi.org/10.1103/PhysRevD.86.095009>. [arXiv:1208.2973](https://arxiv.org/abs/1208.2973) [hep-ph]
 41. M. Endo, K. Hamaguchi, G. Mishima, Constraints on hidden photon models from electron $g - 2$ and hydrogen spectroscopy. *Phys. Rev. D* **86**, 095029 (2012). <https://doi.org/10.1103/PhysRevD.86.095029>. [arXiv:1209.2558](https://arxiv.org/abs/1209.2558) [hep-ph]
 42. H.K. Dreiner, J.-F. Fortin, C. Hanhart, L. Ubaldi, Supernova constraints on MeV dark sectors from $e^+ e^-$ annihilations. *Phys. Rev. D* **89**, 105015 (2014). <https://doi.org/10.1103/PhysRevD.89.105015>. [arXiv:1310.3826](https://arxiv.org/abs/1310.3826) [hep-ph]
 43. J.H. Chang, R. Essig, S.D. McDermott, Supernova 1987A constraints on sub-GeV dark sectors, millicharged particles, the QCD axion, and an axion-like particle. *JHEP* **09**, 051 (2018). [https://doi.org/10.1007/JHEP09\(2018\)051](https://doi.org/10.1007/JHEP09(2018)051). [arXiv:1803.00993](https://arxiv.org/abs/1803.00993) [hep-ph]
 44. BABAR Collaboration, Search for dimuon decays of a light scalar boson in radiative transitions $\Upsilon \rightarrow \gamma A^0$. *Phys. Rev. Lett.* **103**, 081803 (2009). <https://doi.org/10.1103/PhysRevLett.103.081803>. [arXiv:0905.4539](https://arxiv.org/abs/0905.4539) [hep-ex]
 45. KLOE-2 Collaboration, Search for a vector gauge boson in ϕ meson decays with the KLOE detector. *Phys. Lett. B* **706**, 251 (2012). <https://doi.org/10.1016/j.physletb.2011.11.033>. [arXiv:1110.0411](https://arxiv.org/abs/1110.0411) [hep-ex]
 46. BABAR Collaboration, Search for low-mass dark-sector Higgs bosons. *Phys. Rev. Lett.* **108**, 211801 (2012). <https://doi.org/10.1103/PhysRevLett.108.211801>
 47. KLOE-2 Collaboration, Limit on the production of a light vector gauge boson in ϕ meson decays with the KLOE detector. *Phys. Lett. B* **720**, 111 (2013). <https://doi.org/10.1016/j.physletb.2013.01.067>. [arXiv:1210.3927](https://arxiv.org/abs/1210.3927) [hep-ex]

48. BABAR Collaboration, Search for a dark photon in e^+e^- collisions at BaBar. *Phys. Rev. Lett.* **113**, 201801 (2014). <https://doi.org/10.1103/PhysRevLett.113.201801>. arXiv:1406.2980 [hep-ex]
49. BABAR Collaboration, Search for long-lived particles in e^+e^- collisions. *Phys. Rev. Lett.* **114**, 171801 (2015). <https://doi.org/10.1103/PhysRevLett.114.171801>. arXiv:1502.02580 [hep-ex]
50. B. Collaboration, Search for the dark photon and the dark Higgs boson at Belle. *Phys. Rev. Lett.* **114**, 211801 (2015). <https://doi.org/10.1103/PhysRevLett.114.211801>. arXiv:1502.00084 [hep-ex]
51. KLOE-2 Collaboration, Search for dark Higgsstrahlung in $e^+e^- \rightarrow \mu^+\mu^-$ and missing energy events with the KLOE experiment. *Phys. Lett. B* **747**, 365 (2015). <https://doi.org/10.1016/j.physletb.2015.06.015>
52. B. Collaboration, Search for a dark vector gauge boson decaying to $\pi^+\pi^-$ using $\eta \rightarrow \pi^+\pi^-\gamma$ decays. *Phys. Rev. D* **94**, 092006 (2016). <https://doi.org/10.1103/PhysRevD.94.092006>. arXiv:1609.05599 [hep-ex]
53. BESIII Collaboration, Dark photon search in the mass range between 1.5 and 3.4 GeV/ c^2 . *Phys. Lett. B* **774**, 252 (2017). <https://doi.org/10.1016/j.physletb.2017.09.067>. arXiv:1705.04265 [hep-ex]
54. BESIII Collaboration, Measurement of $B(J/\psi \rightarrow \eta' e^+e^-)$ and search for a dark photon. *Phys. Rev. D* **99**, 012013 (2019). <https://doi.org/10.1103/PhysRevD.99.012013>. arXiv:1809.00635 [hep-ex]
55. B. Collaboration, Search for the dark photon in $B^0 \rightarrow A'A'$, $A' \rightarrow e^+e^-$, $\mu^+\mu^-$, and $\pi^+\pi^-$ decays at Belle. *JHEP* **04**, 191 (2021). [https://doi.org/10.1007/JHEP04\(2021\)191](https://doi.org/10.1007/JHEP04(2021)191). arXiv:2012.02538 [hep-ex]
56. Belle II Collaboration, Search for a dark photon and an invisible dark Higgs boson in $\mu^+\mu^-$ and missing energy final states with the Belle II experiment. *Phys. Rev. Lett.* **130**, 071804 (2023). <https://doi.org/10.1103/PhysRevLett.130.071804>
57. ATLAS Collaboration, The ATLAS experiment at the CERN large hadron collider. *JINST* **3**, S08003 (2008). <https://doi.org/10.1088/1748-0221/3/08/S08003>
58. ATLAS Collaboration, ATLAS Insertable B-Layer: Technical Design Report, ATLAS-TDR-19; CERN-LHCC-2010-013 (2010). <https://cds.cern.ch/record/1291633>. Addendum: ATLAS-TDR-19-ADD-1; CERN-LHCC-2012-009 (2012). <https://cds.cern.ch/record/1451888>
59. B. Abbott et al., Production and integration of the ATLAS Insertable B-Layer. *JINST* **13**, T05008 (2018). <https://doi.org/10.1088/1748-0221/13/05/T05008>. arXiv:1803.00844 [physics.ins-det]
60. G. Avoni et al., The new LUCID-2 detector for luminosity measurement and monitoring in ATLAS. *JINST* **13**, P07017 (2018). <https://doi.org/10.1088/1748-0221/13/07/P07017>
61. ATLAS Collaboration, Performance of the ATLAS trigger system in 2015. *Eur. Phys. J. C* **77**, 317 (2017). <https://doi.org/10.1140/epjc/s10052-017-4852-3>. arXiv:1611.09661 [hep-ex]
62. ATLAS Collaboration, Software and computing for Run 3 of the ATLAS experiment at the LHC (2024). arXiv:2404.06335 [hep-ex]
63. ATLAS Collaboration, Performance of electron and photon triggers in ATLAS during LHC Run 2. *Eur. Phys. J. C* **80**, 47 (2020). <https://doi.org/10.1140/epjc/s10052-019-7500-2>. arXiv:1909.00761 [hep-ex]
64. ATLAS Collaboration, Performance of the ATLAS muon triggers in Run 2. *JINST* **15**, P09015 (2020). <https://doi.org/10.1088/1748-0221/15/09/p09015>. arXiv:2004.13447 [physics.ins-det]
65. ATLAS Collaboration, The ATLAS inner detector trigger performance in pp collisions at 13 TeV during LHC Run 2. *Eur. Phys. J. C* **82**, 206 (2022). <https://doi.org/10.1140/epjc/s10052-021-09920-0>. arXiv:2107.02485 [hep-ex]
66. ATLAS Collaboration, ATLAS data quality operations and performance for 2015–2018 data-taking. *JINST* **15**, P04003 (2020). <https://doi.org/10.1088/1748-0221/15/04/P04003>. arXiv:1911.04632 [physics.ins-det]
67. J. Alwall et al., The automated computation of tree-level and next-to-leading order differential cross sections, and their matching to parton shower simulations. *JHEP* **07**, 079 (2014). [https://doi.org/10.1007/JHEP07\(2014\)079](https://doi.org/10.1007/JHEP07(2014)079). arXiv:1405.0301 [hep-ph]
68. T. Sjöstrand, S. Mrenna, P. Skands, A brief introduction to PYTHIA 8.1. *Comput. Phys. Commun.* **178**, 852 (2008). <https://doi.org/10.1016/j.cpc.2008.01.036>. arXiv:0710.3820 [hep-ph]
69. NNPDF Collaboration, R.D. Ball et al., Parton distributions with LHC data. *Nucl. Phys. B* **867**, 244 (2013). <https://doi.org/10.1016/j.nuclphysb.2012.10.003>. arXiv:1207.1303 [hep-ph]
70. M. Cepeda et al., Higgs Physics at the HL-LHC and HE-LHC. CERN Yellow Rep. Monogr. **7**, 221 (2019), ed. by A. Dainese et al. <https://doi.org/10.23731/CYRM-2019-007.221>. arXiv:1902.00134 [hep-ph]
71. C. Anastasiou et al., High precision determination of the gluon fusion Higgs boson cross-section at the LHC. *JHEP* **05**, 058 (2016). [https://doi.org/10.1007/JHEP05\(2016\)058](https://doi.org/10.1007/JHEP05(2016)058). arXiv:1602.00695 [hep-ph]
72. E. Bothmann et al., Event generation with Sherpa 2.2. *SciPost Phys.* **7**, 034 (2019). <https://doi.org/10.21468/SciPostPhys.7.3.034>. arXiv:1905.09127 [hep-ph]
73. T. Gleisberg, S. Höche, Comix, a new matrix element generator. *JHEP* **12**, 039 (2008). <https://doi.org/10.1088/1126-6708/2008/12/039>. arXiv:0808.3674 [hep-ph]
74. F. Bucciioni et al., OpenLoops 2. *Eur. Phys. J. C* **79**, 866 (2019). <https://doi.org/10.1140/epjc/s10052-019-7306-2>. arXiv:1907.13071 [hep-ph]
75. F. Cascioli, P. Maierhöfer, S. Pozzorini, Scattering amplitudes with open loops. *Phys. Rev. Lett.* **108**, 111601 (2012). <https://doi.org/10.1103/PhysRevLett.108.111601>. arXiv:1111.5206 [hep-ph]
76. A. Denner, S. Dittmaier, L. Hofer, Collier: a fortran-based complex one-loop library in extended regularizations. *Comput. Phys. Commun.* **212**, 220 (2017). <https://doi.org/10.1016/j.cpc.2016.10.013>. arXiv:1604.06792 [hep-ph]
77. S. Schumann, F. Krauss, A parton shower algorithm based on Catani–Seymour dipole factorisation. *JHEP* **03**, 038 (2008). <https://doi.org/10.1088/1126-6708/2008/03/038>. arXiv:0709.1027 [hep-ph]
78. S. Höche, F. Krauss, M. Schönherr, F. Siegert, A critical appraisal of NLO+PS matching methods. *JHEP* **09**, 049 (2012). [https://doi.org/10.1007/JHEP09\(2012\)049](https://doi.org/10.1007/JHEP09(2012)049). arXiv:1111.1220 [hep-ph]
79. S. Höche, F. Krauss, M. Schönherr, F. Siegert, QCD matrix elements + parton showers. The NLO case. *JHEP* **04**, 027 (2013). [https://doi.org/10.1007/JHEP04\(2013\)027](https://doi.org/10.1007/JHEP04(2013)027). arXiv:1207.5030 [hep-ph]
80. S. Catani, F. Krauss, B.R. Webber, R. Kuhn, QCD matrix elements + parton showers. *JHEP* **11**, 063 (2001). <https://doi.org/10.1088/1126-6708/2001/11/063>. arXiv:hep-ph/0109231
81. S. Höche, F. Krauss, S. Schumann, F. Siegert, QCD matrix elements and truncated showers. *JHEP* **05**, 053 (2009). <https://doi.org/10.1088/1126-6708/2009/05/053>. arXiv:0903.1219 [hep-ph]
82. NNPDF Collaboration, R.D. Ball et al., Parton distributions for the LHC run II. *JHEP* **04**, 040 (2015). [https://doi.org/10.1007/JHEP04\(2015\)040](https://doi.org/10.1007/JHEP04(2015)040). arXiv:1410.8849 [hep-ph]
83. C. Anastasiou, L. Dixon, K. Melnikov, F. Petriello, High-precision QCD at hadron colliders: electroweak gauge boson rapidity distributions at next-to-next-to leading order. *Phys. Rev. D* **69**, 094008 (2004). <https://doi.org/10.1103/PhysRevD.69.094008>. arXiv:hep-ph/0312266

84. S. Frixione, G. Ridolfi, P. Nason, A positive-weight next-to-leading-order Monte Carlo for heavy flavour hadroproduction. *JHEP* **09**, 126 (2007). <https://doi.org/10.1088/1126-6708/2007/09/126>. [arXiv:0707.3088](https://arxiv.org/abs/0707.3088) [hep-ph]
85. P. Nason, A new method for combining NLO QCD with shower Monte Carlo algorithms. *JHEP* **11**, 040 (2004). <https://doi.org/10.1088/1126-6708/2004/11/040>. [arXiv:hep-ph/0409146](https://arxiv.org/abs/hep-ph/0409146)
86. S. Frixione, P. Nason, C. Oleari, Matching NLO QCD computations with parton shower simulations: the POWHEG method. *JHEP* **11**, 070 (2007). <https://doi.org/10.1088/1126-6708/2007/11/070>. [arXiv:0709.2092](https://arxiv.org/abs/0709.2092) [hep-ph]
87. S. Alioli, P. Nason, C. Oleari, E. Re, A general framework for implementing NLO calculations in shower Monte Carlo programs: the POWHEG BOX. *JHEP* **06**, 043 (2010). [https://doi.org/10.1007/JHEP06\(2010\)043](https://doi.org/10.1007/JHEP06(2010)043). [arXiv:1002.2581](https://arxiv.org/abs/1002.2581) [hep-ph]
88. ATLAS Collaboration, Studies on top-quark Monte Carlo modelling for Top2016, ATL-PHYS-PUB-2016-020 (2016). <https://cds.cern.ch/record/2216168>
89. T. Sjöstrand et al., An introduction to PYTHIA 8.2. *Comput. Phys. Commun.* **191**, 159 (2015). <https://doi.org/10.1016/j.cpc.2015.01.024>. [arXiv:1410.3012](https://arxiv.org/abs/1410.3012) [hep-ph]
90. ATLAS Collaboration, ATLAS Pythia 8 tunes to 7 TeV data, ATL-PHYS-PUB-2014-021 (2014). <https://cds.cern.ch/record/1966419>
91. D.J. Lange, The EvtGen particle decay simulation package. *Nucl. Instrum. Methods A* **462**, 152 (2001). [https://doi.org/10.1016/S0168-9002\(01\)00089-4](https://doi.org/10.1016/S0168-9002(01)00089-4)
92. ATLAS Collaboration, The ATLAS simulation infrastructure. *Eur. Phys. J. C* **70**, 823 (2010). <https://doi.org/10.1140/epjc/s10052-010-1429-9>. [arXiv:1005.4568](https://arxiv.org/abs/1005.4568) [physics.ins-det]
93. S. Agostinelli et al., Geant4—a simulation toolkit. *Nucl. Instrum. Methods A* **506**, 250 (2003). [https://doi.org/10.1016/S0168-9002\(03\)01368-8](https://doi.org/10.1016/S0168-9002(03)01368-8)
94. ATLAS Collaboration, The Pythia 8 A3 tune description of ATLAS minimum bias and inelastic measurements incorporating the Donnachie–Landschoff diffractive model, ATL-PHYS-PUB-2016-017 (2016). <https://cds.cern.ch/record/2206965>
95. ATLAS Collaboration, Vertex Reconstruction Performance of the ATLAS Detector at $\sqrt{s} = 13$ TeV, ATL-PHYS-PUB-2015-026 (2015). <https://cds.cern.ch/record/2037717>
96. ATLAS Collaboration, Electron and photon performance measurements with the ATLAS detector using the 2015–2017 LHC proton–proton collision data. *JINST* **14**, P12006 (2019). <https://doi.org/10.1088/1748-0221/14/12/P12006>. [arXiv:1908.00005](https://arxiv.org/abs/1908.00005) [hep-ex]
97. ATLAS Collaboration, Muon reconstruction and identification efficiency in ATLAS using the full Run 2 pp collision data set at $\sqrt{s} = 13$ TeV. *Eur. Phys. J. C* **81**, 578 (2021). <https://doi.org/10.1140/epjc/s10052-021-09233-2>. [arXiv:2012.00578](https://arxiv.org/abs/2012.00578) [hep-ex]
98. ATLAS Collaboration, Properties of jets and inputs to jet reconstruction and calibration with the ATLAS detector using proton–proton collisions at $\sqrt{s} = 13$ TeV. ATL-PHYS-PUB-2015-036 (2015). <https://cds.cern.ch/record/2044564>
99. M. Cacciari, G.P. Salam, G. Soyez, The anti- k_r jet clustering algorithm. *JHEP* **04**, 063 (2008). <https://doi.org/10.1088/1126-6708/2008/04/063>. [arXiv:0802.1189](https://arxiv.org/abs/0802.1189) [hep-ph]
100. M. Cacciari, G.P. Salam, G. Soyez, FastJet user manual. *Eur. Phys. J. C* **72**, 1896 (2012). <https://doi.org/10.1140/epjc/s10052-012-1896-2>. [arXiv:1111.6097](https://arxiv.org/abs/1111.6097) [hep-ph]
101. ATLAS Collaboration, Jet energy scale measurements and their systematic uncertainties in proton–proton collisions at $\sqrt{s} = 13$ TeV with the ATLAS detector. *Phys. Rev. D* **96**, 072002 (2017). <https://doi.org/10.1103/PhysRevD.96.072002>. [arXiv:1703.09665](https://arxiv.org/abs/1703.09665) [hep-ex]
102. ATLAS Collaboration, Selection of jets produced in 13 TeV proton–proton collisions with the ATLAS detector. ATLAS-CONF-2015-029 (2015). <https://cds.cern.ch/record/2037702>
103. ATLAS Collaboration, Performance of pile-up mitigation techniques for jets in pp collisions at $\sqrt{s} = 8$ TeV using the ATLAS detector. *Eur. Phys. J. C* **76**, 581 (2016). <https://doi.org/10.1140/epjc/s10052-016-4395-z>. [arXiv:1510.03823](https://arxiv.org/abs/1510.03823) [hep-ex]
104. Y.L. Dokshitzer, G.D. Leder, S. Moretti, B.R. Webber, Better jet clustering algorithms. *JHEP* **08**, 001 (1997). <https://doi.org/10.1088/1126-6708/1997/08/001>. [arXiv:hep-ph/9707323](https://arxiv.org/abs/hep-ph/9707323)
105. M. Oreglia, A study of the reactions $\psi' \rightarrow \gamma\gamma\psi$, PhD Thesis (1980). <http://www-public.slac.stanford.edu/sciDoc/docMeta.aspx?slacPubNumber=slac-r-236.html>
106. ATLAS Collaboration, Search for boosted diphoton resonances in the 10 to 70 GeV mass range using 138 fb^{-1} of 13 TeV pp collisions with the ATLAS detector. *JHEP* **07**, 155 (2023). [https://doi.org/10.1007/JHEP07\(2023\)155](https://doi.org/10.1007/JHEP07(2023)155). [arXiv:2211.04172](https://arxiv.org/abs/2211.04172) [hep-ex]
107. ATLAS Collaboration, Luminosity determination in pp collisions at $\sqrt{s} = 13$ TeV using the ATLAS detector at the LHC. *Eur. Phys. J. C* **83**, 982 (2023). <https://doi.org/10.1140/epjc/s10052-023-11747-w>. [arXiv:2212.09379](https://arxiv.org/abs/2212.09379) [hep-ex]
108. ATLAS Collaboration, Measurement of the inelastic proton–proton cross section at $\sqrt{s} = 13$ TeV with the ATLAS detector at the LHC. *Phys. Rev. Lett.* **117**, 182002 (2016). <https://doi.org/10.1103/PhysRevLett.117.182002>. [arXiv:1606.02625](https://arxiv.org/abs/1606.02625) [hep-ex]
109. A.L. Read, Presentation of search results: the CL_S technique. *J. Phys. G* **28**, 2693 (2002). <https://doi.org/10.1088/0954-3899/28/10/313>
110. G. Cowan, K. Cranmer, E. Gross, O. Vitells, Asymptotic formulae for likelihood-based tests of new physics. *Eur. Phys. J. C* **71**, 1554 (2011). <https://doi.org/10.1140/epjc/s10052-011-1554-0>. [arXiv:1007.1727](https://arxiv.org/abs/1007.1727) [physics.data-an]. Erratum: *Eur. Phys. J. C* **73**, 2501 (2013). <https://doi.org/10.1140/epjc/s10052-013-2501-z>
111. B. Batell, M. Pospelov, A. Ritz, Probing a secluded $U(1)$ at B factories. *Phys. Rev. D* **79**, 115008 (2009). <https://doi.org/10.1103/PhysRevD.79.115008>. [arXiv:0903.0363](https://arxiv.org/abs/0903.0363) [hep-ph]
112. ATLAS Collaboration, ATLAS Computing Acknowledgements, ATL-SOFT-PUB-2023-001 (2023). <https://cds.cern.ch/record/2869272>

ATLAS Collaboration*

G. Aad¹⁰⁴, E. Aakvaag¹⁷, B. Abbott¹²³, S. Abdelhameed^{119a}, K. Abeling⁵⁶, N. J. Abicht⁵⁰, S. H. Abidi³⁰, M. Aboeela⁴⁵, A. Aboulhorma^{36c}, H. Abramowicz¹⁵⁵, H. Abreu¹⁵⁴, Y. Abulaiti¹²⁰, B. S. Acharya^{70a,70b,1}, A. Ackermann^{64a}, C. Adam Bourdarios⁴, L. Adamczyk^{87a}, S. V. Addepalli²⁷, M. J. Addison¹⁰³, J. Adelman¹¹⁸, A. Adiguzel^{22c}, T. Adye¹³⁷, A. A. Affolder¹³⁹, Y. Afik⁴⁰, M. N. Agaras¹³, J. Agarwala^{74a,74b}, A. Aggarwal¹⁰², C. Agheorghiesei^{28c}, F. Ahmadov^{39,aa}, W. S. Ahmed¹⁰⁶, S. Ahuja⁹⁷, X. Ai^{63e}, G. Aielli^{77a,77b}, A. Aikot¹⁶⁶, M. Ait Tamlihat^{36e}, B. Aitbenchikh^{36a}, M. Akbiyik¹⁰², T. P. A. Åkesson¹⁰⁰, A. V. Akimov³⁸, D. Akiyama¹⁷¹, N. N. Akolkar²⁵, S. Aktas^{22a}, K. Al Khoury⁴², G. L. Alberghi^{24b}, J. Albert¹⁶⁸, P. Albicocco⁵⁴, G. L. Albouy⁶¹, S. Alderweireldt⁵³, Z. L. Alegria¹²⁴, M. Aleksa³⁷, I. N. Aleksandrov³⁹, C. Alexa^{28b}, T. Alexopoulos¹⁰, F. Alfonsi^{24b}, M. Algren⁵⁷, M. Alhroob¹⁷⁰, B. Ali¹³⁵, H. M. J. Ali^{93,t}, S. Ali³², S. W. Alibocus⁹⁴, M. Aliev^{34c}, G. Alimonti^{72a}, W. Alkakh⁵⁶, C. Allaire⁶⁷, B. M. M. Allbrooke¹⁵⁰, J. S. Allen¹⁰³, J. F. Allen⁵³, C. A. Allendes Flores^{140f}, P. P. Allport²¹, A. Aloisio^{73a,73b}, F. Alonso⁹², C. Alpigiani¹⁴², Z. M. K. Alsolami⁹³, M. Alvarez Estevez¹⁰¹, A. Alvarez Fernandez¹⁰², M. Alves Cardoso⁵⁷, M. G. Alviggi^{73a,73b}, M. Aly¹⁰³, Y. Amaral Coutinho^{84b}, A. Ambler¹⁰⁶, C. Amelung³⁷, M. Ameri¹⁰³, C. G. Ames¹¹¹, D. Amidei¹⁰⁸, B. Amini⁵⁵, K. J. Amirie¹⁵⁸, S. P. Amor Dos Santos^{133a}, K. R. Amos¹⁶⁶, D. Amperidou¹⁵⁶, S. An⁸⁵, V. Ananiev¹²⁸, C. Anastopoulos¹⁴³, T. Andeen¹¹, J. K. Anders³⁷, A. C. Anderson⁶⁰, S. Y. Andreatan^{48a,48b}, A. Andreatza^{72a,72b}, S. Angelidakis⁹, A. Angerami⁴², A. V. Anisenkov³⁸, A. Annovi^{75a}, C. Antel⁵⁷, E. Antipov¹⁴⁹, M. Antonelli⁵⁴, F. Anulli^{76a}, M. Aoki⁸⁵, T. Aoki¹⁵⁷, M. A. Aparo¹⁵⁰, L. Aperio Bella⁴⁹, C. Appelt¹⁹, A. Apyan²⁷, S. J. Arbiol Val⁸⁸, C. Arcangeletti⁵⁴, A. T. H. Arce⁵², J.-F. Arguin¹¹⁰, S. Argyropoulos⁵⁵, J.-H. Arling⁴⁹, O. Arnaez⁴, H. Arnold¹⁴⁹, G. Artoni^{76a,76b}, H. Asada¹¹³, K. Asai¹²¹, S. Asai¹⁵⁷, N. A. Asbah³⁷, R. A. Ashby Pickering¹⁷⁰, K. Assamagan³⁰, R. Astalos^{29a}, K. S. V. Astrand¹⁰⁰, S. Atashi¹⁶², R. J. Atkin^{34a}, M. Atkinson¹⁶⁵, H. Atmani^{36f}, P. A. Atmasiddha¹³¹, K. Augsten¹³⁵, S. Auricchio^{73a,73b}, A. D. Aurio²¹, V. A. Austrup¹⁰³, G. Avolio³⁷, K. Axiotis⁵⁷, G. Azuelos^{110,af}, D. Babal^{29b}, H. Bachacou¹³⁸, K. Bachas^{156,p}, A. Bachiu³⁵, F. Backman^{48a,48b}, A. Badea⁴⁰, T. M. Baer¹⁰⁸, P. Bagnaia^{76a,76b}, M. Bahmani¹⁹, D. Bahner⁵⁵, K. Bai¹²⁶, J. T. Baines¹³⁷, L. Baines⁹⁶, O. K. Baker¹⁷⁵, E. Bakos¹⁶, D. Bakshi Gupta⁸, L. E. Balabram Filho^{84b}, V. Balakrishnan¹²³, R. Balasubramanian⁴, E. M. Baldin³⁸, P. Balek^{87a}, E. Ballabene^{24a,24b}, F. Balli¹³⁸, L. M. Baltes^{64a}, W. K. Balunas³³, J. Balz¹⁰², I. Bamwidhi^{119b}, E. Banas⁸⁸, M. Bandieramonte¹³², A. Bandyopadhyay²⁵, S. Bansal²⁵, L. Barak¹⁵⁵, M. Barakat⁴⁹, E. L. Barberio¹⁰⁷, D. Barberis^{58a,58b}, M. Barbero¹⁰⁴, M. Z. Barel¹¹⁷, T. Barillari¹¹², M.-S. Barisits³⁷, T. Barklow¹⁴⁷, P. Baron¹²⁵, D. A. Baron Moreno¹⁰³, A. Baroncelli^{63a}, A. J. Barr¹²⁹, J. D. Barr⁹⁸, F. Barreiro¹⁰¹, J. Barreiro Guimarães da Costa¹⁴, U. Barron¹⁵⁵, M. G. Barros Teixeira^{133a}, S. Barsov³⁸, F. Bartels^{64a}, R. Bartoldus¹⁴⁷, A. E. Barton⁹³, P. Bartos^{29a}, A. Basan¹⁰², M. Baselga⁵⁰, A. Bassalat^{67,b}, M. J. Basso^{159a}, S. Bataju⁴⁵, R. Bate¹⁶⁷, R. L. Bates⁶⁰, S. Batlamous¹⁰¹, B. Batool¹⁴⁵, M. Battaglia¹³⁹, D. Battulga¹⁹, M. Baucé^{76a,76b}, M. Bauer⁸⁰, P. Bauer²⁵, L. T. Bazzano Hurrell³¹, J. B. Beacham⁵², T. Beau¹³⁰, J. Y. Beauchamp⁹², P. H. Beauchemin¹⁶¹, P. Bechtel²⁵, H. P. Beck^{20,o}, S. F. Beck⁴⁶, K. Becker¹⁷⁰, A. J. Beddall⁸³, V. A. Bednyakov³⁹, C. P. Bee¹⁴⁹, L. J. Beamster¹⁶, T. A. Beermann³⁷, M. Begalli^{84d}, M. Begel³⁰, A. Behera¹⁴⁹, J. K. Behr⁴⁹, J. F. Beirer³⁷, F. Beisiegel²⁵, M. Belfkir^{119b}, G. Bella¹⁵⁵, L. Bellagamba^{24b}, A. Bellerive³⁵, P. Bellos²¹, K. Beloborodov³⁸, D. Benckekroun^{36a}, F. Bendebeba^{36a}, Y. Benhammou¹⁵⁵, K. C. Benkendorfer⁶², L. Beresford⁴⁹, M. Beretta⁵⁴, E. Bergeas Kuutmann¹⁶⁴, N. Berger⁴, B. Bergmann¹³⁵, J. Beringer^{18a}, G. Bernardi⁵, C. Bernius¹⁴⁷, F. U. Bernlochner²⁵, F. Bernon³⁷, A. Berrocal Guardia¹³, T. Berry⁹⁷, P. Berta¹³⁶, A. Berthold⁵¹, S. Bethke¹¹², A. Betti^{76a,76b}, A. J. Bevan⁹⁶, N. K. Bhalla⁵⁵, S. Bhatta¹⁴⁹, D. S. Bhattacharya¹⁶⁹, P. Bhattarai¹⁴⁷, K. D. Bhide⁵⁵, V. S. Bhopatkar¹²⁴, R. M. Bianchi¹³², G. Bianco^{24a,24b}, O. Biebel¹¹¹, R. Bielski¹²⁶, M. Biglietti^{78a}, C. S. Billingsley⁴⁵, Y. Bingdi^{36f}, M. Bindi⁵⁶, A. Bingul^{22b}, C. Bini^{76a,76b}, G. A. Bird³³, M. Birman¹⁷², M. Biros¹³⁶, S. Biryukov¹⁵⁰, T. Bisanz⁵⁰, E. Bisceglie^{44a,44b}, J. P. Biswal¹³⁷, D. Biswas¹⁴⁵, I. Bloch⁴⁹, A. Blue⁶⁰, U. Blumenschein⁹⁶, J. Blumenthal¹⁰², V. S. Bobrovnikov³⁸, M. Boehler⁵⁵, B. Boehm¹⁶⁹, D. Bogavac³⁷, A. G. Bogdanchikov³⁸, L. S. Boggia¹³⁰, C. Bohm^{48a}, V. Boisvert⁹⁷, P. Bokan³⁷, T. Bold^{87a}, M. Bomben⁵, M. Bona⁹⁶, M. Boonekamp¹³⁸, C. D. Booth⁹⁷, A. G. Borbély⁶⁰, I. S. Bordulev³⁸, G. Borissov⁹³, D. Bortoletto¹²⁹, D. Boscherini^{24b}, M. Bosman¹³, J. D. Bossio Sola³⁷, K. Bouaouda^{36a}, N. Bouchhar¹⁶⁶, L. Boudet⁴, J. Boudreau¹³², E. V. Bouhova-Thacker⁹³, D. Boumediene⁴¹, R. Bouquet^{58a,58b}, A. Boveia¹²², J. Boyd³⁷, D. Boye³⁰, I. R. Boyko³⁹, L. Bozianu⁵⁷, J. Bracinik²¹, N. Brahimi⁴, G. Brandt¹⁷⁴, O. Brandt³³

S. J. Dittmeier^{64b}, F. Dittus³⁷, M. Divisek¹³⁶, B. Dixit⁹⁴, F. Djama¹⁰⁴, T. Djobava^{153b}, C. Doglioni^{100,103}, A. Dohnalova^{29a}, J. Dolejsi¹³⁶, Z. Dolezal¹³⁶, K. Domijan^{87a}, K. M. Dona⁴⁰, M. Donadelli^{84d}, B. Dong¹⁰⁹, J. Donini⁴¹, A. D'Onofrio^{73a,73b}, M. D'Onofrio⁹⁴, J. Dopke¹³⁷, A. Doria^{73a}, N. Dos Santos Fernandes^{133a}, P. Dougan¹⁰³, M. T. Dova⁹², A. T. Doyle⁶⁰, M. A. Draguet¹²⁹, M. P. Drescher⁵⁶, E. Dreyer¹⁷², I. Drivas-koulouris¹⁰, M. Drnevich¹²⁰, M. Drozdova⁵⁷, D. Du^{63a}, T. A. du Pree¹¹⁷, F. Dubinin³⁸, M. Dubovsky^{29a}, E. Duchovni¹⁷², G. Duckeck¹¹¹, O. A. Ducu^{28b}, D. Duda⁵³, A. Dudarev³⁷, E. R. Duden²⁷, M. D'uffizi¹⁰³, L. Dufflot⁶⁷, M. Dührssen³⁷, I. Duminica^{28g}, A. E. Dumitriu^{28b}, M. Dunford^{64a}, S. Dungs⁵⁰, K. Dunne^{48a,48b}, A. Duperrin¹⁰⁴, H. Duran Yildiz^{3a}, M. Düren⁵⁹, A. Durglishvili^{153b}, D. Duvnjak³⁵, B. L. Dwyer¹¹⁸, G. I. Dyckes^{18a}, M. Dyndal^{87a}, B. S. Dziedzic³⁷, Z. O. Earnshaw¹⁵⁰, G. H. Eberwein¹²⁹, B. Eckerova^{29a}, S. Eggebrecht⁵⁶, E. Egidio Purcino De Souza^{84c}, L. F. Ehrke⁵⁷, G. Eigen¹⁷, K. Einsweiler^{18a}, T. Ekelof¹⁶⁴, P. A. Ekman¹⁰⁰, S. El Farkh^{36b}, Y. El Ghazali^{63a}, H. El Jarrari³⁷, A. El Moussaouy^{36a}, V. Ellajosyula¹⁶⁴, M. Ellert¹⁶⁴, F. Ellinghaus¹⁷⁴, N. Ellis³⁷, J. Elmsheuser³⁰, M. Elsayy^{119a}, M. Elsing³⁷, D. Emeliyanov¹³⁷, Y. Enari⁸⁵, I. Ene^{18a}, S. Epari¹³, P. A. Erland⁸⁸, D. Ernani Martins Neto⁸⁸, M. Errenst¹⁷⁴, M. Escalier⁶⁷, C. Escobar¹⁶⁶, E. Etzion¹⁵⁵, G. Evans^{133a,133b}, H. Evans⁶⁹, L. S. Evans⁹⁷, A. Ezhilov³⁸, S. Ezzarqtoni^{36a}, F. Fabbri^{24a,24b}, L. Fabbri^{24a,24b}, G. Facini⁹⁸, V. Fadeyev¹³⁹, R. M. Fakhruddinov³⁸, D. Fakoudis¹⁰², S. Falciano^{76a}, L. F. Falda Ulhoa Coelho³⁷, F. Fallavollita¹¹², G. Falsetti^{44a,44b}, J. Faltova¹³⁶, C. Fan¹⁶⁵, K. Y. Fan^{65b}, Y. Fan¹⁴, Y. Fang^{14,114c}, M. Fantì^{72a,72b}, M. Faraj^{70a,70b}, Z. Farazpay⁹⁹, A. Farbin⁸, A. Farilla^{78a}, T. Farooque¹⁰⁹, S. M. Farrington⁵³, F. Fassi^{36e}, D. Fassouliotis⁹, M. Fauci Giannelli^{77a,77b}, W. J. Fawcett³³, L. Fayard⁶⁷, P. Federic¹³⁶, P. Federicova¹³⁴, O. L. Fedin^{38a}, M. Feickert¹⁷³, L. Feligioni¹⁰⁴, D. E. Fellers¹²⁶, C. Feng^{63b}, Z. Feng¹¹⁷, M. J. Fenton¹⁶², L. Ferencz⁴⁹, R. A. M. Ferguson⁹³, S. I. Fernandez Luengo^{140f}, P. Fernandez Martinez⁶⁸, M. J. V. Fernoux¹⁰⁴, J. Ferrando⁹³, A. Ferrari¹⁶⁴, P. Ferrari^{116,117}, R. Ferrari^{74a}, D. Ferrere⁵⁷, C. Ferretti¹⁰⁸, D. Fiacco^{76a,76b}, F. Fiedler¹⁰², P. Fiedler¹³⁵, S. Filimonov³⁸, A. Filipčić⁹⁵, E. K. Filmer^{159a}, F. Filthaut¹¹⁶, M. C. N. Fiolhais^{133a,133c}, L. Fiorini¹⁶⁶, W. C. Fisher¹⁰⁹, T. Fitschen¹⁰³, P. M. Fitzhugh¹³⁸, I. Fleck¹⁴⁵, P. Fleischmann¹⁰⁸, T. Flick¹⁷⁴, M. Flores^{34d,ac}, L. R. Flores Castillo^{65a}, L. Flores Sanz De Acedo³⁷, F. M. Follega^{79a,79b}, N. Fomin³³, J. H. Foo¹⁵⁸, A. Formica¹³⁸, A. C. Forti¹⁰³, E. Fortin³⁷, A. W. Fortman^{18a}, M. G. Foti^{18a}, L. Fountas^{9j}, D. Fournier⁶⁷, H. Fox⁹³, P. Francavilla^{75a,75b}, S. Francescato⁶², S. Franchellucci⁵⁷, M. Franchini^{24a,24b}, S. Franchino^{64a}, D. Francis³⁷, L. Franco¹¹⁶, V. Franco Lima³⁷, L. Franconi⁴⁹, M. Franklin⁶², G. Frattari²⁷, Y. Y. Frid¹⁵⁵, J. Friend⁶⁰, N. Fritzsche³⁷, A. Froch⁵⁵, D. Froidevaux³⁷, J. A. Frost¹²⁹, Y. Fu^{63a}, S. Fuenzalida Garrido^{140f}, M. Fujimoto¹⁰⁴, K. Y. Fung^{65a}, E. Furtado De Simas Filho^{84c}, M. Furukawa¹⁵⁷, J. Fuster¹⁶⁶, A. Gaa⁵⁶, A. Gabrielli^{24a,24b}, A. Gabrielli¹⁵⁸, P. Gadow³⁷, G. Gagliardi^{58a,58b}, L. G. Gagnon^{18a}, S. Gaid¹⁶³, S. Galantzan¹⁵⁵, J. Gallagher¹, E. J. Gallas¹²⁹, B. J. Gallop¹³⁷, K. K. Gan¹²², S. Ganguly¹⁵⁷, Y. Gao⁵³, F. M. Garay Walls^{140a,140b}, B. Garcia³⁰, C. García¹⁶⁶, A. Garcia Alonso¹¹⁷, A. G. Garcia Caffaro¹⁷⁵, J. E. García Navarro¹⁶⁶, M. Garcia-Sciveres^{18a}, G. L. Gardner¹³¹, R. W. Gardner⁴⁰, N. Garelli¹⁶¹, D. Garg⁸¹, R. B. Garg¹⁴⁷, J. M. Gargan⁵³, C. A. Garner¹⁵⁸, C. M. Garvey^{34a}, V. K. Gassmann¹⁶¹, G. Gaudio^{74a}, V. Gautam¹³, P. Gauzzi^{76a,76b}, J. Gavranovic⁹⁵, I. L. Gavrilenko³⁸, A. Gavrilyuk³⁸, C. Gay¹⁶⁷, G. Gaycken¹²⁶, E. N. Gazis¹⁰, A. A. Geanta^{28b}, C. M. Gee¹³⁹, A. Gekow¹²², C. Gemme^{58b}, M. H. Genest⁶¹, A. D. Gentry¹¹⁵, S. George⁹⁷, W. F. George²¹, T. Gerialis⁴⁷, P. Gessinger-Befurt³⁷, M. E. Geyik¹⁷⁴, M. Ghani¹⁷⁰, K. Ghorbanian⁹⁶, A. Ghosal¹⁴⁵, A. Ghosh¹⁶², A. Ghosh⁷, B. Giacobbe^{24b}, S. Giagu^{76a,76b}, T. Giani¹¹⁷, A. Giannini^{63a}, S. M. Gibson⁹⁷, M. Gignac¹³⁹, D. T. Gil^{87b}, A. K. Gilbert^{87a}, B. J. Gilbert⁴², D. Gillberg³⁵, G. Gilles¹¹⁷, L. Ginabat¹³⁰, D. M. Gingrich^{2,af}, M. P. Giordani^{70a,70c}, P. F. Giraud¹³⁸, G. Giugliarelli^{70a,70c}, D. Giugni^{72a}, F. Giuli^{77a,77b}, I. Gkialas^{9j}, L. K. Gladilin³⁸, C. Glasman¹⁰¹, G. R. Gledhill¹²⁶, G. Glemža⁴⁹, M. Glisic¹²⁶, I. Gnesi^{44b}, Y. Go³⁰, M. Goblirsch-Kolb³⁷, B. Gocke⁵⁰, D. Godin¹¹⁰, B. Gokturk^{22a}, S. Goldfarb¹⁰⁷, T. Golling⁵⁷, M. G. D. Gololo^{34g}, D. Golubkov³⁸, J. P. Gombas¹⁰⁹, A. Gomes^{133a,133b}, G. Gomes Da Silva¹⁴⁵, A. J. Gomez Delegido¹⁶⁶, R. Gonçalves^{133a}, L. Gonella²¹, A. Gongadze^{153c}, F. Gonnella²¹, J. L. Gonski¹⁴⁷, R. Y. González Andana⁵³, S. González de la Hoz¹⁶⁶, R. Gonzalez Lopez⁹⁴, C. Gonzalez Renteria^{18a}, M. V. Gonzalez Rodrigues⁴⁹, R. Gonzalez Suarez¹⁶⁴, S. Gonzalez-Sevilla⁵⁷, L. Goossens³⁷, B. Gorini³⁷, E. Gorini^{71a,71b}, A. Gorišek⁹⁵, T. C. Gosart¹³¹, A. T. Goshaw⁵², M. I. Gostkin³⁹, S. Goswami¹²⁴, C. A. Gottardo³⁷, S. A. Gotz¹¹¹, M. Gouighri^{36b}, V. Goumarre⁴⁹, A. G. Goussiou¹⁴², N. Govender^{34c}, R. P. Grabarczyk¹²⁹, I. Grabowska-Bold^{87a}, K. Graham³⁵, E. Gramstad¹²⁸, S. Grancagnolo^{71a,71b}, C. M. Grant^{1,138}, P. M. Gravila^{28f}, F. G. Gravili^{71a,71b}, H. M. Gray^{18a}, M. Greco^{71a,71b}, M. J. Green¹, C. Grefe²⁵, A. S. Grefsrud¹⁷, I. M. Gregor⁴⁹, K. T. Greif¹⁶², P. Grenier¹⁴⁷, S. G. Grewe¹¹², A. A. Grillo¹³⁹, K. Grimm³², S. Grinstein^{13,u}, J.-F. Grivaz⁶⁷, E. Gross¹⁷², J. Grosse-Knetter⁵⁶

L. Guan¹⁰⁸, J. G. R. Guerrero Rojas¹⁶⁶, G. Guerrieri³⁷, R. Gugel¹⁰², J. A. M. Guhit¹⁰⁸, A. Guida¹⁹, E. Guilloton¹⁷⁰, S. Guindon³⁷, F. Guo^{14,114c}, J. Guo^{63c}, L. Guo⁴⁹, Y. Guo¹⁰⁸, A. Gupta⁵⁰, R. Gupta¹³², S. Gurbuz²⁵, S. S. Gurdasani⁵⁵, G. Gustavino^{76a,76b}, P. Gutierrez¹²³, L. F. Gutierrez Zagazeta¹³¹, M. Gutsche⁵¹, C. Gutschow⁹⁸, C. Gwenlan¹²⁹, C. B. Gwilliam⁹⁴, E. S. Haaland¹²⁸, A. Haas¹²⁰, M. Habedank⁶⁰, C. Haber^{18a}, H. K. Hadavand⁸, A. Hadeef⁵¹, S. Hadzic¹¹², A. I. Hagan⁹³, J. J. Hahn¹⁴⁵, E. H. Haines⁹⁸, M. Haleem¹⁶⁹, J. Haley¹²⁴, G. D. Hallowell¹⁰⁴, L. Halser²⁰, K. Hamano¹⁶⁸, M. Hamer²⁵, E. J. Hampshire⁹⁷, J. Han^{63b}, L. Han^{114a}, L. Han^{63a}, S. Han^{18a}, Y. F. Han¹⁵⁸, K. Hanagaki⁸⁵, M. Hance¹³⁹, D. A. Hangal⁴², H. Hanif¹⁴⁶, M. D. Hank¹³¹, J. B. Hansen⁴³, P. H. Hansen⁴³, D. Harada⁵⁷, T. Harenberg¹⁷⁴, S. Harkusha³⁸, M. L. Harris¹⁰⁵, Y. T. Harris²⁵, J. Harrison¹³, N. M. Harrison¹²², P. F. Harrison¹⁷⁰, N. M. Hartman¹¹², N. M. Hartmann¹¹¹, R. Z. Hasan^{97,137}, Y. Hasegawa¹⁴⁴, F. Haslbeck¹²⁹, S. Hassan¹⁷, R. Hauser¹⁰⁹, C. M. Hawkes²¹, R. J. Hawkins³⁷, Y. Hayashi¹⁵⁷, D. Hayden¹⁰⁹, C. Hayes¹⁰⁸, R. L. Hayes¹¹⁷, C. P. Hays¹²⁹, J. M. Hays⁹⁶, H. S. Hayward⁹⁴, F. He^{63a}, M. He^{14,114c}, Y. He⁴⁹, Y. He⁹⁸, N. B. Heatley⁹⁶, V. Hedberg¹⁰⁰, A. L. Heggelund¹²⁸, N. D. Hehir^{96,*}, C. Heidegger⁵⁵, K. K. Heidegger⁵⁵, J. Heilman³⁵, S. Heim⁴⁹, T. Heim^{18a}, J. G. Heinlein¹³¹, J. J. Heinrich¹²⁶, L. Heinrich^{112,ad}, J. Hejbal¹³⁴, A. Held¹⁷³, S. Hellesund¹⁷, C. M. Helling¹⁶⁷, S. Hellman^{48a,48b}, R. C. W. Henderson⁹³, L. Henkelmann³³, A. M. Henriques Correia³⁷, H. Herde¹⁰⁰, Y. Hernández Jiménez¹⁴⁹, L. M. Herrmann²⁵, T. Herrmann⁵¹, G. Herten⁵⁵, R. Hertenberger¹¹¹, L. Hervas³⁷, M. E. Hespings¹⁰², N. P. Hessey^{159a}, J. Hessler¹¹², M. Hidaoui^{36b}, N. Hidic¹³⁶, E. Hill¹⁵⁸, S. J. Hillier²¹, J. R. Hinds¹⁰⁹, F. Hinterkeuser²⁵, M. Hirose¹²⁷, S. Hirose¹⁶⁰, D. Hirschbuehl¹⁷⁴, T. G. Hitchings¹⁰³, B. Hiti⁹⁵, J. Hobbs¹⁴⁹, R. Hobincu^{28e}, N. Hod¹⁷², M. C. Hodgkinson¹⁴³, B. H. Hodgkinson¹²⁹, A. Hoecker³⁷, D. D. Hofer¹⁰⁸, J. Hofer¹⁶⁶, T. Holm²⁵, M. Holzbock³⁷, L. B. A. H. Hommels³³, B. P. Honan¹⁰³, J. J. Hong⁶⁹, J. Hong^{63c}, T. M. Hong¹³², B. H. Hooberman¹⁶⁵, W. H. Hopkins⁶, M. C. Hoppesch¹⁶⁵, Y. Horii¹¹³, M. E. Horstmann¹¹², S. Hou¹⁵², A. S. Howard⁹⁵, J. Howarth⁶⁰, J. Hoya⁶, M. Hrabovsky¹²⁵, A. Hrynevich⁴⁹, T. Hryn'ova⁴, P. J. Hsu⁶⁶, S.-C. Hsu¹⁴², T. Hsu⁶⁷, M. Hu^{18a}, Q. Hu^{63a}, S. Huang^{65b}, X. Huang^{14,114c}, Y. Huang¹⁴³, Y. Huang¹⁰², Y. Huang¹⁴, Z. Huang¹⁰³, Z. Hubacek¹³⁵, M. Huebner²⁵, F. Huegging²⁵, T. B. Huffman¹²⁹, M. Hufnagel Maranha De Faria^{84a}, C. A. Hugli⁴⁹, M. Huhtinen³⁷, S. K. Huiberts¹⁷, R. Hulsken¹⁰⁶, N. Huseynov^{12,g}, J. Huston¹⁰⁹, J. Huth⁶², R. Hyneman¹⁴⁷, G. Iacobucci⁵⁷, G. Iakovidis³⁰, L. Iconomidou-Fayard⁶⁷, J. P. Iddon³⁷, P. Iengo^{73a,73b}, R. Iguchi¹⁵⁷, Y. Iiyama¹⁵⁷, T. Iizawa¹²⁹, Y. Ikegami⁸⁵, N. Ilic¹⁵⁸, H. Imam^{84c}, G. Inacio Goncalves^{84d}, T. Ingebretsen Carlson^{48a,48b}, J. M. Inglis⁹⁶, G. Introzzi^{74a,74b}, M. Iodice^{78a}, V. Ippolito^{76a,76b}, R. K. Irwin⁹⁴, M. Ishino¹⁵⁷, W. Islam¹⁷³, C. Issever¹⁹, S. Istin^{22a,aj}, H. Ito¹⁷¹, R. Iuppa^{79a,79b}, A. Ivina¹⁷², J. M. Izen⁴⁶, V. Izzo^{73a}, P. Jacka¹³⁴, P. Jackson¹, C. S. Jagfeld¹¹¹, G. Jain^{159a}, P. Jain⁴⁹, K. Jakobs⁵⁵, T. Jakoubek¹⁷², J. Jamieson⁶⁰, W. Jang¹⁵⁷, M. Javurkova¹⁰⁵, P. Jawahar¹⁰³, L. Jeanty¹²⁶, J. Jejelava^{153a,ab}, P. Jenni^{55,f}, C. E. Jessiman³⁵, C. Jia^{63b}, H. Jia¹⁶⁷, J. Jia¹⁴⁹, X. Jia^{14,114c}, Z. Jia^{114a}, C. Jiang⁵³, S. Jiggins⁴⁹, J. Jimenez Pena¹³, S. Jin^{114a}, A. Jinaru^{28b}, O. Jinnouchi¹⁴¹, P. Johansson¹⁴³, K. A. Johns⁷, J. W. Johnson¹³⁹, F. A. Jolly⁴⁹, D. M. Jones¹⁵⁰, E. Jones⁴⁹, K. S. Jones⁸, P. Jones³³, R. W. L. Jones⁹³, T. J. Jones⁹⁴, H. L. Joos^{37,56}, R. Joshi¹²², J. Jovicevic¹⁶, X. Ju^{18a}, J. J. Junggeburth¹⁰⁵, T. Junkermann^{64a}, A. Juste Rozas^{13,u}, M. K. Juzek⁸⁸, S. Kabana^{140e}, A. Kaczmarek⁸⁸, M. Kado¹¹², H. Kagan¹²², M. Kagan¹⁴⁷, A. Kahn¹³¹, C. Kahra¹⁰², T. Kaji¹⁵⁷, E. Kajomovitz¹⁵⁴, N. Kakati¹⁷², I. Kalaitzidou⁵⁵, C. W. Kalderon³⁰, N. J. Kang¹³⁹, D. Kar^{34g}, K. Karava¹²⁹, M. J. Kareem^{159b}, E. Karentzos⁵⁵, O. Karkout¹¹⁷, S. N. Karpov³⁹, Z. M. Karpova³⁹, V. Kartvelishvili⁹³, A. N. Karyukhin³⁸, E. Kasimi¹⁵⁶, J. Katzy⁴⁹, S. Kaur³⁵, K. Kawade¹⁴⁴, M. P. Kawale¹²³, C. Kawamoto⁸⁹, T. Kawamoto^{63a}, E. F. Kay³⁷, F. I. Kaya¹⁶¹, S. Kazakos¹⁰⁹, V. F. Kazanin³⁸, Y. Ke¹⁴⁹, J. M. Keaveney^{34a}, R. Keeler¹⁶⁸, G. V. Kehris⁶², J. S. Keller³⁵, J. J. Kempster¹⁵⁰, O. Kepka¹³⁴, B. P. Kerridge¹³⁷, S. Kersten¹⁷⁴, B. P. Kerševan⁹⁵, L. Keszeghova^{29a}, S. Ketabchi Haghghat¹⁵⁸, R. A. Khan¹³², A. Khanov¹²⁴, A. G. Kharlamov³⁸, T. Kharlamova³⁸, E. E. Khoda¹⁴², M. Kholodenko^{133a}, T. J. Khoo¹⁹, G. Khorauli¹⁶⁹, J. Khubua^{153b,*}, Y. A. R. Khwaira¹³⁰, B. Kibirige^{34g}, D. Kim⁶, D. W. Kim^{48a,48b}, Y. K. Kim⁴⁰, N. Kimura⁹⁸, M. K. Kingston⁵⁶, A. Kirchoff⁵⁶, C. Kirfel²⁵, F. Kirfel²⁵, J. Kirk¹³⁷, A. E. Kiryunin¹¹², S. Kita¹⁶⁰, C. Kitsaki¹⁰, O. Kivernyk²⁵, M. Klassen¹⁶¹, C. Klein³⁵, L. Klein¹⁶⁹, M. H. Klein⁴⁵, S. B. Klein⁵⁷, U. Klein⁹⁴, A. Klimentov³⁰, T. Klioutchnikova³⁷, P. Kluit¹¹⁷, S. Kluth¹¹², E. Kneringer⁸⁰, T. M. Knight¹⁵⁸, A. Knue⁵⁰, D. Kobylanski¹⁷², S. F. Koch¹²⁹, M. Kocian¹⁴⁷, P. Kodyš¹³⁶, D. M. Koeck¹²⁶, P. T. Koenig²⁵, T. Koffas³⁵, O. Kolay⁵¹, I. Koletsou⁴, T. Komarek⁸⁸, K. Köneke⁵⁵, A. X. Y. Kong¹, T. Kono¹²¹, N. Konstantinidis⁹⁸, P. Kontaxakis⁵⁷, B. Konya¹⁰⁰, R. Kopelianny⁴², S. Koperny^{87a}, K. Korcyl⁸⁸, K. Kordas^{156,e}, A. Korn⁹⁸, S. Korn⁵⁶, I. Korolkov¹³

N. Korotkova³⁸, B. Kortman¹¹⁷, O. Kortner¹¹², S. Kortner¹¹², W. H. Kostecka¹¹⁸, V. V. Kostyukhin¹⁴⁵, A. Kotsokechagia³⁷, A. Kotwal⁵², A. Koulouris³⁷, A. Kourkoumeli-Charalampidi^{74a,74b}, C. Kourkoumelis⁹, E. Kourlitis¹¹², O. Kovanda¹²⁶, R. Kowalewski¹⁶⁸, W. Kozanecki¹²⁶, A. S. Kozhin³⁸, V. A. Kramarenko³⁸, G. Kramberger⁹⁵, P. Kramer¹⁰², M. W. Krasny¹³⁰, A. Krasznahorkay³⁷, A. C. Kraus¹¹⁸, J. W. Kraus¹⁷⁴, J. A. Kremer⁴⁹, T. Kresse⁵¹, L. Kretschmann¹⁷⁴, J. Kretzschmar⁹⁴, K. Kreul¹⁹, P. Krieger¹⁵⁸, M. Krivos¹³⁶, K. Krizka²¹, K. Kroeninger⁵⁰, H. Kroha¹¹², J. Kroll¹³⁴, J. Kroll¹³¹, K. S. Krowpman¹⁰⁹, U. Kruchonak³⁹, H. Krüger²⁵, N. Krumnack⁸², M. C. Kruse⁵², O. Kuchinskaia³⁸, S. Kuday^{3a}, S. Kuehn³⁷, R. Kuesters⁵⁵, T. Kuhl⁴⁹, V. Kukhtin³⁹, Y. Kulchitsky^{38,a}, S. Kuleshov^{140b,140d}, M. Kumar^{34g}, N. Kumari⁴⁹, P. Kumari^{159b}, A. Kupco¹³⁴, T. Kupfer⁵⁰, A. Kupich³⁸, O. Kuprash⁵⁵, H. Kurashige⁸⁶, L. L. Kurchaninov^{159a}, O. Kurdysh⁶⁷, Y. A. Kurochkin³⁸, A. Kurova³⁸, M. Kuze¹⁴¹, A. K. Kvam¹⁰⁵, J. Kvita¹²⁵, T. Kwan¹⁰⁶, N. G. Kyriacou¹⁰⁸, L. A. O. Laatu¹⁰⁴, C. Lacasta¹⁶⁶, F. Lacava^{76a,76b}, H. Lacker¹⁹, D. Lacour¹³⁰, N. N. Lad⁹⁸, E. Ladygin³⁹, A. Lafarge⁴¹, B. Laforge¹³⁰, T. Lagouri¹⁷⁵, F. Z. Lahbabi^{36a}, S. Lai⁵⁶, J. E. Lambert¹⁶⁸, S. Lammers⁶⁹, W. Lampl⁷, C. Lampoudis^{156,e}, G. Lamprinoudis¹⁰², A. N. Lancaster¹¹⁸, E. Lançon³⁰, U. Landgraf⁵⁵, M. P. J. Landon⁹⁶, V. S. Lang⁵⁵, O. K. B. Langrekken¹²⁸, A. J. Lankford¹⁶², F. Lanni³⁷, K. Lantzsch²⁵, A. Lanza^{74a}, M. Lanzac Berrocal¹⁶⁶, J. F. Laporte¹³⁸, T. Lari^{72a}, F. Lasagni Manghi^{24b}, M. Lassnig³⁷, V. Latonova¹³⁴, A. Laurier¹⁵⁴, S. D. Lawlor¹⁴³, Z. Lawrence¹⁰³, R. Lazaridou¹⁷⁰, M. Lazzaroni^{72a,72b}, B. Le¹⁰³, H. D. M. Le¹⁰⁹, E. M. Le Boulicaut¹⁷⁵, L. T. Le Pottier^{18a}, B. Leban^{24a,24b}, A. Lebedev⁸², M. LeBlanc¹⁰³, F. Ledroit-Guillon⁶¹, S. C. Lee¹⁵², S. Lee^{48a,48b}, T. F. Lee⁹⁴, L. L. Leuw^{34c}, H. P. Lefebvre⁹⁷, M. Lefebvre¹⁶⁸, C. Leggett^{18a}, G. Lehmann Miotto³⁷, M. Leigh⁵⁷, W. A. Leight¹⁰⁵, W. Leinonen¹¹⁶, A. Leisos^{156,s}, M. A. L. Leite^{84c}, C. E. Leitgeb¹⁹, R. Leitner¹³⁶, K. J. C. Leney⁴⁵, T. Lenz²⁵, S. Leone^{75a}, C. Leonidopoulos⁵³, A. Leopold¹⁴⁸, R. Les¹⁰⁹, C. G. Lester³³, M. Levchenko³⁸, J. Levêque⁴, L. J. Levinson¹⁷², G. Levrimi^{24a,24b}, M. P. Lewicki⁸⁸, C. Lewis¹⁴², D. J. Lewis⁴, L. Lewitt¹⁴³, A. Li³⁰, B. Li^{63b}, C. Li^{63a}, C-Q. Li¹¹², H. Li^{63a}, H. Li^{63b}, H. Li^{114a}, H. Li¹⁵, H. Li^{63b}, J. Li^{63c}, K. Li¹⁴, L. Li^{63c}, M. Li^{14,114c}, S. Li^{14,114c}, S. Li^{63c,63d,d}, T. Li⁵, X. Li¹⁰⁶, Z. Li¹⁵⁷, Z. Li^{14,114c}, Z. Li^{63a}, S. Liang^{14,114c}, Z. Liang¹⁴, M. Liberatore¹³⁸, B. Liberti^{77a}, K. Lie^{65c}, J. Lieber Marin^{84e}, H. Lien⁶⁹, H. Lin¹⁰⁸, K. Lin¹⁰⁹, R. E. Lindley⁷, J. H. Lindon², J. Ling⁶², E. Lipeles¹³¹, A. Lipniacka¹⁷, A. Lister¹⁶⁷, J. D. Little⁶⁹, B. Liu¹⁴, B. X. Liu^{114b}, D. Liu^{63c,63d}, E. H. L. Liu²¹, J. B. Liu^{63a}, J. K. K. Liu³³, K. Liu^{63d}, K. Liu^{63c,63d}, M. Liu^{63a}, M. Y. Liu^{63a}, P. Liu¹⁴, Q. Liu^{63c,63d,142}, X. Liu^{63a}, X. Liu^{63b}, Y. Liu^{114b,114c}, Y. L. Liu^{63b}, Y. W. Liu^{63a}, S. L. Lloyd⁹⁶, E. M. Lobodzinska⁴⁹, P. Loch⁷, E. Lodhi¹⁵⁸, T. Lohse¹⁹, K. Lohwasser¹⁴³, E. Loiacono⁴⁹, M. Lokajicek^{134,*}, J. D. Lomas²¹, J. D. Long⁴², I. Longarini¹⁶², R. Longo¹⁶⁵, I. Lopez Paz⁶⁸, A. Lopez Solis⁴⁹, N. A. Lopez-canelas⁷, N. Lorenzo Martinez⁴, A. M. Lory¹¹¹, M. Losada^{119a}, G. Löschcke Centeno¹⁵⁰, O. Loseva³⁸, X. Lou^{48a,48b}, X. Lou^{14,114c}, A. Lounis⁶⁷, P. A. Love⁹³, G. Lu^{14,114c}, M. Lu⁶⁷, S. Lu¹³¹, Y. J. Lu⁶⁶, H. J. Lubatti¹⁴², C. Luci^{76a,76b}, F. L. Lucio Alves^{114a}, F. Luehring⁶⁹, O. Lukianchuk⁶⁷, B. S. Lunday¹³¹, O. Lundberg¹⁴⁸, B. Lund-Jensen^{148,*}, N. A. Luongo⁶, M. S. Lutz³⁷, A. B. Lux²⁶, D. Lynn³⁰, R. Lysak¹³⁴, E. Lytken¹⁰⁰, V. Lyubushkin³⁹, T. Lyubushkina³⁹, M. M. Lyukova¹⁴⁹, M. Firdaus M. Soberi⁵³, H. Ma³⁰, K. Ma^{63a}, L. L. Ma^{63b}, W. Ma^{63a}, Y. Ma¹²⁴, J. C. MacDonald¹⁰², P. C. Machado De Abreu Farias^{84e}, R. Madar⁴¹, T. Madula⁹⁸, J. Maeda⁸⁶, T. Maeno³⁰, H. Maguire¹⁴³, V. Maiboroda¹³⁸, A. Maio^{133a,133b,133d}, K. Maj^{87a}, O. Majersky⁴⁹, S. Majewski¹²⁶, N. Makovec⁶⁷, V. Maksimovic¹⁶, B. Malaescu¹³⁰, Pa. Malecki⁸⁸, V. P. Maleev³⁸, F. Malek^{61,n}, M. Mali⁹⁵, D. Malito⁹⁷, U. Mallik^{81,*}, S. Maltezos¹⁰, S. Malyukov³⁹, J. Mamuzic¹³, G. Mancini⁵⁴, M. N. Mancini²⁷, G. Manco^{74a,74b}, J. P. Mandalia⁹⁶, S. S. Mandarray¹⁵⁰, I. Mandić⁹⁵, L. Manhaes de Andrade Filho^{84a}, I. M. Maniatis¹⁷², J. Manjarres Ramos⁹¹, D. C. Mankad¹⁷², A. Mann¹¹¹, S. Manzoni³⁷, L. Mao^{63c}, X. Mapekula^{34c}, A. Marantis^{156,s}, G. Marchiori⁵, M. Marcisovsky¹³⁴, C. Marcon^{72a}, M. Marinescu²¹, S. Marium⁴⁹, M. Marjanovic¹²³, A. Markhoos⁵⁵, M. Markovitch⁶⁷, E. J. Marshall⁹³, Z. Marshall^{18a}, S. Marti-Garcia¹⁶⁶, J. Martin⁹⁸, T. A. Martin¹³⁷, V. J. Martin⁵³, B. Martin dit Latour¹⁷, L. Martinelli^{76a,76b}, M. Martinez^{13,u}, P. Martinez Agullo¹⁶⁶, V. I. Martinez Outschoorn¹⁰⁵, P. Martinez Suarez¹³, S. Martin-Haugh¹³⁷, G. Martinovicova¹³⁶, V. S. Martoiu^{28b}, A. C. Martyniuk⁹⁸, A. Marzin³⁷, D. Mascione^{79a,79b}, L. Masetti¹⁰², J. Masik¹⁰³, A. L. Maslennikov³⁸, S. L. Mason⁴², P. Massarotti^{73a,73b}, P. Mastrandrea^{75a,75b}, A. Mastroberardino^{44a,44b}, T. Masubuchi¹²⁷, T. T. Mathew¹²⁶, T. Mathisen¹⁶⁴, J. Matousek¹³⁶, D. M. Mattern⁵⁰, J. Maurer^{28b}, T. Maurin⁶⁰, A. J. Maury⁶⁷, B. Mačec⁹⁵, D. A. Maximov³⁸, A. E. May¹⁰³, R. Mazini¹⁵², I. Maznas¹¹⁸, M. Mazza¹⁰⁹, S. M. Mazza¹³⁹, E. Mazzeo^{72a,72b}, C. Mc Ginn³⁰, J. P. Mc Gowan¹⁶⁸, S. P. Mc Kee¹⁰⁸, C. A. Mc Lean⁶, C. C. McCracken¹⁶⁷, E. F. McDonald¹⁰⁷, A. E. McDougall¹¹⁷, J. A. MCFayden¹⁵⁰, R. P. McGovern¹³¹

R. P. McKenzie^{34g}, T. C. Mclachlan⁴⁹, D. J. Mclaughlin⁹⁸, S. J. McMahon¹³⁷, C. M. Mcpartland⁹⁴, R. A. McPherson^{168,y}, S. Mehlhase¹¹¹, A. Mehta⁹⁴, B. Meirose⁴⁶, D. Melini¹⁶⁶, B. R. Mellado Garcia^{34g}, A. H. Melo⁵⁶, F. Meloni⁴⁹, A. M. Mendes Jacques Da Costa¹⁰³, H. Y. Meng¹⁵⁸, L. Meng⁹³, S. Menke¹¹², M. Mentink³⁷, E. Meoni^{44a,44b}, G. Mercado¹¹⁸, S. Merianos¹⁵⁶, C. Merlassino^{70a,70c}, L. Merola^{73a,73b}, C. Meroni^{72a,72b}, J. Metcalfe⁶, A. S. Mete⁶, E. Meuser¹⁰², C. Meyer⁶⁹, J-P. Meyer¹³⁸, R. P. Middleton¹³⁷, L. Mijović⁵³, G. Mikenberg¹⁷², M. Mikestikova¹³⁴, M. Mikuz⁹⁵, H. Mildner¹⁰², A. Milic³⁷, D. W. Miller⁴⁰, E. H. Miller¹⁴⁷, L. S. Miller³⁵, A. Milov¹⁷², D. A. Milstead^{48a,48b}, T. Min^{114a}, A. A. Minaenko³⁸, I. A. Minashvili^{153b}, L. Mince⁶⁰, A. I. Mincer¹²⁰, B. Mindur^{87a}, M. Mineev³⁹, Y. Mino⁸⁹, L. M. Mir¹³, M. Miralles Lopez⁶⁰, M. Mironova^{18a}, M. C. Missio¹¹⁶, A. Mitra¹⁷⁰, V. A. Mitsou¹⁶⁶, Y. Mitsumori¹¹³, O. Miu¹⁵⁸, P. S. Miyagawa⁹⁶, T. Mkrtychyan^{64a}, M. Mlinarevic⁹⁸, T. Mlinarevic⁹⁸, M. Mlynarikova³⁷, S. Mobius²⁰, P. Mogg¹¹¹, M. H. Mohamed Farook¹¹⁵, A. F. Mohammed^{14,114c}, S. Mohapatra⁴², G. Mokgatitswane^{34g}, L. Moleri¹⁷², B. Mondal¹⁴⁵, S. Mondal¹³⁵, K. Mönig⁴⁹, E. Monnier¹⁰⁴, L. Monsonis Romero¹⁶⁶, J. Montejo Berlingen¹³, A. Montella^{48a,48b}, M. Montella¹²², F. Montereali^{78a,78b}, F. Monticelli⁹², S. Monzani^{70a,70c}, A. Morancho Tarda⁴³, N. Morange⁶⁷, A. L. Moreira De Carvalho⁴⁹, M. Moreno Llácer¹⁶⁶, C. Moreno Martinez⁵⁷, J. M. Moreno Perez^{23b}, P. Morettini^{58b}, S. Morgenstern³⁷, M. Mori⁶², M. Morinaga¹⁵⁷, M. Moritsu⁹⁰, F. Morodei^{76a,76b}, P. Moschovakos³⁷, B. Moser¹²⁹, M. Mosidze^{153b}, T. Moskalets⁴⁵, P. Moskvitina¹¹⁶, J. Moss^{32,k}, P. Moszkowicz^{87a}, A. Moussa^{36d}, E. J. W. Moyse¹⁰⁵, O. Mtintsilana^{34g}, S. Muanza¹⁰⁴, J. Mueller¹³², D. Muenstermann⁹³, R. Müller³⁷, G. A. Mullier¹⁶⁴, A. J. Mullin³³, J. J. Mullin¹³¹, A. E. Mulski⁶², D. P. Mungo¹⁵⁸, D. Munoz Perez¹⁶⁶, F. J. Munoz Sanchez¹⁰³, M. Murin¹⁰³, W. J. Murray^{137,170}, M. Muškinja⁹⁵, C. Mwewa³⁰, A. G. Myagkov^{38,a}, A. J. Myers⁸, G. Myers¹⁰⁸, M. Myska¹³⁵, B. P. Nachman^{18a}, O. Nackenhorst⁵⁰, K. Nagai¹²⁹, K. Nagano⁸⁵, R. Nagasaka¹⁵⁷, J. L. Nagle^{30,ah}, E. Nagy¹⁰⁴, A. M. Nairz³⁷, Y. Nakahama⁸⁵, K. Nakamura⁸⁵, K. Nakkalil⁵, H. Nanjo¹²⁷, E. A. Narayanan⁴⁵, I. Naryshkin³⁸, L. Nasella^{72a,72b}, M. Naseri³⁵, S. Nasri^{119b}, C. Nass²⁵, G. Navarro^{23a}, J. Navarro-Gonzalez¹⁶⁶, R. Nayak¹⁵⁵, A. Nayaz¹⁹, P. Y. Nechaeva³⁸, S. Nechaeva^{24a,24b}, F. Nechansky¹³⁴, L. Nedic¹²⁹, T. J. Neep²¹, A. Negri^{74a,74b}, M. Negrini^{24b}, C. Nellist¹¹⁷, C. Nelson¹⁰⁶, K. Nelson¹⁰⁸, S. Nemecek¹³⁴, M. Nessi^{37,h}, M. S. Neubauer¹⁶⁵, F. Neuhaus¹⁰², J. Neundorff⁴⁹, J. Newell⁹⁴, P. R. Newman²¹, C. W. Ng¹³², Y. W. Y. Ng⁴⁹, B. Ngair^{119a}, H. D. N. Nguyen¹¹⁰, R. B. Nickerson¹²⁹, R. Nicolaidou¹³⁸, J. Nielsen¹³⁹, M. Niemeyer⁵⁶, J. Niermann⁵⁶, N. Nikiforou³⁷, V. Nikolaenko^{38,a}, I. Nikolic-Audit¹³⁰, K. Nikolopoulos²¹, P. Nilsson³⁰, I. Ninca⁴⁹, G. Ninio¹⁵⁵, A. Nisati^{76a}, N. Nishu², R. Nisius¹¹², N. Nitika^{70a,70c}, J-E. Nitschke⁵¹, E. K. Nkademeng^{34g}, T. Nobe¹⁵⁷, T. Nommensen¹⁵¹, M. B. Norfolk¹⁴³, B. J. Norman³⁵, M. Noury^{36a}, J. Novak⁹⁵, T. Novak⁹⁵, L. Novotny¹³⁵, R. Novotny¹¹⁵, L. Nozka¹²⁵, K. Ntekas¹⁶², N. M. J. Nunes De Moura Junior^{84b}, J. Ocariz¹³⁰, A. Ochi⁸⁶, I. Ochoa^{133a}, S. Oerdek^{49,v}, J. T. Offermann⁴⁰, A. Ogrodnik¹³⁶, A. Oh¹⁰³, C. C. Ohm¹⁴⁸, H. Oide⁸⁵, R. Oishi¹⁵⁷, M. L. Ojeda³⁷, Y. Okumura¹⁵⁷, L. F. Oleiro Seabra^{133a}, I. Oleksiyuk⁵⁷, S. A. Olivares Pino^{140d}, G. Oliveira Correa¹³, D. Oliveira Damazio³⁰, J. L. Oliver¹⁶², Ö. O. Öncel⁵⁵, A. P. O'Neill²⁰, A. Onofre^{133a,133e}, P. U. E. Onyisi¹¹, M. J. Oreglia⁴⁰, G. E. Orellana⁹², D. Orestano^{78a,78b}, N. Orlando¹³, R. S. Orr¹⁵⁸, L. M. Osojnak¹³¹, R. Ospanov^{63a}, Y. Osumi¹¹³, G. Otero y Garzon³¹, H. Otono⁹⁰, P. S. Ott^{64a}, G. J. Ottino^{18a}, M. Ouchrif^{36d}, F. Ould-Saada¹²⁸, T. Ovsiannikova¹⁴², M. Owen⁶⁰, R. E. Owen¹³⁷, V. E. Ozcan^{22a}, F. Ozturk⁸⁸, N. Ozturk⁸, S. Ozturk⁸³, H. A. Pacey¹²⁹, A. Pacheco Pages¹³, C. Padilla Aranda¹³, G. Padovano^{76a,76b}, S. Pagan Griso^{18a}, G. Palacino⁶⁹, A. Palazzo^{71a,71b}, J. Pampel²⁵, J. Pan¹⁷⁵, T. Pan^{65a}, D. K. Panchal¹¹, C. E. Pandini¹¹⁷, J. G. Panduro Vazquez¹³⁷, H. D. Pandya¹, H. Pang¹⁵, P. Pani⁴⁹, G. Panizzo^{70a,70c}, L. Panwar¹³⁰, L. Paolozzi⁵⁷, S. Parajuli¹⁶⁵, A. Paramonov⁶, C. Paraskevopoulos⁵⁴, D. Paredes Hernandez^{65b}, A. Pareti^{74a,74b}, K. R. Park⁴², T. H. Park¹⁵⁸, M. A. Parker³³, F. Parodi^{58a,58b}, E. W. Parrish¹¹⁸, V. A. Parrish⁵³, J. A. Parsons⁴², U. Parzefall⁵⁵, B. Pascual Dias¹¹⁰, L. Pascual Dominguez¹⁰¹, E. Pasqualucci^{76a}, S. Passaggio^{58b}, F. Pastore⁹⁷, P. Patel⁸⁸, U. M. Patel⁵², J. R. Pater¹⁰³, T. Pauly³⁷, F. Pauwels¹³⁶, C. I. Pazos¹⁶¹, M. Pedersen¹²⁸, R. Pedro^{133a}, S. V. Peleganchuk³⁸, O. Penc³⁷, E. A. Pender⁵³, S. Peng¹⁵, G. D. Penn¹⁷⁵, K. E. Penski¹¹¹, M. Penzin³⁸, B. S. Peralva^{84d}, A. P. Pereira Peixoto¹⁴², L. Pereira Sanchez¹⁴⁷, D. V. Perepelitsa^{30,ah}, G. Perera¹⁰⁵, E. Perez Codina^{159a}, M. Perganti¹⁰, H. Pernegger³⁷, S. Perrella^{76a,76b}, O. Perrin⁴¹, K. Peters⁴⁹, R. F. Y. Peters¹⁰³, B. A. Petersen³⁷, T. C. Petersen⁴³, E. Petit¹⁰⁴, V. Petousis¹³⁵, C. Petridou^{156,e}, T. Petru¹³⁶, A. Petrukhin¹⁴⁵, M. Pettee^{18a}, A. Petukhov³⁸, K. Petukhova³⁷, R. Pezoa^{140f}, L. Pezzotti³⁷, G. Pezzullo¹⁷⁵, A. J. Pflieger³⁷, T. M. Pham¹⁷³, T. Pham¹⁰⁷, P. W. Phillips¹³⁷, G. Piacquadio¹⁴⁹, E. Pianori^{18a}, F. Piazza¹²⁶, R. Piegaia³¹, D. Pietreanu^{28b}, A. D. Pilkington¹⁰³, M. Pinamonti^{70a,70c}, J. L. Pinfold²,

B. C. Pinheiro Pereira^{133a}, J. Pinol Bel¹³, A. E. Pinto Pinoargote¹³⁸, L. Pintucci^{70a,70c}, K. M. Piper¹⁵⁰, A. Pirttikoski⁵⁷, D. A. Pizzi³⁵, L. Pizzimento^{65b}, A. Pizzini¹¹⁷, M.-A. Pleier³⁰, V. Pleskot¹³⁶, E. Plotnikova³⁹, G. Poddar⁹⁶, R. Poettgen¹⁰⁰, L. Poggioli¹³⁰, I. Pokharel⁵⁶, S. Polacek¹³⁶, G. Polesello^{74a}, A. Poley^{146,159a}, A. Polini^{24b}, C. S. Pollard¹⁷⁰, Z. B. Pollock¹²², E. Pompa Pacchi^{76a,76b}, N. I. Pond⁹⁸, D. Ponomarenko⁶⁹, L. Pontecorvo³⁷, S. Popa^{28a}, G. A. Popeneciu^{28d}, A. Poreba³⁷, D. M. Portillo Quintero^{159a}, S. Pospisil¹³⁵, M. A. Postill¹⁴³, P. Postolache^{28c}, K. Potamianos¹⁷⁰, P. A. Potepa^{87a}, I. N. Potrap³⁹, C. J. Potter³³, H. Potti¹⁵¹, J. Poveda¹⁶⁶, M. E. Pozo Astigarraga³⁷, A. Prades Ibanez^{77a,77b}, J. Pretel¹⁶⁸, D. Price¹⁰³, M. Primavera^{71a}, L. Primomo^{70a,70c}, M. A. Principe Martin¹⁰¹, R. Privara¹²⁵, T. Procter⁶⁰, M. L. Proffitt¹⁴², N. Proklova¹³¹, K. Prokofiev^{65c}, G. Proto¹¹², J. Proudfoot⁶, M. Przybycien^{87a}, W. W. Przygoda^{87b}, A. Psallidas⁴⁷, J. E. Puddefoot¹⁴³, D. Pudzha⁵⁵, D. Pyatiizbyantseva³⁸, J. Qian¹⁰⁸, D. Qichen¹⁰³, Y. Qin¹³, T. Qiu⁵³, A. Quadt⁵⁶, M. Queitsch-Maitland¹⁰³, G. Quetant⁵⁷, R. P. Quinn¹⁶⁷, G. Rabanal Bolanos⁶², D. Rafanoharana⁵⁵, F. Raffaelli^{77a,77b}, F. Ragusa^{72a,72b}, J. L. Rainbolt⁴⁰, J. A. Raine⁵⁷, S. Rajagopalan³⁰, E. Ramakoti³⁸, L. Rambelli^{58a,58b}, I. A. Ramirez-Berend³⁵, K. Ran^{49,114c}, D. S. Rankin¹³¹, N. P. Rappheeha^{34g}, H. Rasheed^{28b}, V. Raskina¹³⁰, D. F. Rassloff^{64a}, A. Rastogi^{18a}, S. Rave¹⁰², S. Ravera^{58a,58b}, B. Ravina⁵⁶, I. Ravinovich¹⁷², M. Raymond³⁷, A. L. Read¹²⁸, N. P. Readioff¹⁴³, D. M. Rebuffi^{74a,74b}, G. Redlinger³⁰, A. S. Reed¹¹², K. Reeves²⁷, J. A. Reidelsturz¹⁷⁴, D. Reikher¹²⁶, A. Rej⁵⁰, C. Rembser³⁷, M. Renda^{28b}, F. Renner⁴⁹, A. G. Rennie¹⁶², A. L. Rescia⁴⁹, S. Resconi^{72a}, M. Ressegotti^{58a,58b}, S. Rettie³⁷, J. G. Reyes Rivera¹⁰⁹, E. Reynolds^{18a}, O. L. Rezanova³⁸, P. Reznicek¹³⁶, H. Riani^{36d}, N. Ribaric⁵², B. Ricci^{70c}, E. Ricci^{79a,79b}, R. Richter¹¹², S. Richter^{48a,48b}, E. Richter-Was^{87b}, M. Ridel¹³⁰, S. Ridouani^{36d}, P. Rieck¹²⁰, P. Riedler³⁷, E. M. Riefel^{48a,48b}, J. O. Rieger¹¹⁷, M. Rijssenbeek¹⁴⁹, M. Rimoldi³⁷, L. Rinaldi^{24a,24b}, P. Rincke^{56,164}, T. T. Rinn³⁰, M. P. Rinnagel¹¹¹, G. Ripellino¹⁶⁴, I. Riu¹³, J. C. Rivera Vergara¹⁶⁸, F. Rizatdinova¹²⁴, E. Rizvi⁹⁶, B. R. Roberts^{18a}, S. S. Roberts¹³⁹, S. H. Robertson^{106,y}, D. Robinson³³, M. Robles Manzano¹⁰², A. Robson⁶⁰, A. Rocchi^{77a,77b}, C. Roda^{75a,75b}, S. Rodriguez Bosca³⁷, Y. Rodriguez Garcia^{23a}, A. Rodriguez Rodriguez⁵⁵, A. M. Rodríguez Vera¹¹⁸, S. Roe³⁷, J. T. Roemer³⁷, A. R. Roepe-Gier¹³⁹, O. Røhne¹²⁸, R. A. Rojas¹⁰⁵, C. P. A. Roland¹³⁰, J. Roloff³⁰, A. Romaniouk⁸⁰, E. Romano^{74a,74b}, M. Romano^{24b}, A. C. Romero Hernandez¹⁶⁵, N. Rompotis⁹⁴, L. Roos¹³⁰, S. Rosati^{76a}, B. J. Rosser⁴⁰, E. Rossi¹²⁹, E. Rossi^{73a,73b}, L. P. Rossi⁶², L. Rossini⁵⁵, R. Rosten¹²², M. Rotaru^{28b}, B. Rottler⁵⁵, C. Rougier⁹¹, D. Rousseau⁶⁷, D. Rouso⁴⁹, A. Roy¹⁶⁵, S. Roy-Garand¹⁵⁸, A. Rozanov¹⁰⁴, Z. M. A. Rozario⁶⁰, Y. Rozen¹⁵⁴, A. Rubio Jimenez¹⁶⁶, A. J. Ruby⁹⁴, V. H. Ruelas Rivera¹⁹, T. A. Ruggeri¹, A. Ruggiero¹²⁹, A. Ruiz-Martinez¹⁶⁶, A. Rummler³⁷, Z. Rurikova⁵⁵, N. A. Rusakovich³⁹, H. L. Russell¹⁶⁸, G. Russo^{76a,76b}, J. P. Rutherford⁷, S. Rutherford Colmenares³³, M. Rybar¹³⁶, E. B. Rye¹²⁸, A. Ryzhov⁴⁵, J. A. Sabater Iglesias⁵⁷, H. F.-W. Sadrozinski¹³⁹, F. Safai Tehrani^{76a}, B. Safarzadeh Samani¹³⁷, S. Saha¹, M. Sahinsoy⁸³, A. Saibel¹⁶⁶, M. Saimpert¹³⁸, M. Saito¹⁵⁷, T. Saito¹⁵⁷, A. Sala^{72a,72b}, D. Salamani³⁷, A. Salnikov¹⁴⁷, J. Salt¹⁶⁶, A. Salvador Salas¹⁵⁵, D. Salvatore^{44a,44b}, F. Salvatore¹⁵⁰, A. Salzburger³⁷, D. Sammel⁵⁵, E. Sampson⁹³, D. Sampsonidis^{156,e}, D. Sampsonidou¹²⁶, J. Sánchez¹⁶⁶, V. Sanchez Sebastian¹⁶⁶, H. Sandaker¹²⁸, C. O. Sander⁴⁹, J. A. Sandesara¹⁰⁵, M. Sandhoff¹⁷⁴, C. Sandoval^{23b}, L. Sanfilippo^{64a}, D. P. C. Sankey¹³⁷, T. Sano⁸⁹, A. Sansoni⁵⁴, L. Santi^{37,76b}, C. Santoni⁴¹, H. Santos^{133a,133b}, A. Santra¹⁷², E. Sanzani^{24a,24b}, K. A. Saoucha¹⁶³, J. G. Saraiva^{133a,133d}, J. Sardain⁷, O. Sasaki⁸⁵, K. Sato¹⁶⁰, C. Sauer^{64b}, E. Sauvan⁴, P. Savard^{158,af}, R. Sawada¹⁵⁷, C. Sawyer¹³⁷, L. Sawyer⁹⁹, C. Sbarra^{24b}, A. Sbrizzi^{24a,24b}, T. Scanlon⁹⁸, J. Schaarschmidt¹⁴², U. Schäfer¹⁰², A. C. Schaffer^{45,67}, D. Schaile¹¹¹, R. D. Schamberger¹⁴⁹, C. Scharf¹⁹, M. M. Schefer²⁰, V. A. Schegelsky³⁸, D. Scheirich¹³⁶, M. Schernau¹⁶², C. Scheulen⁵⁶, C. Schiavi^{58a,58b}, M. Schioppa^{44a,44b}, B. Schlag¹⁴⁷, S. Schlenker³⁷, J. Schmeing¹⁷⁴, M. A. Schmidt¹⁷⁴, K. Schmieden¹⁰², C. Schmitt¹⁰², N. Schmitt¹⁰², S. Schmitt⁴⁹, L. Schoeffel¹³⁸, A. Schoening^{64b}, P. G. Scholer³⁵, E. Schopf¹²⁹, M. Schott²⁵, J. Schovancova³⁷, S. Schramm⁵⁷, T. Schroer⁵⁷, H.-C. Schultz-Coulon^{64a}, M. Schumacher⁵⁵, B. A. Schumm¹³⁹, Ph. Schune¹³⁸, A. J. Schuy¹⁴², H. R. Schwartz¹³⁹, A. Schwartzman¹⁴⁷, T. A. Schwarz¹⁰⁸, Ph. Schwemling¹³⁸, R. Schwienhorst¹⁰⁹, F. G. Sciacca²⁰, A. Sciandra³⁰, G. Sciolla²⁷, F. Scuri^{75a}, C. D. Sebastiani⁹⁴, K. Sedlaczek¹¹⁸, S. C. Seidel¹¹⁵, A. Seiden¹³⁹, B. D. Seidlitz⁴², C. Seitz⁴⁹, J. M. Seixas^{84b}, G. Sekhniaidze^{73a}, L. Selem⁶¹, N. Semprini-Cesari^{24a,24b}, D. Sengupta⁵⁷, V. Senthilkumar¹⁶⁶, L. Serin⁶⁷, M. Sessa^{77a,77b}, H. Severini¹²³, F. Sforza^{58a,58b}, A. Sfyrta⁵⁷, Q. Sha¹⁴, E. Shabalina⁵⁶, A. H. Shah³³, R. Shaheen¹⁴⁸, J. D. Shahinian¹³¹, D. Shaked Renous¹⁷², L. Y. Shan¹⁴, M. Shapiro^{18a}, A. Sharma³⁷, A. S. Sharma¹⁶⁷, P. Sharma⁸¹, P. B. Shatalov³⁸, K. Shaw¹⁵⁰, S. M. Shaw¹⁰³, Q. Shen^{63c}, D. J. Sheppard¹⁴⁶, P. Sherwood⁹⁸, L. Shi⁹⁸, X. Shi¹⁴, S. Shimizu⁸⁵, C. O. Shimmin¹⁷⁵, J. D. Shinner⁹⁷, I. P. J. Shipsey^{129,*}, S. Shirabe⁹⁰

M. Shiyakova^{39,w}, M. J. Shochet⁴⁰, D. R. Shope¹²⁸, B. Shrestha¹²³, S. Shrestha^{122,ai}, I. Shreyber³⁸, M. J. Shroff¹⁶⁸, P. Sicho¹³⁴, A. M. Sickles¹⁶⁵, E. Sideras Haddad^{34g}, A. C. Sidley¹¹⁷, A. Sidoti^{24b}, F. Siegert⁵¹, Dj. Sijacki¹⁶, F. Sili⁹², J. M. Silva⁵³, I. Silva Ferreira^{84b}, M. V. Silva Oliveira³⁰, S. B. Silverstein^{48a}, S. Simion⁶⁷, R. Simoniello³⁷, E. L. Simpson¹⁰³, H. Simpson¹⁵⁰, L. R. Simpson¹⁰⁸, S. Simsek⁸³, S. Sindhu⁵⁶, P. Sinervo¹⁵⁸, S. Singh¹⁵⁸, S. Sinha⁴⁹, S. Sinha¹⁰³, M. Sioli^{24a,24b}, I. Siral³⁷, E. Sitnikova⁴⁹, J. Sjölin^{48a,48b}, A. Skaf⁵⁶, E. Skorda²¹, P. Skubic¹²³, M. Slawinska⁸⁸, V. Smakhtin¹⁷², B. H. Smart¹³⁷, S. Yu. Smirnov³⁸, Y. Smirnov³⁸, L. N. Smirnova^{38,a}, O. Smirnova¹⁰⁰, A. C. Smith⁴², D. R. Smith¹⁶², E. A. Smith⁴⁰, J. L. Smith¹⁰³, R. Smith¹⁴⁷, M. Smizanska⁹³, K. Smolek¹³⁵, A. A. Snesarev³⁸, H. L. Snoek¹¹⁷, S. Snyder³⁰, R. Sobie^{168,y}, A. Soffer¹⁵⁵, C. A. Solans Sanchez³⁷, E. Yu. Soldatov³⁸, U. Soldevila¹⁶⁶, A. A. Solodkov³⁸, S. Solomon²⁷, A. Soloshenko³⁹, K. Solovieva⁵⁵, O. V. Solovyanov⁴¹, P. Sommer⁵¹, A. Sonay¹³, W. Y. Song^{159b}, A. Sopczak¹³⁵, A. L. Sopio⁵³, F. Sopkova^{29b}, J. D. Sorenson¹¹⁵, I. R. Sotarriva Alvarez¹⁴¹, V. Sothilingam^{64a}, O. J. Soto Sandoval^{140b,140c}, S. Sottocornola⁶⁹, R. Soualah¹⁶³, Z. Soumami^{36e}, D. South⁴⁹, N. Soybelman¹⁷², S. Spagnolo^{71a,71b}, M. Spalla¹¹², D. Sperlich⁵⁵, G. Spigo³⁷, B. Spisso^{73a,73b}, D. P. Spiteri⁶⁰, M. Spousta¹³⁶, E. J. Staats³⁵, R. Stamen^{64a}, A. Stampekis²¹, E. Stanecka⁸⁸, W. Stanek-Maslouska⁴⁹, M. V. Stange⁵¹, B. Stanislaus^{18a}, M. M. Stanitzki⁴⁹, B. Stapf⁴⁹, E. A. Starchenko³⁸, G. H. Stark¹³⁹, J. Stark⁹¹, P. Staroba¹³⁴, P. Starovoitov^{64a}, S. Stärz¹⁰⁶, R. Staszewski⁸⁸, G. Stavropoulos⁴⁷, A. Steffl³⁷, P. Steinberg³⁰, B. Stelzer^{146,159a}, H. J. Stelzer¹³², O. Stelzer-Chilton^{159a}, H. Stenzel⁵⁹, T. J. Stevenson¹⁵⁰, G. A. Stewart³⁷, J. R. Stewart¹²⁴, M. C. Stockton³⁷, G. Stoicea^{28b}, M. Stolarski^{133a}, S. Stonjek¹¹², A. Straessner⁵¹, J. Strandberg¹⁴⁸, S. Strandberg^{48a,48b}, M. Stratmann¹⁷⁴, M. Strauss¹²³, T. Streblor¹⁰⁴, P. Strizenc^{29b}, R. Ströhmer¹⁶⁹, D. M. Strom¹²⁶, R. Stroynowski⁴⁵, A. Strubig^{48a,48b}, S. A. Stucci³⁰, B. Stugu¹⁷, J. Stupak¹²³, N. A. Styles⁴⁹, D. Su¹⁴⁷, S. Su^{63a}, W. Su^{63d}, X. Su^{63a}, D. Suchy^{29a}, K. Sugizaki¹⁵⁷, V. V. Sulim³⁸, M. J. Sullivan⁹⁴, D. M. S. Sultan¹²⁹, L. Sultanaliyeva³⁸, S. Sultansoy^{3b}, T. Sumida⁸⁹, S. Sun¹⁷³, O. Sunneborn Gudnadottir¹⁶⁴, N. Sur¹⁰⁴, M. R. Sutton¹⁵⁰, H. Suzuki¹⁶⁰, M. Svatos¹³⁴, M. Swiatlowski^{159a}, T. Swirski¹⁶⁹, I. Sykora^{29a}, M. Sykora¹³⁶, T. Sykora¹³⁶, D. Ta¹⁰², K. Tackmann^{49,v}, A. Taffard¹⁶², R. Tafirout^{159a}, J. S. Tafoya Vargas⁶⁷, Y. Takubo⁸⁵, M. Talby¹⁰⁴, A. A. Talyshev³⁸, K. C. Tam^{65b}, N. M. Tamir¹⁵⁵, A. Tanaka¹⁵⁷, J. Tanaka¹⁵⁷, R. Tanaka⁶⁷, M. Tanasini¹⁴⁹, Z. Tao¹⁶⁷, S. Tapia Araya^{140f}, S. Tapprogge¹⁰², A. Tarek Abouelfadl Mohamed¹⁰⁹, S. Tarem¹⁵⁴, K. Tariq¹⁴, G. Tarna^{28b}, G. F. Tartarelli^{72a}, M. J. Tartarin⁹¹, P. Tas¹³⁶, M. Tasevsky¹³⁴, E. Tassi^{44a,44b}, A. C. Tate¹⁶⁵, G. Tateno¹⁵⁷, Y. Tayalati^{36e,x}, G. N. Taylor¹⁰⁷, W. Taylor^{159b}, R. Teixeira De Lima¹⁴⁷, P. Teixeira-Dias⁹⁷, J. J. Teoh¹⁵⁸, K. Terashi¹⁵⁷, J. Terron¹⁰¹, S. Terzo¹³, M. Testa⁵⁴, R. J. Teuscher^{158,y}, A. Thaler⁸⁰, O. Theiner⁵⁷, T. Theveneaux-Pelzer¹⁰⁴, O. Thielmann¹⁷⁴, D. W. Thomas⁹⁷, J. P. Thomas²¹, E. A. Thompson^{18a}, P. D. Thompson²¹, E. Thomson¹³¹, R. E. Thornberry⁴⁵, C. Tian^{63a}, Y. Tian⁵⁷, V. Tikhomirov^{38,a}, Yu. A. Tikhonov³⁸, S. Timoshenko³⁸, D. Timoshyn¹³⁶, E. X. L. Ting¹, P. Tipton¹⁷⁵, A. Tishelman-Charny³⁰, S. H. Tlou^{34g}, K. Todome¹⁴¹, S. Todorova-Nova¹³⁶, S. Todt⁵¹, L. Toffolin^{70a,70c}, M. Togawa⁸⁵, J. Tojo⁹⁰, S. Tokár^{29a}, K. Tokushuku⁸⁵, O. Toldaiev⁶⁹, M. Tomoto^{85,113}, L. Tompkins^{147,m}, K. W. Topolnicki^{87b}, E. Torrence¹²⁶, H. Torres⁹¹, E. Torró Pastor¹⁶⁶, M. Toscani³¹, C. Toscri⁴⁰, M. Tost¹¹, D. R. Tovey¹⁴³, I. S. Trandafir^{28b}, T. Trefzger¹⁶⁹, A. Tricoli³⁰, I. M. Trigger^{159a}, S. Trincz-Duvold¹³⁰, D. A. Trischuk²⁷, B. Trocme⁶¹, A. Tropina³⁹, L. Truong^{34c}, M. Trzebinski⁸⁸, A. Trzupek⁸⁸, F. Tsai¹⁴⁹, M. Tsai¹⁰⁸, A. Tsiamis¹⁵⁶, P. V. Tsiarehka³⁸, S. Tsigaridas^{159a}, A. Tsigotis^{156,s}, V. Tsiskaridze¹⁵⁸, E. G. Tskhadadze^{153a}, M. Tsopoulou¹⁵⁶, Y. Tsujikawa⁸⁹, I. I. Tsukerman³⁸, V. Tsulaia^{18a}, S. Tsuno⁸⁵, K. Tsurii¹²¹, D. Tsybychev¹⁴⁹, Y. Tu^{65b}, A. Tudorache^{28b}, V. Tudorache^{28b}, A. N. Tuna⁶², S. Turchikhin^{58a,58b}, I. Turk Cakir^{3a}, R. Turra^{72a}, T. Turtuvshin^{39,z}, P. M. Tuts⁴², S. Tzamarias^{156,e}, E. Tzovara¹⁰², F. Ukegawa¹⁶⁰, P. A. Ulloa Poblete^{140b,140c}, E. N. Umaka³⁰, G. Unal³⁷, A. Undrus³⁰, G. Unel¹⁶², J. Urban^{29b}, P. Urrejola^{140a}, G. Usai⁸, R. Ushioda¹⁴¹, M. Usman¹¹⁰, F. Ustuner⁵³, Z. Uysal⁸³, V. Vacek¹³⁵, B. Vachon¹⁰⁶, T. Vafeiadis³⁷, A. Vaitkus⁹⁸, C. Valderanis¹¹¹, E. Valdes Santurio^{48a,48b}, M. Valente^{159a}, S. Valentinetti^{24a,24b}, A. Valero¹⁶⁶, E. Valiente Moreno¹⁶⁶, A. Vallier⁹¹, J. A. Valls Ferrer¹⁶⁶, D. R. Van Arneman¹¹⁷, T. R. Van Daalen¹⁴², A. Van Der Graaf⁵⁰, P. Van Gemmeren⁶, M. Van Rijnbach³⁷, S. Van Stroud⁹⁸, I. Van Vulpen¹¹⁷, P. Vana¹³⁶, M. Vanadia^{77a,77b}, U. M. Vande Voorde¹⁴⁸, W. Vandelli³⁷, E. R. Vandewall¹²⁴, D. Vannicola¹⁵⁵, L. Vannoli⁵⁴, R. Vari^{76a}, E. W. Varnes⁷, C. Varni^{18b}, T. Varol¹⁵², D. Varouchas⁶⁷, L. Varriale¹⁶⁶, K. E. Varvell¹⁵¹, M. E. Vasile^{28b}, L. Vaslin⁸⁵, G. A. Vasquez¹⁶⁸, A. Vasyukov³⁹, L. M. Vaughan¹²⁴, R. Vavricka¹⁰², T. Vazquez Schroeder³⁷, J. Veatch³², V. Vecchio¹⁰³, M. J. Veen¹⁰⁵, I. Veliscek³⁰, L. M. Veloce¹⁵⁸, F. Veloso^{133a,133c}, S. Veneziano^{76a}, A. Ventura^{71a,71b}, S. Ventura Gonzalez¹³⁸, A. Verbytskyi¹¹², M. Verducci^{75a,75b}, C. Vergis⁹⁶, M. Verissimo De Araujo^{84b}

W. Verkerke¹¹⁷, J. C. Vermeulen¹¹⁷, C. Vernieri¹⁴⁷, M. Vessella¹⁰⁵, M. C. Vetterli^{146.af}, A. Vgenopoulos¹⁰², N. Viaux Maira^{140f}, T. Vickey¹⁴³, O. E. Vickey Boeriu¹⁴³, G. H. A. Viehhauser¹²⁹, L. Vigani^{64b}, M. Vigi¹¹², M. Villa^{24a.24b}, M. Villaplana Perez¹⁶⁶, E. M. Villhauer⁵³, E. Vilucchi⁵⁴, M. G. Vincter³⁵, A. Visibile¹¹⁷, C. Vittori³⁷, I. Vivarelli^{24a.24b}, E. Voevodina¹¹², F. Vogel¹¹¹, J. C. Voigt⁵¹, P. Vokac¹³⁵, Yu. Volkotrub^{87b}, E. Von Toerne²⁵, B. Vormwald³⁷, V. Vorobel¹³⁶, K. Vorobev³⁸, M. Vos¹⁶⁶, K. Voss¹⁴⁵, M. Vozak¹¹⁷, L. Vozdecky¹²³, N. Vranjes¹⁶, M. Vranjes Milosavljevic¹⁶, M. Vreeswijk¹¹⁷, N. K. Vu^{63c.63d}, R. Vuillermet³⁷, O. Vujanovic¹⁰², I. Vukotic⁴⁰, I. K. Vyas³⁵, S. Wada¹⁶⁰, C. Wagner¹⁴⁷, J. M. Wagner^{18a}, W. Wagner¹⁷⁴, S. Wahdan¹⁷⁴, H. Wahlberg⁹², C. H. Waits¹²³, J. Walder¹³⁷, R. Walker¹¹¹, W. Walkowiak¹⁴⁵, A. Wall¹³¹, E. J. Wallin¹⁰⁰, T. Wamorkar⁶, A. Z. Wang¹³⁹, C. Wang¹⁰², C. Wang¹¹, H. Wang^{18a}, J. Wang^{65c}, P. Wang⁹⁸, R. Wang⁶², R. Wang⁶, S. M. Wang¹⁵², S. Wang^{63b}, S. Wang¹⁴, T. Wang^{63a}, W. T. Wang⁸¹, W. Wang¹⁴, X. Wang^{114a}, X. Wang¹⁶⁵, X. Wang^{63c}, Y. Wang^{63d}, Y. Wang^{114a}, Y. Wang^{63a}, Z. Wang¹⁰⁸, Z. Wang^{52.63c.63d}, Z. Wang¹⁰⁸, A. Warburton¹⁰⁶, R. J. Ward²¹, N. Warrack⁶⁰, S. Waterhouse⁹⁷, A. T. Watson²¹, H. Watson⁵³, M. F. Watson²¹, E. Watton^{60.137}, G. Watts¹⁴², B. M. Waugh⁹⁸, J. M. Webb⁵⁵, C. Weber³⁰, H. A. Weber¹⁹, M. S. Weber²⁰, S. M. Weber^{64a}, C. Wei^{63a}, Y. Wei⁵⁵, A. R. Weidberg¹²⁹, E. J. Weik¹²⁰, J. Weingarten⁵⁰, C. Weiser⁵⁵, C. J. Wells⁴⁹, T. Wenaus³⁰, B. Wendland⁵⁰, T. Wengler³⁷, N. S. Wenke¹¹², N. Wermes²⁵, M. Wessels^{64a}, A. M. Wharton⁹³, A. S. White⁶², A. White⁸, M. J. White¹, D. Whiteson¹⁶², L. Wickremasinghe¹²⁷, W. Wiedenmann¹⁷³, M. Wielers¹³⁷, C. Wiglesworth⁴³, D. J. Wilbern¹²³, H. G. Wilkens³⁷, J. J. H. Wilkinson³³, D. M. Williams⁴², H. H. Williams¹³¹, S. Williams³³, S. Willocq¹⁰⁵, B. J. Wilson¹⁰³, P. J. Windischhofer⁴⁰, F. I. Winkel³¹, F. Winklmeier¹²⁶, B. T. Winter⁵⁵, J. K. Winter¹⁰³, M. Wittgen¹⁴⁷, M. Wobisch⁹⁹, T. Wojtkowski⁶¹, Z. Wolffs¹¹⁷, J. Wollrath¹⁶², M. W. Wolter⁸⁸, H. Wolters^{133a.133c}, M. C. Wong¹³⁹, E. L. Woodward⁴², S. D. Worm⁴⁹, B. K. Wosiek⁸⁸, K. W. Woźniak⁸⁸, S. Wozniowski⁵⁶, K. Wraight⁶⁰, C. Wu²¹, M. Wu^{114b}, M. Wu¹¹⁶, S. L. Wu¹⁷³, X. Wu⁵⁷, Y. Wu^{63a}, Z. Wu⁴, J. Wuerzinger^{112.ad}, T. R. Wyatt¹⁰³, B. M. Wynne⁵³, S. Xella⁴³, L. Xia^{114a}, M. Xia¹⁵, M. Xie^{63a}, S. Xin^{14.114c}, A. Xiong¹²⁶, J. Xiong^{18a}, D. Xu¹⁴, H. Xu^{63a}, L. Xu^{63a}, R. Xu¹³¹, T. Xu¹⁰⁸, Y. Xu¹⁵, Z. Xu⁵³, Z. Xu^{114a}, B. Yabsley¹⁵¹, S. Yacoub^{34a}, Y. Yamaguchi⁸⁵, E. Yamashita¹⁵⁷, H. Yamauchi¹⁶⁰, T. Yamazaki^{18a}, Y. Yamazaki⁸⁶, S. Yan⁶⁰, Z. Yan¹⁰⁵, H. J. Yang^{63c.63d}, H. T. Yang^{63a}, S. Yang^{63a}, T. Yang^{65c}, X. Yang³⁷, X. Yang¹⁴, Y. Yang⁴⁵, Y. Yang^{63a}, Z. Yang^{63a}, W.-M. Yao^{18a}, H. Ye^{114a}, H. Ye⁵⁶, J. Ye¹⁴, S. Ye³⁰, X. Ye^{63a}, Y. Yeh⁹⁸, I. Yeletsikh³⁹, B. Yeo^{18b}, M. R. Yexley⁹⁸, T. P. Yildirim¹²⁹, P. Yin⁴², K. Yorita¹⁷¹, S. Younas^{28b}, C. J. S. Young³⁷, C. Young¹⁴⁷, C. Yu^{14.114c}, Y. Yu^{63a}, J. Yuan^{14.114c}, M. Yuan¹⁰⁸, R. Yuan^{63c.63d}, L. Yue⁹⁸, M. Zaazoua^{63a}, B. Zabinski⁸⁸, E. Zaid⁵³, Z. K. Zak⁸⁸, T. Zakareishvili¹⁶⁶, S. Zambito⁵⁷, J. A. Zamora Saa^{140b.140d}, J. Zang¹⁵⁷, D. Zanzi⁵⁵, O. Zaplatilek¹³⁵, C. Zeitnitz¹⁷⁴, H. Zeng¹⁴, J. C. Zeng¹⁶⁵, D. T. Zenger Jr²⁷, O. Zenin³⁸, T. Ženiš^{29a}, S. Zenz⁹⁶, S. Zerradi^{36a}, D. Zerwas⁶⁷, M. Zhai^{14.114c}, D. F. Zhang¹⁴³, J. Zhang^{63b}, J. Zhang⁶, K. Zhang^{14.114c}, L. Zhang^{63a}, L. Zhang^{114a}, P. Zhang^{14.114c}, R. Zhang¹⁷³, S. Zhang¹⁰⁸, S. Zhang⁹¹, T. Zhang¹⁵⁷, X. Zhang^{63c}, X. Zhang^{63b}, Y. Zhang^{63c}, Y. Zhang⁹⁸, Y. Zhang^{114a}, Z. Zhang^{18a}, Z. Zhang^{63b}, Z. Zhang⁶⁷, H. Zhao¹⁴², T. Zhao^{63b}, Y. Zhao¹³⁹, Z. Zhao^{63a}, Z. Zhao^{63a}, A. Zhemchugov³⁹, J. Zheng^{114a}, K. Zheng¹⁶⁵, X. Zheng^{63a}, Z. Zheng¹⁴⁷, D. Zhong¹⁶⁵, B. Zhou¹⁰⁸, H. Zhou⁷, N. Zhou^{63c}, Y. Zhou¹⁵, Y. Zhou^{114a}, Y. Zhou⁷, C. G. Zhu^{63b}, J. Zhu¹⁰⁸, X. Zhu^{63d}, Y. Zhu^{63c}, Y. Zhu^{63a}, X. Zhuang¹⁴, K. Zhukov⁶⁹, N. I. Zimine³⁹, J. Zinsser^{64b}, M. Ziolkowski¹⁴⁵, L. Živković¹⁶, A. Zoccoli^{24a.24b}, K. Zoch⁶², T. G. Zorbas¹⁴³, O. Zormpa⁴⁷, W. Zou⁴², L. Zwalinski³⁷

¹ Department of Physics, University of Adelaide, Adelaide, Australia

² Department of Physics, University of Alberta, Edmonton, AB, Canada

³ (a) Department of Physics, Ankara University, Ankara, Türkiye; (b) Division of Physics, TOBB University of Economics and Technology, Ankara, Türkiye

⁴ LAPP, CNRS/IN2P3, Université Savoie Mont Blanc, Annecy, France

⁵ APC, CNRS/IN2P3, Université Paris Cité, Paris, France

⁶ High Energy Physics Division, Argonne National Laboratory, Argonne, IL, USA

⁷ Department of Physics, University of Arizona, Tucson, AZ, USA

⁸ Department of Physics, University of Texas at Arlington, Arlington, TX, USA

⁹ Physics Department, National and Kapodistrian University of Athens, Athens, Greece

¹⁰ Physics Department, National Technical University of Athens, Zografou, Greece

¹¹ Department of Physics, University of Texas at Austin, Austin, TX, USA

- ¹² Institute of Physics, Azerbaijan Academy of Sciences, Baku, Azerbaijan
- ¹³ Institut de Física d'Altes Energies (IFAE), Barcelona Institute of Science and Technology, Barcelona, Spain
- ¹⁴ Institute of High Energy Physics, Chinese Academy of Sciences, Beijing, China
- ¹⁵ Physics Department, Tsinghua University, Beijing, China
- ¹⁶ Institute of Physics, University of Belgrade, Belgrade, Serbia
- ¹⁷ Department for Physics and Technology, University of Bergen, Bergen, Norway
- ¹⁸ ^(a)Physics Division, Lawrence Berkeley National Laboratory, Berkeley, CA, USA; ^(b)University of California, Berkeley, CA, USA
- ¹⁹ Institut für Physik, Humboldt Universität zu Berlin, Berlin, Germany
- ²⁰ Albert Einstein Center for Fundamental Physics and Laboratory for High Energy Physics, University of Bern, Bern, Switzerland
- ²¹ School of Physics and Astronomy, University of Birmingham, Birmingham, UK
- ²² ^(a)Department of Physics, Bogazici University, Istanbul, Türkiye; ^(b)Department of Physics Engineering, Gaziantep University, Gaziantep, Türkiye; ^(c)Department of Physics, Istanbul University, Istanbul, Türkiye
- ²³ ^(a)Facultad de Ciencias y Centro de Investigaciones, Universidad Antonio Nariño, Bogotá, Colombia; ^(b)Departamento de Física, Universidad Nacional de Colombia, Bogotá, Colombia
- ²⁴ ^(a)Dipartimento di Fisica e Astronomia A. Righi, Università di Bologna, Bologna, Italy; ^(b)INFN Sezione di Bologna, Bologna, Italy
- ²⁵ Physikalisches Institut, Universität Bonn, Bonn, Germany
- ²⁶ Department of Physics, Boston University, Boston, MA, USA
- ²⁷ Department of Physics, Brandeis University, Waltham, MA, USA
- ²⁸ ^(a)Transilvania University of Brasov, Brasov, Romania; ^(b)Horia Hulubei National Institute of Physics and Nuclear Engineering, Bucharest, Romania; ^(c)Department of Physics, Alexandru Ioan Cuza University of Iasi, Iasi, Romania; ^(d)Physics Department, National Institute for Research and Development of Isotopic and Molecular Technologies, Cluj-Napoca, Romania; ^(e)National University of Science and Technology Politehnica, Bucharest, Romania; ^(f)West University in Timisoara, Timisoara, Romania; ^(g)Faculty of Physics, University of Bucharest, Bucharest, Romania
- ²⁹ ^(a)Faculty of Mathematics, Physics and Informatics, Comenius University, Bratislava, Slovak Republic; ^(b)Department of Subnuclear Physics, Institute of Experimental Physics of the Slovak Academy of Sciences, Kosice, Slovak Republic
- ³⁰ Physics Department, Brookhaven National Laboratory, Upton, NY, USA
- ³¹ Facultad de Ciencias Exactas y Naturales, Departamento de Física, y CONICET, Instituto de Física de Buenos Aires (IFIBA), Universidad de Buenos Aires, Buenos Aires, Argentina
- ³² California State University, Los Angeles, CA, USA
- ³³ Cavendish Laboratory, University of Cambridge, Cambridge, UK
- ³⁴ ^(a)Department of Physics, University of Cape Town, Cape Town, South Africa; ^(b)iThemba Labs, Western Cape, South Africa; ^(c)Department of Mechanical Engineering Science, University of Johannesburg, Johannesburg, South Africa; ^(d)National Institute of Physics, University of the Philippines Diliman (Philippines), Quezon City, Philippines; ^(e)University of South Africa, Department of Physics, Pretoria, South Africa; ^(f)University of Zululand, KwaDlangezwa, South Africa; ^(g)School of Physics, University of the Witwatersrand, Johannesburg, South Africa
- ³⁵ Department of Physics, Carleton University, Ottawa, ON, Canada
- ³⁶ ^(a)Faculté des Sciences Ain Chock, Université Hassan II de Casablanca, Casablanca, Morocco; ^(b)Faculté des Sciences, Université Ibn-Tofail, Kénitra, Morocco; ^(c)Faculté des Sciences Semlalia, Université Cadi Ayyad, LPHEA-Marrakech, Marrakech, Morocco; ^(d)LPMR, Faculté des Sciences, Université Mohamed Premier, Oujda, Morocco; ^(e)Faculté des sciences, Université Mohammed V, Rabat, Morocco; ^(f)Institute of Applied Physics, Mohammed VI Polytechnic University, Ben Guerir, Morocco
- ³⁷ CERN, Geneva, Switzerland
- ³⁸ Affiliated with an Institute Covered by a Cooperation Agreement with CERN, Geneva, Switzerland
- ³⁹ Affiliated with an International Laboratory Covered by a Cooperation Agreement with CERN, Geneva, Switzerland
- ⁴⁰ Enrico Fermi Institute, University of Chicago, Chicago, IL, USA
- ⁴¹ LPC, CNRS/IN2P3, Université Clermont Auvergne, Clermont-Ferrand, France
- ⁴² Nevis Laboratory, Columbia University, Irvington, NY, USA
- ⁴³ Niels Bohr Institute, University of Copenhagen, Copenhagen, Denmark
- ⁴⁴ ^(a)Dipartimento di Fisica, Università della Calabria, Rende, Italy; ^(b)Laboratori Nazionali di Frascati, INFN Gruppo Collegato di Cosenza, Cosenza, Italy

- ⁴⁵ Physics Department, Southern Methodist University, Dallas, TX, USA
- ⁴⁶ Physics Department, University of Texas at Dallas, Richardson, TX, USA
- ⁴⁷ National Centre for Scientific Research “Demokritos”, Agia Paraskevi, Greece
- ⁴⁸ ^(a)Department of Physics, Stockholm University, Stockholm, Sweden; ^(b)Oskar Klein Centre, Stockholm, Sweden
- ⁴⁹ Deutsches Elektronen-Synchrotron DESY, Hamburg and Zeuthen, Germany
- ⁵⁰ Fakultät Physik, Technische Universität Dortmund, Dortmund, Germany
- ⁵¹ Institut für Kern- und Teilchenphysik, Technische Universität Dresden, Dresden, Germany
- ⁵² Department of Physics, Duke University, Durham, NC, USA
- ⁵³ SUPA-School of Physics and Astronomy, University of Edinburgh, Edinburgh, UK
- ⁵⁴ INFN e Laboratori Nazionali di Frascati, Frascati, Italy
- ⁵⁵ Physikalisches Institut, Albert-Ludwigs-Universität Freiburg, Freiburg, Germany
- ⁵⁶ II. Physikalisches Institut, Georg-August-Universität Göttingen, Göttingen, Germany
- ⁵⁷ Département de Physique Nucléaire et Corpusculaire, Université de Genève, Geneva, Switzerland
- ⁵⁸ ^(a)Dipartimento di Fisica, Università di Genova, Genoa, Italy; ^(b)INFN Sezione di Genova, Genoa, Italy
- ⁵⁹ II. Physikalisches Institut, Justus-Liebig-Universität Giessen, Giessen, Germany
- ⁶⁰ SUPA-School of Physics and Astronomy, University of Glasgow, Glasgow, UK
- ⁶¹ LPSC, CNRS/IN2P3, Grenoble INP, Université Grenoble Alpes, Grenoble, France
- ⁶² Laboratory for Particle Physics and Cosmology, Harvard University, Cambridge, MA, USA
- ⁶³ ^(a)Department of Modern Physics and State Key Laboratory of Particle Detection and Electronics, University of Science and Technology of China, Hefei, China; ^(b)Institute of Frontier and Interdisciplinary Science and Key Laboratory of Particle Physics and Particle Irradiation (MOE), Shandong University, Qingdao, China; ^(c)School of Physics and Astronomy, Key Laboratory for Particle Astrophysics and Cosmology (MOE), SKLPPC, Shanghai Jiao Tong University, Shanghai, China; ^(d)Tsung-Dao Lee Institute, Shanghai, China; ^(e)School of Physics, Zhengzhou University, Zhengzhou, China
- ⁶⁴ ^(a)Kirchhoff-Institut für Physik, Ruprecht-Karls-Universität Heidelberg, Heidelberg, Germany; ^(b)Physikalisches Institut, Ruprecht-Karls-Universität Heidelberg, Heidelberg, Germany
- ⁶⁵ ^(a)Department of Physics, Chinese University of Hong Kong, Shatin, N.T., Hong Kong, China; ^(b)Department of Physics, University of Hong Kong, Hong Kong, China; ^(c)Department of Physics and Institute for Advanced Study, Hong Kong University of Science and Technology, Clear Water Bay, Kowloon, Hong Kong, China
- ⁶⁶ Department of Physics, National Tsing Hua University, Hsinchu, Taiwan
- ⁶⁷ IJCLab, CNRS/IN2P3, Université Paris-Saclay, 91405 Orsay, France
- ⁶⁸ Centro Nacional de Microelectrónica (IMB-CNM-CSIC), Barcelona, Spain
- ⁶⁹ Department of Physics, Indiana University, Bloomington, IN, USA
- ⁷⁰ ^(a)INFN Gruppo Collegato di Udine, Sezione di Trieste, Udine, Italy; ^(b)ICTP, Trieste, Italy; ^(c)Dipartimento Politecnico di Ingegneria e Architettura, Università di Udine, Udine, Italy
- ⁷¹ ^(a)INFN Sezione di Lecce, Lecce, Italy; ^(b)Dipartimento di Matematica e Fisica, Università del Salento, Lecce, Italy
- ⁷² ^(a)INFN Sezione di Milano, Milan, Italy; ^(b)Dipartimento di Fisica, Università di Milano, Milan, Italy
- ⁷³ ^(a)INFN Sezione di Napoli, Naples, Italy; ^(b)Dipartimento di Fisica, Università di Napoli, Naples, Italy
- ⁷⁴ ^(a)INFN Sezione di Pavia, Pavia, Italy; ^(b)Dipartimento di Fisica, Università di Pavia, Pavia, Italy
- ⁷⁵ ^(a)INFN Sezione di Pisa, Pisa, Italy; ^(b)Dipartimento di Fisica E. Fermi, Università di Pisa, Pisa, Italy
- ⁷⁶ ^(a)INFN Sezione di Roma, Rome, Italy; ^(b)Dipartimento di Fisica, Sapienza Università di Roma, Rome, Italy
- ⁷⁷ ^(a)INFN Sezione di Roma Tor Vergata, Rome, Italy; ^(b)Dipartimento di Fisica, Università di Roma Tor Vergata, Rome, Italy
- ⁷⁸ ^(a)INFN Sezione di Roma Tre, Rome, Italy; ^(b)Dipartimento di Matematica e Fisica, Università Roma Tre, Rome, Italy
- ⁷⁹ ^(a)INFN-TIFPA, Povo, Italy; ^(b)Università degli Studi di Trento, Trento, Italy
- ⁸⁰ Universität Innsbruck, Department of Astro and Particle Physics, Innsbruck, Austria
- ⁸¹ University of Iowa, Iowa City, IA, USA
- ⁸² Department of Physics and Astronomy, Iowa State University, Ames, IA, USA
- ⁸³ Istinye University, Sariyer, Istanbul, Türkiye
- ⁸⁴ ^(a)Departamento de Engenharia Elétrica, Universidade Federal de Juiz de Fora (UFJF), Juiz de Fora, Brazil; ^(b)Universidade Federal do Rio De Janeiro COPPE/EE/IF, Rio de Janeiro, Brazil; ^(c)Instituto de Física, Universidade de São Paulo, São Paulo, Brazil; ^(d)Rio de Janeiro State University, Rio de Janeiro, Brazil; ^(e)Federal University of Bahia, Bahia, Brazil

- 85 KEK, High Energy Accelerator Research Organization, Tsukuba, Japan
- 86 Graduate School of Science, Kobe University, Kobe, Japan
- 87 ^(a)Faculty of Physics and Applied Computer Science, AGH University of Krakow, Kraków, Poland; ^(b)Marian Smoluchowski Institute of Physics, Jagiellonian University, Kraków, Poland
- 88 Institute of Nuclear Physics Polish Academy of Sciences, Kraków, Poland
- 89 Faculty of Science, Kyoto University, Kyoto, Japan
- 90 Research Center for Advanced Particle Physics and Department of Physics, Kyushu University, Fukuoka, Japan
- 91 L2IT, CNRS/IN2P3, UPS, Université de Toulouse, Toulouse, France
- 92 Instituto de Física La Plata, Universidad Nacional de La Plata and CONICET, La Plata, Argentina
- 93 Physics Department, Lancaster University, Lancaster, UK
- 94 Oliver Lodge Laboratory, University of Liverpool, Liverpool, UK
- 95 Department of Experimental Particle Physics, Jožef Stefan Institute and Department of Physics, University of Ljubljana, Ljubljana, Slovenia
- 96 School of Physics and Astronomy, Queen Mary University of London, London, UK
- 97 Department of Physics, Royal Holloway University of London, Egham, UK
- 98 Department of Physics and Astronomy, University College London, London, UK
- 99 Louisiana Tech University, Ruston, LA, USA
- 100 Fysiska institutionen, Lunds universitet, Lund, Sweden
- 101 Departamento de Física Teórica C-15 and CIAFF, Universidad Autónoma de Madrid, Madrid, Spain
- 102 Institut für Physik, Universität Mainz, Mainz, Germany
- 103 School of Physics and Astronomy, University of Manchester, Manchester, UK
- 104 CPPM, CNRS/IN2P3, Aix-Marseille Université, Marseille, France
- 105 Department of Physics, University of Massachusetts, Amherst, MA, USA
- 106 Department of Physics, McGill University, Montreal, QC, Canada
- 107 School of Physics, University of Melbourne, Victoria, Australia
- 108 Department of Physics, University of Michigan, Ann Arbor, MI, USA
- 109 Department of Physics and Astronomy, Michigan State University, East Lansing, MI, USA
- 110 Group of Particle Physics, University of Montreal, Montreal, QC, Canada
- 111 Fakultät für Physik, Ludwig-Maximilians-Universität München, Munich, Germany
- 112 Max-Planck-Institut für Physik (Werner-Heisenberg-Institut), Munich, Germany
- 113 Graduate School of Science and Kobayashi-Maskawa Institute, Nagoya University, Nagoya, Japan
- 114 ^(a)Department of Physics, Nanjing University, Nanjing, China; ^(b)School of Science, Shenzhen Campus of Sun Yat-sen University, Shenzhen, China; ^(c)University of Chinese Academy of Science (UCAS), Beijing, China
- 115 Department of Physics and Astronomy, University of New Mexico, Albuquerque, NM, USA
- 116 Institute for Mathematics, Astrophysics and Particle Physics, Radboud University/Nikhef, Nijmegen, Netherlands
- 117 Nikhef National Institute for Subatomic Physics and University of Amsterdam, Amsterdam, Netherlands
- 118 Department of Physics, Northern Illinois University, DeKalb, IL, USA
- 119 ^(a)New York University Abu Dhabi, Abu Dhabi, United Arab Emirates; ^(b)United Arab Emirates University, Al Ain, United Arab Emirates
- 120 Department of Physics, New York University, New York, NY, USA
- 121 Ochanomizu University, Otsuka, Bunkyo-ku, Tokyo, Japan
- 122 Ohio State University, Columbus, OH, USA
- 123 Homer L. Dodge Department of Physics and Astronomy, University of Oklahoma, Norman, OK, USA
- 124 Department of Physics, Oklahoma State University, Stillwater, OK, USA
- 125 Joint Laboratory of Optics, Palacký University, Olomouc, Czech Republic
- 126 Institute for Fundamental Science, University of Oregon, Eugene, OR, USA
- 127 Graduate School of Science, Osaka University, Osaka, Japan
- 128 Department of Physics, University of Oslo, Oslo, Norway
- 129 Department of Physics, Oxford University, Oxford, UK
- 130 LPNHE, CNRS/IN2P3, Sorbonne Université, Université Paris Cité, Paris, France
- 131 Department of Physics, University of Pennsylvania, Philadelphia, PA, USA
- 132 Department of Physics and Astronomy, University of Pittsburgh, Pittsburgh, PA, USA

- 133 (a) Laboratório de Instrumentação e Física Experimental de Partículas-LIP, Lisbon, Portugal; (b) Departamento de Física, Faculdade de Ciências, Universidade de Lisboa, Lisbon, Portugal; (c) Departamento de Física, Universidade de Coimbra, Coimbra, Portugal; (d) Centro de Física Nuclear da Universidade de Lisboa, Lisbon, Portugal; (e) Departamento de Física, Universidade do Minho, Braga, Portugal; (f) Departamento de Física Teórica y del Cosmos, Universidad de Granada, Granada, Spain; (g) Departamento de Física, Instituto Superior Técnico, Universidade de Lisboa, Lisbon, Portugal
- 134 Institute of Physics of the Czech Academy of Sciences, Prague, Czech Republic
- 135 Czech Technical University in Prague, Prague, Czech Republic
- 136 Charles University, Faculty of Mathematics and Physics, Prague, Czech Republic
- 137 Particle Physics Department, Rutherford Appleton Laboratory, Didcot, UK
- 138 IRFU, CEA, Université Paris-Saclay, Gif-sur-Yvette, France
- 139 Santa Cruz Institute for Particle Physics, University of California Santa Cruz, Santa Cruz, CA, USA
- 140 (a) Departamento de Física, Pontificia Universidad Católica de Chile, Santiago, Chile; (b) Millennium Institute for Subatomic Physics at High Energy Frontier (SAPHIR), Santiago, Chile; (c) Instituto de Investigación Multidisciplinario en Ciencia y Tecnología y Departamento de Física, Universidad de La Serena, La Serena, Chile; (d) Department of Physics, Universidad Andres Bello, Santiago, Chile; (e) Instituto de Alta Investigación, Universidad de Tarapacá, Arica, Chile; (f) Departamento de Física, Universidad Técnica Federico Santa María, Valparaíso, Chile
- 141 Department of Physics, Institute of Science, Tokyo, Japan
- 142 Department of Physics, University of Washington, Seattle, WA, USA
- 143 Department of Physics and Astronomy, University of Sheffield, Sheffield, UK
- 144 Department of Physics, Shinshu University, Nagano, Japan
- 145 Department Physik, Universität Siegen, Siegen, Germany
- 146 Department of Physics, Simon Fraser University, Burnaby, BC, Canada
- 147 SLAC National Accelerator Laboratory, Stanford, CA, USA
- 148 Department of Physics, Royal Institute of Technology, Stockholm, Sweden
- 149 Departments of Physics and Astronomy, Stony Brook University, Stony Brook, NY, USA
- 150 Department of Physics and Astronomy, University of Sussex, Brighton, UK
- 151 School of Physics, University of Sydney, Sydney, Australia
- 152 Institute of Physics, Academia Sinica, Taipei, Taiwan
- 153 (a) E. Andronikashvili Institute of Physics, Iv. Javakishvili Tbilisi State University, Tbilisi, Georgia; (b) High Energy Physics Institute, Tbilisi State University, Tbilisi, Georgia; (c) University of Georgia, Tbilisi, Georgia
- 154 Department of Physics, Technion, Israel Institute of Technology, Haifa, Israel
- 155 Raymond and Beverly Sackler School of Physics and Astronomy, Tel Aviv University, Tel Aviv, Israel
- 156 Department of Physics, Aristotle University of Thessaloniki, Thessaloníki, Greece
- 157 International Center for Elementary Particle Physics and Department of Physics, University of Tokyo, Tokyo, Japan
- 158 Department of Physics, University of Toronto, Toronto, ON, Canada
- 159 (a) TRIUMF, Vancouver, BC, Canada; (b) Department of Physics and Astronomy, York University, Toronto, ON, Canada
- 160 Division of Physics and Tomonaga Center for the History of the Universe, Faculty of Pure and Applied Sciences, University of Tsukuba, Tsukuba, Japan
- 161 Department of Physics and Astronomy, Tufts University, Medford, MA, USA
- 162 Department of Physics and Astronomy, University of California Irvine, Irvine, CA, USA
- 163 University of Sharjah, Sharjah, United Arab Emirates
- 164 Department of Physics and Astronomy, University of Uppsala, Uppsala, Sweden
- 165 Department of Physics, University of Illinois, Urbana, IL, USA
- 166 Instituto de Física Corpuscular (IFIC), Centro Mixto Universidad de Valencia-CSIC, Valencia, Spain
- 167 Department of Physics, University of British Columbia, Vancouver, BC, Canada
- 168 Department of Physics and Astronomy, University of Victoria, Victoria, BC, Canada
- 169 Fakultät für Physik und Astronomie, Julius-Maximilians-Universität Würzburg, Würzburg, Germany
- 170 Department of Physics, University of Warwick, Coventry, UK
- 171 Waseda University, Tokyo, Japan
- 172 Department of Particle Physics and Astrophysics, Weizmann Institute of Science, Rehovot, Israel
- 173 Department of Physics, University of Wisconsin, Madison, WI, USA
- 174 Fakultät für Mathematik und Naturwissenschaften, Fachgruppe Physik, Bergische Universität Wuppertal, Wuppertal, Germany

¹⁷⁵ Department of Physics, Yale University, New Haven, CT, USA

^a Also Affiliated with an Institute Covered by a Cooperation Agreement with CERN, Geneva, Switzerland

^b Also at An-Najah National University, Nablus, Palestine

^c Also at Borough of Manhattan Community College, City University of New York, New York, NY, USA

^d Also at Center for High Energy Physics, Peking University, Beijing, China

^e Also at Center for Interdisciplinary Research and Innovation (CIRI-AUTH), Thessaloníki, Greece

^f Also at CERN, Geneva, Switzerland

^g Also at CMD-AC UNEC Research Center, Azerbaijan State University of Economics (UNEC), Baku, Azerbaijan

^h Also at Département de Physique Nucléaire et Corpusculaire, Université de Genève, Geneva, Switzerland

ⁱ Also at Departament de Física de la Universitat Autònoma de Barcelona, Barcelona, Spain

^j Also at Department of Financial and Management Engineering, University of the Aegean, Chios, Greece

^k Also at Department of Physics, California State University, Sacramento, USA

^l Also at Department of Physics, King's College London, London, UK

^m Also at Department of Physics, Stanford University, Stanford, CA, USA

ⁿ Also at Department of Physics, Stellenbosch University, Stellenbosch, South Africa

^o Also at Department of Physics, University of Fribourg, Fribourg, Switzerland

^p Also at Department of Physics, University of Thessaly, Volos, Greece

^q Also at Department of Physics, Westmont College, Santa Barbara, USA

^r Also at Faculty of Physics, Sofia University, 'St. Kliment Ohridski', Sofia, Bulgaria

^s Also at Hellenic Open University, Patras, Greece

^t Also at Imam Mohammad Ibn Saud Islamic University, Riyadh, Saudi Arabia

^u Also at Institutio Catalana de Recerca i Estudis Avancats, ICREA, Barcelona, Spain

^v Also at Institut für Experimentalphysik, Universität Hamburg, Hamburg, Germany

^w Also at Institute for Nuclear Research and Nuclear Energy (INRNE) of the Bulgarian Academy of Sciences, Sofia, Bulgaria

^x Also at Institute of Applied Physics, Mohammed VI Polytechnic University, Ben Guerir, Morocco

^y Also at Institute of Particle Physics (IPP), Toronto, Canada

^z Also at Institute of Physics and Technology, Mongolian Academy of Sciences, Ulaanbaatar, Mongolia

^{aa} Also at Institute of Physics, Azerbaijan Academy of Sciences, Baku, Azerbaijan

^{ab} Also at Institute of Theoretical Physics, Ilia State University, Tbilisi, Georgia

^{ac} Also at National Institute of Physics, University of the Philippines Diliman (Philippines), Quezon City, Philippines

^{ad} Also at Technical University of Munich, Munich, Germany

^{ae} Also at The Collaborative Innovation Center of Quantum Matter (CICQM), Beijing, China

^{af} Also at TRIUMF, Vancouver, BC, Canada

^{ag} Also at Università di Napoli Parthenope, Naples, Italy

^{ah} Also at University of Colorado Boulder, Department of Physics, Colorado, USA

^{ai} Also at Washington College, Chestertown, MD, USA

^{aj} Also at Yeditepe University, Physics Department, Istanbul, Türkiye

* Deceased